Single Bubble-Electrospinning of Polyvinyl Alcohol and Polyacrylonitrile Solutions

By
Carla Pringle

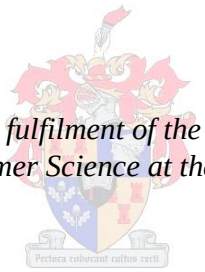

Thesis presented in partial fulfilment of the requirements for the degree Master of Science in Polymer Science at the University of Stellenbosch

Supervisor: Dr. Eugene Smit
Co-supervisor: Mrs. Lizl Cronje
Polymer Science
Department of Chemistry and Polymer Science

December 2011

Firstly, I give God all glory
for His awesome love and grace.
He was my strength when I had none.

I would then like to dedicate this work
to my loving and supportive husband, James Pringle,
who has been a pillar of strength.

Finally I dedicate this work to
my father, Leon Egen,
who encouraged me and made these past few years a reality.

Declaration

By submitting this thesis/dissertation electronically, I declare that the entirety of the work contained therein is my own, original work, that I am the sole author thereof (save to the extent explicitly otherwise stated), that reproduction and publication thereof by Stellenbosch University will not infringe any third party rights and that I have not previously in its entirety or in part submitted it for obtaining any qualification.

December 2011

Abstract

Needle-electrospinning is an uncomplicated and highly versatile nanofiber (fiber diameter of 50 to 500 nm) production technique. Nevertheless the process can only produce 0.01 to 1.0 g/h/m^2 of nanofibers, unpractical for large-scale productions. Bubble-electrospinning, in the presence of surfactants, is a novel nanofiber mass-production technique developed at Stellenbosch University.[1] The technique is similar to needle-electrospinning only that the surface area of a bubble surpasses that of a solution droplet, making it possible for multiple jets to form on the bubble surface at high field strengths. Thus far little research has been done on the influence of solution properties on the bubble-electrospinning technique.

During electrospinning the solution experiences three competing forces, namely, surface tension (contracting force), charge repulsion (expanding force), and viscosity (resistance to flow). The first aim of this study was to obtain better understanding on the influence of three significant solution properties (viscosity, conductivity and surface tension) on bubble-electrospinning in terms of bubble lifetime, bubble size, average number of jets and the resultant fibers. The solution properties were varied using a range of polymer and surfactant concentrations. A second aim was to obtain better understanding on the comparison of the bubble-electrospinning process between two polymer solutions, namely Polyvinyl alcohol (PVOH) solutions containing sodium lauryl ether sulphate (SLES) surfactant, and Polyacrylonitrile (PAN) solutions containing silicone surfactant.

Results indicated that the solution viscosity and conductivity increased with increasing polymer concentrations for both polymer solutions. In addition, both the solution surface tensions were not influenced by polymer concentration. With regards to bubble-electrospinning of PVOH solutions, results indicated that the average number of jets per bubble was influenced by the polymer concentration. Regarding PAN solutions, bubble lifetime and the average number of jets was influenced by polymer concentration.

Results indicated that the solution viscosity increased and surface tension decreased with increasing surfactant concentration for both polymer solutions. PVOH solution conductivity increased whilst PAN solution conductivity decreased with increasing surfactant concentrations. With regards to bubble-electrospinning of PVOH solutions, the bubble lifetime and bubble size was significantly influenced by the SLES concentration. Regarding PAN solutions, the silicone surfactant concentration had no significant effect on the bubble-electrospinning process. Overall, PVOH fiber diameters decreased with increasing surfactant concentration.

There was no common trend between the bubble-electrospinning of PVOH and PAN solutions in relation to their solution properties. It was concluded that solution viscosity, conductivity and surface tension are not the only significant contributing parameters to the bubble-electrospinning process.

Opsomming

Die naald-elektrospinproses is ‗n eenvoudige, hoogsaanpasbare tegniek wat gebruik word vir die maak van nanovesels. Nanovesels het tipies ‗n deursnee van 50nm tot 500nm. Ongelukkig is dit onprakties vir grootskaalse produksie omdat die uitset daarvan beperk is tot 0.01 tot 1.0 g/h/m^2. Die borrel-elektrospinproses, waar elektrospinstrale gespin word vanaf die oppervlak van borrels op die oppervlak van die spinoplossing en waar die borrels gestabiliseer is m.b.v. sepe, is ‗n nuwe tegniek wat ontwikkel is by die Universiteit van Stellenbosch. [1]. Die tegniek is soortgelyk aan die naald-elektrospinproses in dié sin dat die elektrospinstraal vorm vanaf ‗n gelaaide halfsfeervormige oppervlak in die spinoplossing, maar die aansienlik groter oppervlakarea van die borrel in die borrel-elektrospinproses maak dit moontlik om verskeie elektrospinstrale gelyktydig op die oppervlak van die borrel te onderhou. Dit lei tot baie hoër doeltreffendheid in die saamgroeppering van die strale en gevolglik tot hoër nanoveseluitsette. Tot dusver is daar weinig navorsing aangaande die invloed van oplossingseienskappe op die borrel- elektrospintegniek gedoen.

Tydens die elektrospinproses ervaar die oplossing drie kompeterende kragte, naamlik: oppervlakspanning (sametrekkende krag), elektrostatiese afstoting (afstotende krag) en viskositeit (vertragende effek op vloei van die oplossing). Die hoofdoelwit van hierdie navorsing was om ‗n beter begrip te kry van die invloed van drie gemete oplossingswaardes, d.w.s. viskositeit, elektriese geleidingsvermoë en oppervlakspanning op die borrel-elektrospinproses. Die impak van hierde waardes is spesifiek geëvalueer in terme van borrellewensduur, borrelgrootte, gemiddelde hoeveelheid elektrospinstrale per borrel en die morfologie van die vesels wat in die proses gevorm is. Die tweede doelwit van die studie was om ‗n vergelyking te tref tussen die mees optimale oplossingswaardes in die borrel-elektrospinproses van twee baie uiteenlopende polimeerspinoplossings, naamlik polivinielalkohol (PVOH), met natrium dodesieletersulfaat (SLES) as die borrelstabiliserende seep en poliakrilonitriel (PAN) oplossing, met ‗n silikoonseep as die borrelstabiliserende seep.

Resultate het getoon dat die viskositeit en elektriese geleidingsvermoë toeneem met toename in polimeerkonsentrasie vir beide PVOH- en PAN-oplossings. Verder is oppervlakspanning in beide gevalle nie beduidend beïnvloed deur die polimeerkonsentrasie nie. In die geval van die borrel-elektrospin van die PVOH-oplossings het resultate daarop gedui dat die gemiddelde aantal elektrospinstrale per borrel moontlik beïnvloed kon word deur die polimeerkonsentrasie. In die geval van borrel-elektrospin van PAN-oplossing is

bevind dat polimeerkonsentrasie die borrelleeftyd en die gemiddelde aantal elektrospinstrale per borrel beïnvloed.

Resultate het ook getoon dat die viskositeit vermeerder en die oppervlakspanning afneem met toename in die konsentrasie van die sepe in beide die polimeeroplossings. Die PVOH-oplossing se elektriese geleidingsvermoë het vermeerder terwyl dit verminder in die geval van die PAN-oplossings met ‗n toename in die seepkonsentrasie. Tydens borrel-elektrospin van die PVOH-oplossings is beide borrelleeftyd en borrelgrootte beduidend beïnvloed deur die SLES konsentrasie. By die borrel-elektrospin van PAN-oplossings het die silikoonseepkonsentrasie nie ‗n beduidende invloed gehad op die borrelleeftyd en borrelgrootte nie. Oor die algemeen het die gemiddelde PVOH veseldeursnee afgeneem met toename in seepkonsentrasie.

Geen algemene tendens kon waargeneem word tussen die optimale oplossingswaardes vir borrel-elektrospin van die PVOH- en die PAN-oplossings onderskeidelik nie. Die gevolgtrekking is dat die viskositeit, elektriese geleidingsvermoë en oppervlakspanning nie die enigste beduidende waardes is wat bepaal of die borrel-elektrospinproses sal werk vir ‗n spesifieke polimeeroplossing nie.

Acknowledgements

I would just like to thank my promoter and co-promoter for their unending support and encouragement. I would also just like to thank the following people or companies for the role they played in bringing this study to a close:

- Electrospinning and nanofiber yarns group – for all the support, knowledge and laughs.
- MPak laboratories – for allowing me to use the equipment extensively. Thank you Pauline for always being willing to offer help.
- Ulrich Buttner – Thank you for all your technical support.
- Mr. Busson at GBX company – Thank you for always being ready to provide answers. Your assistance was irreplaceable.
- Staff in the 1st year Chemistry Building (Anthony and Gabriel) for always serving.
- NRF and CTFL SETA for funding. Thank you for making this study a possibility.

Table of Contents

Table of Figures

List of Tables

Chapter 1: Introduction

The handle of an everyday fabric, such as natural cotton or synthetic polyester, is largely based on the flexibility of a textile fiber.[2] The fiber diameters of synthetic fibers can be controlled during fiber manufacturing by simply altering solution or process parameters. Synthetic microfibers, fine fibers with a cross-section diameter range of 1 to 10 µm, are a recent development in the textile industry. The fineness of the fibers gives a textile handle that is softer than elegant silk fibers. In addition, microfiber textiles have unique technical properties such as water repellency whilst giving vapour permeability (breathability), due simply to a larger packing density of fibers per unit area.

Over the past two decades, researchers have managed to stretch boundaries in textile manufacturing, producing fibers with a cross section diameter of between 50 and 500 nm, called nanofibers. These fibers go beyond the unique technical properties provided by microfibers because of their even higher surface area to volume ratio. A range of nanofiber applications are shown in Figure 1-1.

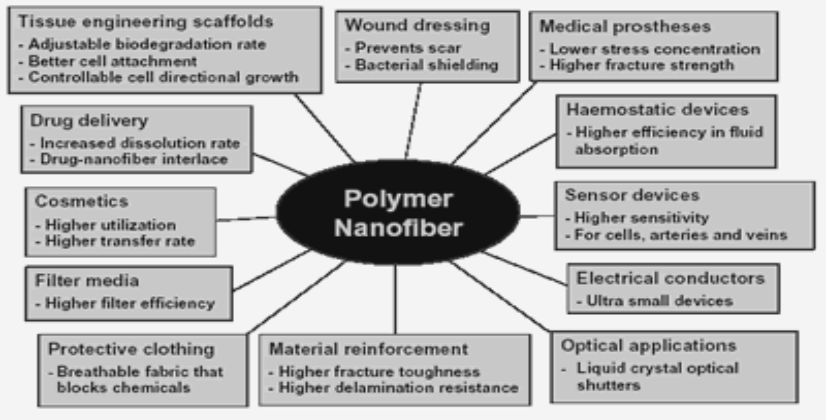

Figure 1-1: Applications of nanofibers. [3]

Nanofibers cannot be produced using ordinary fiber spinning techniques, e.g. melt-, wet-, and dry- spinning. Instead, an electrospinning phenomenon has been used since the early 1900‘s to spin very fine fibers from polymer solutions in the presence of a strong electric field.[4]

In the past two decades, research has focused primarily on electrospinning process development and innovative applications.[5-10] The needle-electrospinning process is a laboratory scale process that has a production rate of 0.1 – 1.0 g/h, depending on the polymer solution system.[1,11,12] The production rates are unfeasible for large-scale

production industries, especially when comparing the needle-electrospun nanofiber production rates to conventional fiber production rates. Thus far, a handful of nanofiber mass-production techniques have been developed to improve production rates of nanofibers.[1,11,13-23]

Bubble-electrospinning, in the presence of surfactants, is a nanofiber mass-production technique developed at Stellenbosch University. In his research, Smit [1] studied the influence of polymer and surfactant concentrations on the bubble-electrospinning process in terms of number of jets, production rates and bubble lifetimes for polyvinyl alcohol (PVOH) solutions. His work also briefly covered the bubble-electrospinning of Polyacrylonitrile solutions. It was suggested within Smit's study to investigate the influence of solution properties on the bubble lifetime in future research.

The novel bubble-electrospinning technique requires fundamental research on the influence of solution properties (viscosity, electrical conductivity and surface tension) on the entire bubble-electrospinning process. In addition, it is necessary to investigate the translational ability of the bubble-electrospinning technique across different polymer systems in order to mass-produce nanofibers from a large selection of polymer solutions in future.

1.1 Aims and Objectives

The aims of this study were to:

- Obtain better understanding of the influence of solution properties (viscosity, conductivity and surface tension) on the bubble-electrospinning process, in terms of bubble lifetime, bubble size, average number of jets and the resultant fibers.
- Compare the bubble-electrospinning of two polymer systems, polyvinyl alcohol (PVOH) and polyacrylonitrile (PAN) solutions, in terms of their solution properties.

The objectives of this study were as follows:

1. To define trends between solution properties and polymer- and surfactant-concentrations.
2. To investigate the influence of solution properties on needle-electrospun fibers for both polymer systems. The influence of solution properties were determined using fiber images, average fiber diameters and fiber diameter distributions.

3. To evaluate the influence of solution properties on the bubble-electrospinning process for both polymer systems. The influence of solution properties were determined using data from average bubble lifetimes, bubble sizes and average number of jets per bubble.
4. To evaluate the influence of solution properties on morphology of resultant fibers obtained from bubble-electrospinning of both polymer solutions. The influence of solution properties were determined using fiber images, average fiber diameters and fiber diameter distributions.
5. To determine whether two solutions would needle- and bubble-electrospin with similar surface tension, conductivity and viscosity values. The two polymer solutions were compared in terms of their solution properties, needle- and bubble-electrospinning process results, fiber quality and fiber production rates, all relative to their solution properties.

1.2 Chapter Description

Chapter 2: A literature study done on the fields applicable to this study. The chapter includes theory on the needle- and bubble-electrospinning process, as well as theory on polymer-solvent-surfactant interactions within solution.

Chapter 3: The experimental procedures chapter includes a list of materials and preparation of solutions. Solution property measurement procedures, needle- and bubble-electrospinning experimental procedures, and fiber analysis are described.

Chapter 4: Results and discussion is divided into five sections. Section one and two discuss solution properties and needle-electrospinning results concerning PVOH and PAN solutions, respectively. Section three and four discuss bubble-electrospinning results, the resultant fibers and fiber production rates. The last section draws comparisons between the bubble-electrospinnability of both polymer solutions.

Chapter 5: Conclusions drawn from this study based on the defined objectives of this study.

Chapter 2: Literature Study

This literature study covers the theoretical knowledge behind conventional needle electrospinning through to the novel bubble-electrospinning technique. This chapter includes theory on the influence of solution-, process- and ambient- parameters on the needle- and bubble-electrospinning process, as well as the influence of surfactants in bubble-electrospinning. The chapter is concluded with basic literature on Polyvinyl alcohol (PVOH) and Polyacrylonitrile (PAN) polymers.

2.1 Needle-Electrospinning

Nanofibers are continuous polymer filaments with diameters typically between 50 – 500 nm. These fibers are spun from a polymer solution exposed to a strong electric field, a process called electrospinning.[24-26] Other methods, such as self-assembly [27,28], phase separation [29,30] and even melt spinning [31,32], lack the simplicity and versatility of electrospinning. Electrospinning holds the potential to increase production rates of nanofibers to an industrial scale.[1,33]

The concept of electrospinning of polymer solutions was first introduced by Cooley [4] far back in 1902. In his study, fibers were spun from nitrocellulose solutions. The polymer solution flowed from a glass nozzle into an electric field. A solution jet ejected from the polymer solution droplet, was guided through an electric field using charged electrodes, and was collected onto a drum. The electrospinning phenomenon drew little attention at the time, not knowing that possible nanofibers were produced. Only a handful of patents were published between 1902 and 1960.

Taylor [34] made a large contribution in 1964 to today‘s knowledge of polymer solution droplets exposed to an electric field. His work explained droplet deformation prior to jetting during electrospinning.[34] Increasing numbers of patents followed Taylor‘s work, investigating the influence of solution-, process-, and ambient parameters on the needle-electrospinning process.[35] Today, and especially over the past two decades, there are thousands of papers concerning electrospinning and nanofiber applications.[9,10,36,37]

2.1.1 Needle-Electrospinning Set-Up

Figure 2-1 is an illustration of the basic electrospinning set-up. An explanation on the needle-electrospinning process is to follow.

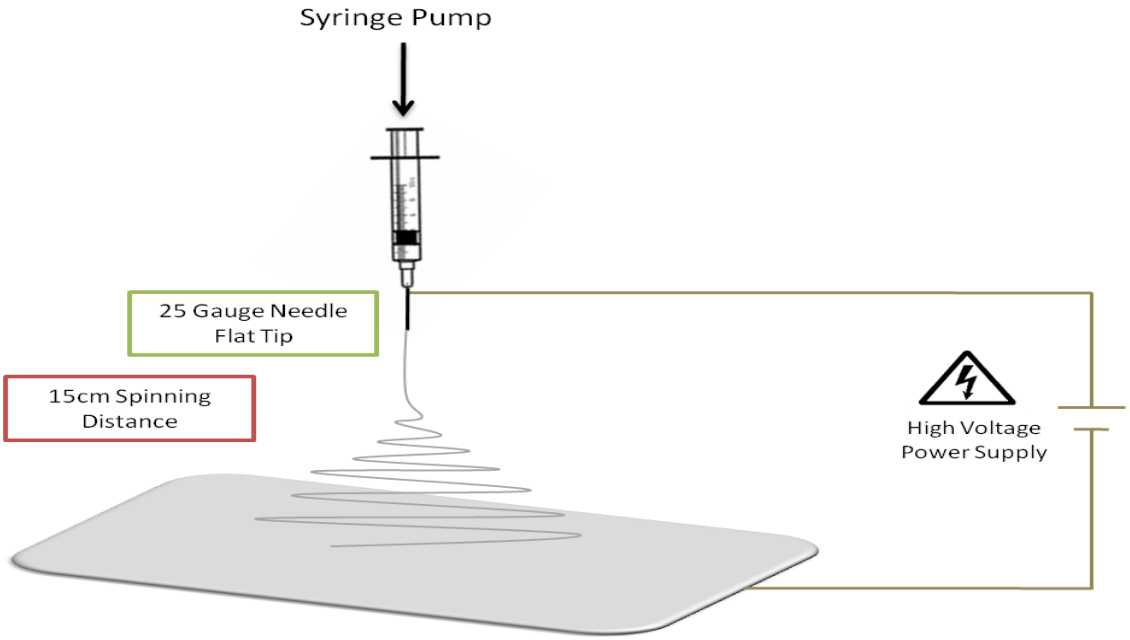

Figure 2-1: Needle-electrospinning set-up and process.

Polymer solution, consisting of a polymer dissolved in a suitable solvent, is placed in a syringe. A flat tip needle is attached to the syringe nozzle. The polymer solution flows to the end of the needle tip and forms a spherical droplet. One end of a copper wire is attached to the metal needle containing solution, whilst the other end of the copper wire is connected to the positive potential of a high voltage power supply.

The collector is placed approximately 15 cm away from the needle tip (the distance can be varied). The collector is either grounded or connected to the negative potential of the voltage source. The collector is also covered with a conductive sheet of foil. The syringe is pumped at a steady rate that provides continuous jet formation and minimal dripping.

2.2 Needle-electrospinning Process

The polymer solution forms a droplet at the end of the needle and is exposed to an electric field. A polymer solution droplet in an electric field experiences three competing forces:

1. The surface tension of the solution is a contractive force that aims to reduce the surface area of the droplet.
2. Like charges at the droplet surface repel each other. The charge repulsion forces result in expansion of the droplet surface.

3. Viscosity of the polymer solution, i.e. having a resistance to flow, resists sudden expansions or contractions.

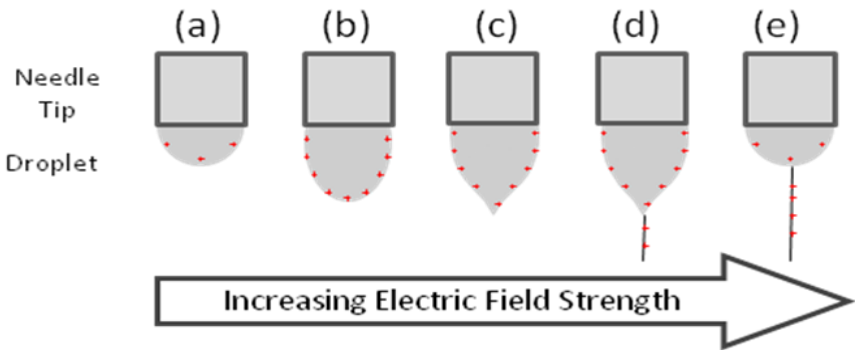

Figure 2-2: Process of droplet deformation in an electric field of increasing strength. Small crosses indicate the electric charge density at the droplet surface.

Figure 2-2 shows a charged polymer droplet exposed to an electric field of increasing intensity. In a weak electric field where positive voltage is applied to the solution, positive electric charges from the polymer solution move outwards towards to the droplet surface (Figure 2-2 (a)). Charge repulsion within the droplet increases as the electric field strengthens. The charge density on the droplet surface increases and the droplet deforms into an egg-shape (Figure 2-2 (b)). Further increases in electric field strength forces the droplet to deform into a pointed Taylor cone shape (Figure 2-2 (c)).[34]

Increasing the electric field strength further, the charge repulsion forces overcome the surface tension and resistance to flow of the solution. With sufficient chain entanglements in the polymer solution, a continuous polymer solution jet ejects from the droplet Taylor cone (Figure 2-2 (d)). The droplet relaxes immediately as charge is carried away from the droplet surface (Figure 2-2 (e)).

The jet elongates along a straight path towards the collector after ejecting from the solution droplet. The straight path is also referred to as the straight segment of the jet.[38] Once again, the same three opposing forces are at work on the solution jet. The surface tension of the solution continually attempts to contract and break up the jet into spherical droplets of smallest surface area whilst the like charges on the surface of the jet oppose such forces. In addition, the viscosity of polymer solution, and the chain entanglements of the polymer chains, resists the change brought about by surface tension and charge repulsion forces.

The charge density on the surface of the jet increases per unit area as the jet elongates within the straight segment. Repulsion forces begin to dominate over surface tension and

viscosity, and the jet becomes increasingly unstable. The jet starts to whip rapidly in the form of a downward expanding coil, the whipping often referred to as bending or whipping instability. Throughout the bending instability segment, solvent evaporates as the jet stretches and rapidly decreases in diameter.

The jet undergoes continuous destabilisation from repelling surface charges, resulting in coiling within the present coil (second degree bending instability). This coiling within a coil can repeat itself up to the point of fiber deposition (Refer to Figure 2-3).[24] As a result, dry, thin fibers deposit on the collector.

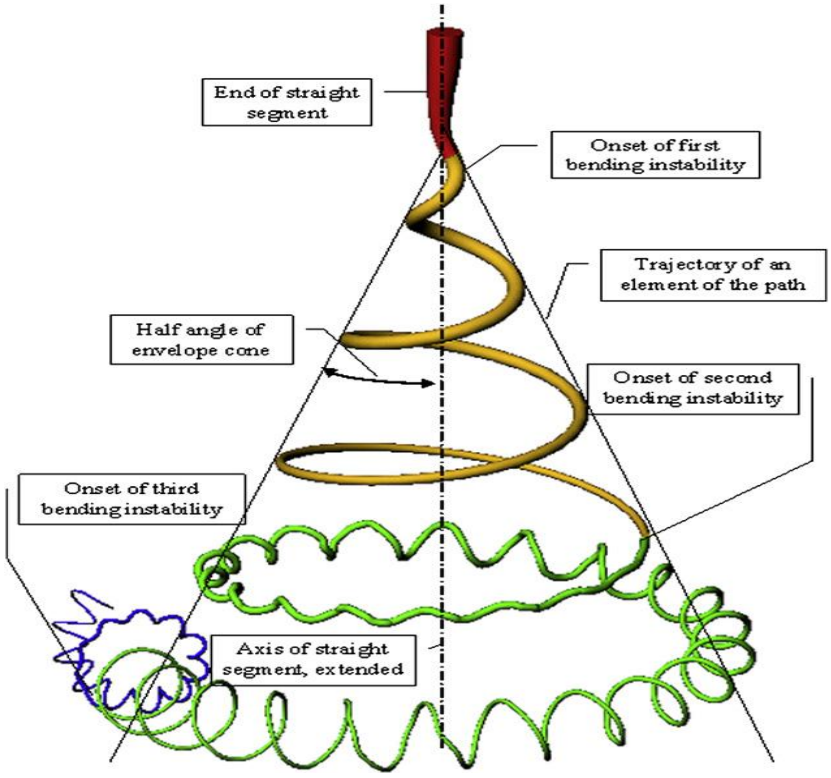

Figure 2-3: Bending instability of a polymer solution jet during electrospinning. The illustration shows bending instability of the jet up to the third degree.[24]

The needle-electrospinning process is a simple process but have numerous variables that control the process. It is tedious to discuss every variable that could possibly influence the needle-electrospinning process, thus only those factors which have the most significant influence on the electrospinning process are discussed.

2.3 Solution Parameters and Their Effect on Electrospinning

There are various controlled solution properties that influence the solution viscosity (resistance to solution flow), surface tension (contracting force), and the electrical conductivity of the solution (influences the charge density at droplet surface). These controlling parameters include polymer concentration, polymer molecular weight, solvent selection, presence of surfactants or other additives, and the solution temperature.

2.3.1 Solution Viscosity

The resistance to flow of any fluid is known as the solution viscosity. Polymer solutions, specifically, are made up of high molecular weight molecules solvated in a suitable solvent. The length of the chains, the concentration of polymer chains, and the interactions between molecules, be it polymer-polymer, polymer-solvent, polymer-additive, etc., all influence the rate of solution flow, i.e. solution viscosity.

During the electrospinning process, the solution jet travels along the straight segment and then undergoes bending instability. The jet experiences both contracting and repulsion forces from surface tension and like charges, respectively. At the same time the jet experiences drastic stretching. The resistance to solution flow along the jet influences the change brought about by the other two contracting and repelling forces. The higher the solution viscosity, the less the influence of contracting and expanding forces. Even more, the jet experiences stretching relative to the resistance to solution flow. The higher the solution viscosity, the less ability the jet has to elongate and the larger the resultant fiber diameters.

Viscosity of the polymer solutions can be increased by increasing the molecular weight of the polymer [39] and/or increasing the polymer concentration within a fixed solution volume.[40] Other influences on solution viscosity are the solvent system [41], additives, and the solution temperature.[42-44] The influences of these parameters are discussed further on in section 2.3.

2.3.2 Electrical Conductivity of a Solution

The electrical conductivity of a solution is its ability to facilitate the flow of charge through the solution, whether by the polymer molecules, solvent molecules, or even impurities. Solutions with zero conductivity cannot be electrospun. Highly conductive solutions require lower field strengths than poorly conductive solutions, to overcome the surface tension of a droplet and to form a continuous jet during electrospinning.

A high electrical charge density at the surface of the polymer solution jet during electrospinning applies resultant horizontal and vertical forces to the jet, expanding the surface area of the jet (Refer to Figure 2-4 below). Repulsion forces, along with the viscosity of the polymer solution, resist surface tension forces that aim to reduce the surface area and form spherical beads (discussed in section 2.3.3) along the jet length.

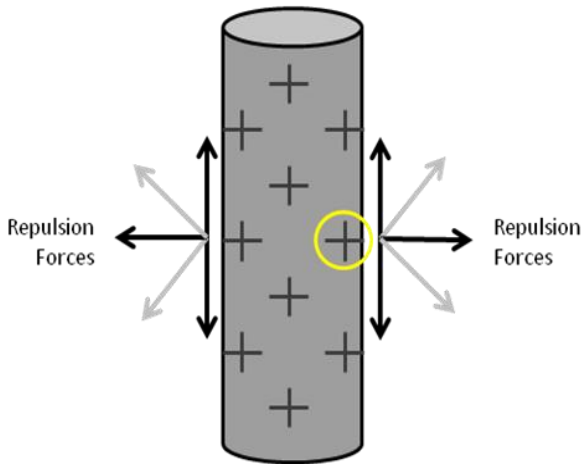

Figure 2-4: Repulsion of electrical charge along the polymer solution jet axis.

As the jet stretches along the straight segment during electrospinning, the charge density on the surface of the jet only increases. The jet begins to whip rapidly and thins at a rapid rate. A solution with high conductivity will have a shorter straight segment, i.e. bending instability starts earlier, than that of a poorly conductive solution. The charge repulsion forces acting on the jet dominate the other two mentioned forces, earlier. As a result, the resultant fibers will be thinner and more uniform.

Polymer solution conductivity can be increased either by changing the solvent system, increase in solution temperature or by addition of ions.

2.3.3 Surface Tension of a Solution

The surface tension of a solution is the strength of the interactive forces between molecules at the solution surface. A charged polymer solution droplet in an electric field deforms to a great extent before the surface tension is overcome and a jet is formed (refer to Figure 2-2). The lower the surface tension of a solution, the less charge density is required at the solution droplet surface to form a jet from a polymer solution droplet during electrospinning, assuming that all else remains constant.

The surface tension forces attempt to contract the jet surface into spherical shapes. Polymer chain entanglements prevent the jet from breaking up into droplets. Instead, small spherical beads form along the jet length, often referred to as beads on a string. The more the surface tension dominates over charge repulsion and viscosity, the more beading will occur. Beads-on-a-string is very common in low viscosity solutions.

The surface tension of a solution can be reduced either by adding surface active agents (surfactants) or increasing the solution temperature.

2.3.4 Influence of Polymer Concentration and Molecular Weight

Polymer molecular chains generally overlap and entangle in a polymer solution. As a result, the entangled polymer molecules in solution form a continuous jet when exposed to a strong electric field, such as in electrospinning. Polymer molecules of low molecular weight lack sufficient entanglement for continuous jets to form. Instead the jet breaks up into rows of droplets that ‗spray' towards the collector. This phenomenon is known as electrospraying.[45,46]

Throughout the jet elongation process in electrospinning, the entangled polymer molecules are stretched and forced to align with the pulling force. Highly concentrated polymer solutions, and/or solutions containing high molecular weight polymers, have a slower response to the elongating force acting on the entangled polymer chains. Hence, the chains orientate at a slower rate due to a high number of polymer chain entanglements. These polymer solutions are generally highly viscous. Polymer solutions with higher flow resistance result in fibers with larger diameters.[24,47]

Lower viscosity solutions align with the electric field pulling force. A low viscosity polymer solution results in an electrospinning jet that is more prone to be dominated by surface tension and charge repulsion forces.

2.3.5 Influence of the Solvent System

Various solvents are used to solvate polymers, but not all solvate the polymer to the same degree. When a polymer is placed in a ―good" solvent for a specific polymer, the solvent molecules interact with the polymer chains, overcoming the polymer-polymer interactions. The polymer swells in the solvent and eventually becomes a homogeneous solution. A poor solvent for a specific polymer, on the other hand, will fail to overcome polymer-polymer

interactions and fail to form a homogeneous solution. A solvent is primarily selected for its ability to solvate the polymer. [48,49]

Most polymers can be solvated in more than one solvent. It is therefore necessary to look at other variables concerning solvents that might influence the electrospinning process. In addition to being a good solvent, the solvent requires minimal conductivity. A polymer system that has no solution conductivity cannot be electrospun. As mentioned before, the conductivity of a solution influences the fineness and uniformity of the fibers to a large extent.

One of the factors influencing the solvent conductivity is the dielectric constant.[50] The dielectric constant of solvents plays a role in electrospinning, especially with poorly conductive organic solvents. The dielectric constant is the degree of polarization of the solvent molecules in an electric field. The higher the dielectric constant, the larger the degree of solvent molecule orientation and the greater the effect of the electric field applied to the system.[51]

The solvent must also be of the correct volatility. Highly volatile solvents could evaporate even before a jet has ejected from the droplet. Solvents that evaporate soon after jet formation prevent polymer molecules to orientate along the axis of the pulling force and for the polymer jet to elongate. Solvents that evaporate too quickly generally result in clogging of the needle. The resultant fibers will have larger diameters. Polymer solutions made up with low volatility solvents result in wet fibers depositing on the collector. An ideal solvent system for electrospinning evaporates slowly enough for maximum fiber elongation but undergoes sufficient evaporation for dry fiber collection.

2.3.6 Influence of Surfactants

Surface active agents, or surfactants, are most often used in aqueous solutions to reduce surface tension. Surface tension is reduced by a layer of surfactant molecules adsorbed at the water/air interface. A conventional hydrocarbon surfactant molecule consists of an apolar (often referred to as hydrophobic) tail and a polar (hydrophilic) head. The polar head has a strong affinity for water. The apolar tail orientates itself towards the water/air interface to minimise contact with water.

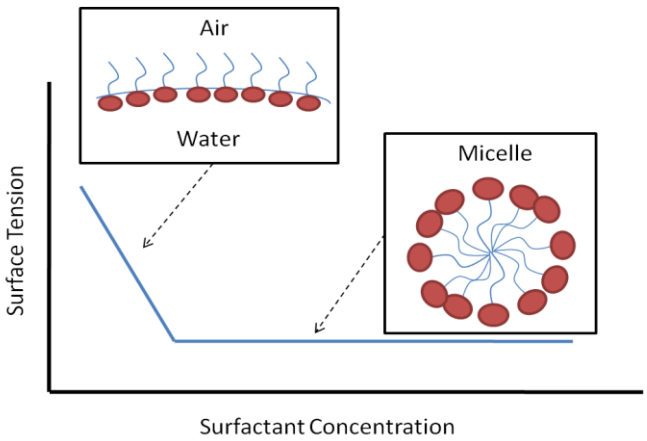

Figure 2-5: Behaviour of surfactant molecules in aqueous solution with increasing surfactant concentration.

Figure 2-5 shows the behaviour of surfactant molecules in an aqueous solution with increasing surfactant concentration. At a low surfactant concentration, the surfactant molecules migrate to the water-air interface. The interactions between the surfactant molecules are weak, lowering the surface tension of the solution. As the surfactant concentration increases, more and more surfactant molecules migrate to the solution surface until the solution surface becomes ―saturated" (Although literature uses the term ―saturation" it is understood that surfactant molecules are constantly adsorbing and desorbing to and from the interface, respectively). This point of saturation is known as the critical micelle concentration (cmc).[52]

In the case where the surfactant concentration is increased further, the surfactant molecules form micelles (refer to Figure 2-5). Micelles are groupings of surfactant molecules with the hydrophilic heads facing the water interface and the hydrophobic tails facing inwards. Micelles form to prevent the hydrophobic tail to come in contact with water molecules.

In a polymer solution, the surfactant molecules are also likely to associate with the polymer molecules via electrostatic and/or hydrophilic/hydrophobic interactions. Depending on the degree of interactions and the molecular weight of the surfactant, this interaction can significantly increase the solution viscosity.[53-55]

Electrospinning of solutions containing surfactants is expected to produce nanofibers with finer fiber diameters if the solution viscosity is not significantly increased by polymer-surfactant interactions.

2.3.7 Solution Temperature

An increase in solution temperature adds energy to the molecules in solution. More rapid molecular vibrations create space around the molecule in which the molecules can move more freely. The polymer molecules possess more energy to disentangle and orientate, reducing the viscosity of the solution.

Electrical conductivity of the solution increases with an increase in solution temperature. Molecules, carrying charge, move at a more rapid pace and so does the flow of charge. The polymer solution charge density at the droplet surface builds up more rapidly.[42,43]

Increases in solution temperature reduce the surface tension of the solution. The strong interaction between surrounding molecules at the surface lessen due to the more rapid movements of molecules. The charge repulsion forces overcome the surface tension more easily, thus, lower electric field strength is required for jet formation during electrospinning. [42,43]

Electrospinning a solution with a lower surface tension and viscosity, and a higher electrical conductivity, bending instability is prone to occur early along the straight segment. The polymer solution jet will whip rapidly over a further distance, in comparison to a solution with a high surface tension, high viscosity, and low conductivity (Refer to Figure 2-6). The resultant fibers from a high temperature electrospinning solution will have finer diameters than that of low temperature solutions.

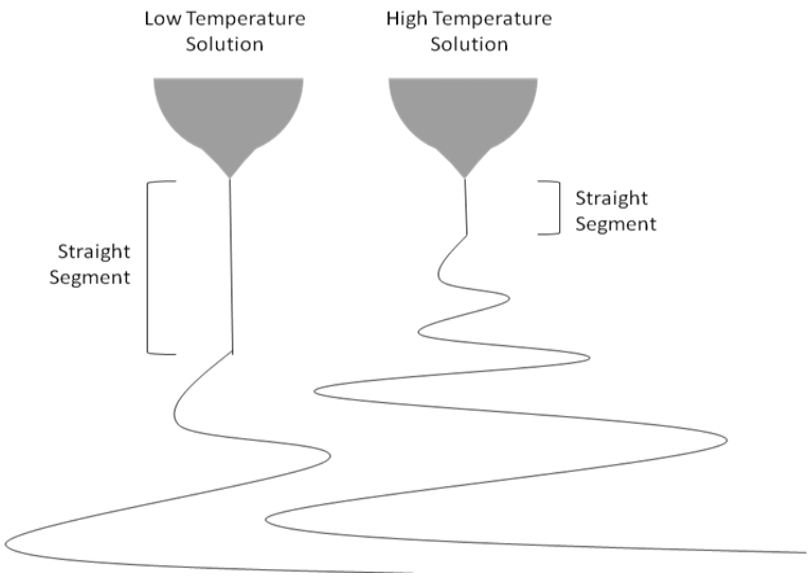

Figure 2-6: Length of the straight segment during the electrospinning of low and high temperature solutions.

2.4 Process Parameters and Their Effect on Electrospinning

Electrospinning process parameters are variables specific to the electrospinning set-up, including the voltage applied, the distance between the needle tip and collector, the feed rate, and the type of collector used. The processing parameters determine the strength of the electric field acting on the solution jet, which influences the degree of whipping instability, and hence the average fiber diameter, and sufficient solvent evaporation. The feed rate and collector type also influences the fiber diameter and resultant fiber mat, respectively.

2.4.1 Applied Voltage, Collector Distance and Electric Field Strength

An electric field is applied to an electrospinning setup between a polymer solution droplet and a collector. A positive voltage is applied to the polymer solution and a negative voltage is applied to the collector. Electric field strength (ε) is defined in terms of applied voltage (V) and the distance between the needle tip and the collector (d):

$$\varepsilon = V/d$$

The applied positive voltage to solution induces charges within the polymer solution. The positive charges in solution are repelled by the applied positive potential and flows through solution towards the droplet surface. Increases in applied voltage result in a higher electrical charge density at the droplet surface.

Repelling charges in solution force the droplet to increase its surface area. The droplet elongates towards the oppositely charged collector in the form of a Taylor cone. At sufficient applied field strength, the charge density at the droplet surface overcomes surface tension and the viscous flow of the solution and a jet ejects towards the collector.

At high electric field strengths, the charge density at the surface of the jet is high and results in more rapid whipping of the jet, producing finer and more uniform fibers. In the case where the electric field strength is too high and distance, d, is too small, the polymer solution jet has insufficient time to undergo sufficient whipping and solvent evaporation. As a result, wet fibers with large diameters deposit on the collector. The voltage, V, and the distance, d, between the polymer solution droplet and the collector, can thus be altered to create the ideal electric field strength that results in both efficient jet elongation and dry fiber collection.

2.4.2 Feed Rate

The term ‗feed rate' in needle-electrospinning refers to the rate at which polymer solution is pumped into the needle. The faster the feed rate, the more polymer solution is available for electrospinning. High feed rates give rise to a larger volume of solution being pulled away from the needle. The resultant fibers have larger fiber diameters and possibly beading due to insufficient solvent evaporation.[56]

At too low feed rates the Taylor cone literally disappears or even moves into the needle, resulting in discontinuous jetting from the polymer solution. The ideal feed rate in needle-electrospinning is the same rate at which solution is carried away from the droplet.[24]

2.4.3 Collector Material

A collector in electrospinning, be it stationary or in motion, is used to collect the deposited fibers. Teo, et al. [57] did a comprehensive review on different forms of collector materials that will not be discussed in this section. Rotating drum collectors, used for fiber collection during electrospinning, was the only collector of interest in this study. Figure 2-7 illustrates a typical rotating drum collector.

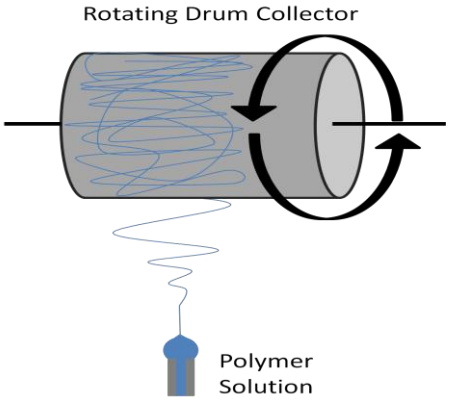

Figure 2-7: Rotating drum collector for electrospinning nanofiber collection.

Rotating drum collectors are commonly used to align and stretch deposited fibers collected after the electrospinning process. Fiber alignment increases with the rotation speed of the drum collector. High rotation speeds of the collector cause fibers to stretch resulting in reduced fiber diameters.[58] Rotating collectors can also facilitate further solvent evaporation.[59]

More importantly, rotating collectors eliminates the risk of backbuilding [60] of fibers from collector back to the droplet Taylor cone. A charged jet spins towards the closest possible

collection point. Hanging fibers on a stationary collector could serve as shorter-distanced collection points. Eventually the fibers collect downwards in the form of a yarn that stretches down to the Taylor cone, making it difficult to electrospin continuous dry fibers. Continuous rotation of the drum eliminates the possibility of self-assembly during fiber collection.

2.5 Ambient Parameters and Their Effect on Electrospinning

Ambient parameters, such as absolute humidity, atmospheric temperature, and the resultant relative humidity, play a significant role in electrospinning. Humidity can be described in terms of absolute humidity and relative humidity. Absolute humidity is the grams of water vapour per cubic meter volume of air. Relative humidity, on the other hand, is the water vapour in the air relative to the atmospheric temperature.[61]

The relative humidity gives an indication of moisture saturation in the air and is expressed as a percentage. Warm air can hold a larger volume of moisture in comparison to cool air; hence the relative humidity and vapour pressure will be lower at high air temperatures with the same amount of vapour in the air, in comparison with cool air.[62]

Moisture in the atmosphere surrounding the solution droplet and jet, conducts charge away from the jet, reducing the overall charge on the droplet and jet surface. In air with high moisture content, a stronger electric field is required to overcome the surface tension of the droplet and to eject a jet.[56]

Lastly, the rate of solvent evaporation in electrospinning is also increased with increasing air temperature i.e. increased heat energy.

2.6 Bubble Electrospinning

Bubble-electrospinning is carried out in a similar method to needle-electrospinning: A polymer solution is exposed to a strong electric field. As charge is increasingly built-up at the solution surface a Taylor cone is formed and, with further increases in charge density, a jet ejects from the Taylor cone. The jet travels along a straight path, the jet begins to whip rapidly, solvent evaporates as the jet thins rapidly, and dry fibers deposit on the collector.

The difference between the two methods is this: in bubble-electrospinning an air bubble is blown in a polymer solution. The bubble wall then plays the same role as the polymer solution droplet in needle-electrospinning. Figure 2-8 shows an image captured during a bubble-electrospinning experiment from this study.

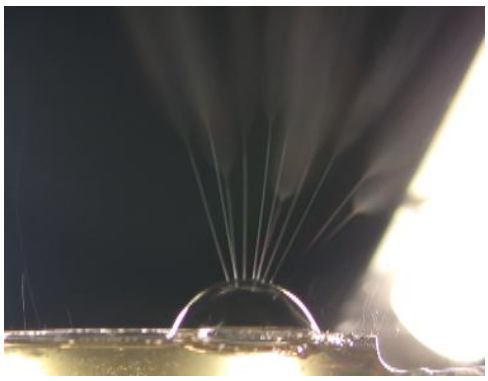

Figure 2-8: Bubble-electrospinning of PAN solutions. Image was captured during experiments done within this study.

2.6.1 Bubble Formation in a Polymer Solution

Polymer solutions used for bubble-electrospinning purposes generally consist of polymer, a solvent, and surfactant. The polymer solution is placed in a bowl that has an air inlet below the solution surface. Air is pumped into the polymer solution and an air bubble forms on the solution surface. Refer to Figure 2-9.

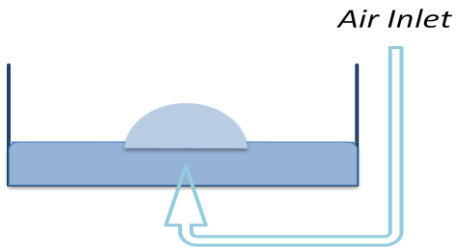

Figure 2-9: Bubble formation

If a bubble is blown in a solution that doesn‘t contain surfactant, the bubble is prone to instability. Drainage of the fluid down the bubble wall, evaporation of solvent, local vibrations or temperature variations along the bubble wall can create weak spots in the bubble wall.[63,64] Although these weaknesses form much slower in viscous polymer solutions than pure liquids, the weak spots eventually lead to bubble rupture if not stabilised or ~~–~~self-healed”.

2.6.2 Surfactants and Bubble Stabilisation

Section 2.3.6 described the influence of surfactants in polymer solution during needle-electrospinning. In needle-electrospinning surfactants are primarily used to lower the surface tension of solutions. In bubble-electrospinning surfactants are also used to stabilise the bubble by creating surface tension (γ) gradients along the bubble wall.

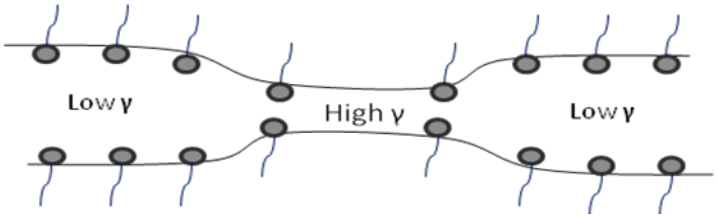

Figure 2-10: Description of a weak spot in the bubble wall. Surfactants are illustrated as a head and tail figure at the surfaces of the bubble wall. Areas of high and low surface tensions (γ) are shown.

Surfactant molecules are well known for their ability to stabilise bubbles. In the presence of surfactants, weak spots along the bubble wall bring about areas of low and high surface tensions. Refer to Figure 2-10. The surface tension gradient results in fluid flowing from areas of low surface tension to the areas of higher surface tension, i.e. to the weak spot areas along the bubble wall. The shape of the bubble wall becomes uniform and the bubble is stabilised. The process of bubble stabilisation is an ongoing process throughout the life of the bubble. The phenomenon is referred to as the Gibbs-Marangoni effect.[65,66]

The solution surface tension must be lowered sufficiently by surfactants to create a strong surface tension gradient along the bubble wall for bubble stabilisation. Surfactants containing a methylene tail, often referred to as hydrocarbon surfactants, lower the surface tension of aqueous solutions down to 30 – 40mN/m. An example of such a surfactant is sodium lauryl ether sulphate (SLES) (Refer to Figure 2-11).

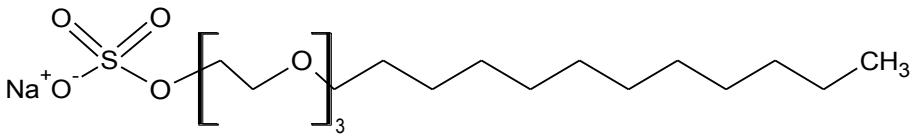

Figure 2-11: Sodium lauryl ether sulphate (SLES) surfactant.

The surface tension of an organic solvent (not containing surfactant) such as N,N-dimethyl formamide (DMF), has a surface tension of 37 mN/m. The surface tension value is similar to that of aqueous solutions already lowered by hydrocarbon surfactants (30 – 40mN/m). Hydrocarbon surfactants can therefore not effectively lower the surface tension of organic solutions.

Silicone surfactants differ from hydrocarbon surfactants in that the molecule consists of a hydrophilic, a lyophilic and a silophilic segment. A basic silicone surfactant, poly dimethyl siloxane (PDMS), is made up of a flexible siloxane backbone, masked off with methyl

pendant groups, essential in lowering the surface tension of solutions down to 20 – 30mN/m (Refer to Figure 2-12). [65]

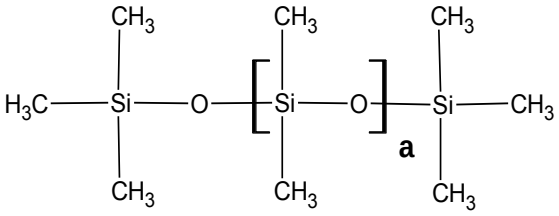

Poly Dimethyl Siloxane (PDMS)

Figure 2-12: Polydimethyl siloxane silicone surfactant.

Silicone surfactants behave similarly to hydrocarbon surfactants in the following ways:

1. The surface tension of the solution is reduced with increasing surfactant concentration, up to the critical micellular concentration (cmc). After the cmc is reached, the surface tension remains constant with further increases in surfactant concentration.
2. Both surfactants form micelles in solution and other forms of self-association.
3. Both surfactants behave similarly in foam stabilisation.

PDMS polymers specifically are often modified to perform a desired function (such as pro-foaming, anti-foaming, emulsifying etc.) within a particular solution system. A comprehensive review on silicone surfactant activity (In aqueous and non-aqueous systems), silicone surfactant modification and applications was done by Hill [67].

One such modification, applicable to this study, is silicone-polyether surfactants. These surfactants are generally used to stabilise foam in the polyurethane foam industry. The modified silicone surfactant is a silicone-polyether graft copolymer consisting of a PDMS backbone and polyether chains of polyethylene oxide (PEO) and polypropylene oxide (PPO) segments. Refer to Figure 2-13.

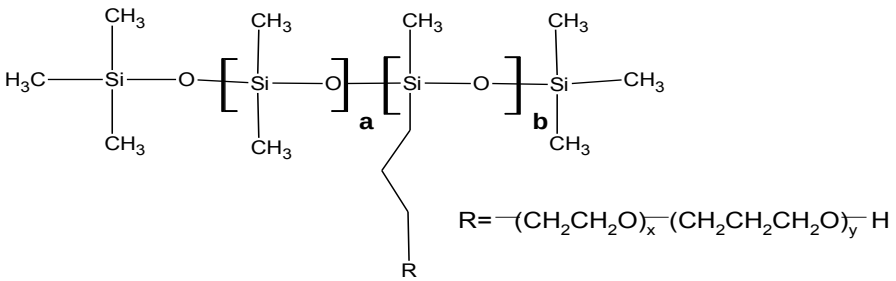

Silicone-Polyether Graft Copolymer Surfacrtant

Figure 2-13: Polyether silicone surfactant molecular structure.

The polyether segments are hydrophilic, with PEO more hydrophilic than PPO, whilst the PDMS backbone is hydrophobic. In highly polar and aqueous solutions the hydrophobic PDMS segment positions itself on the air side of the interface whilst the ether segments are anchored to the solution surface. Refer to Figure 2-14.

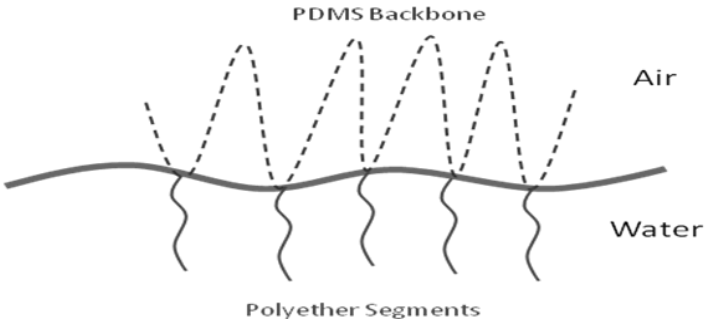

Figure 2-14: Positioning of silicone-polyether surfactant molecule at the water-air interface. The dotted line above water level symbolises the PDMS backbone whilst the solid line below water level symbolises the polyether segments.

Silicone surfactants have three unique properties that set them apart and make them superior to hydrocarbon surfactants. These unique properties enable silicone surfactants to lower the surface tensions of both aqueous and non-aqueous solutions to values as low as 20mN/m. The unique properties are listed below and are discussed in the paragraphs to follow.

1. A film of methyl groups at the interface
2. Flexible PDMS chain
3. Molecular Structure of the silicone surfactant

A film of methyl groups at the Water-Air interface

In Figure 2-15, a hydrocarbon and silicone surfactant have adsorbed to the water-air interface of an aqueous solution. In the case of the hydrocarbon surfactant molecule, the water-air interface of the solution is dominated by methylene groups. Silicone surfactants dominate the surface with methyl groups. Methyl groups have a much lower surface energy than the methylene groups. The methyl groups also cover a larger solution surface area per molecule than the hydrocarbon molecules.[67]

In general, a surface dominated by methylene groups (hydrocarbon surfactants) has a surface tension of approximately 30-32mN/m, whilst a surface dominated by methyl groups (silicone surfactants) has a surface energy of 20mN/m.[67]

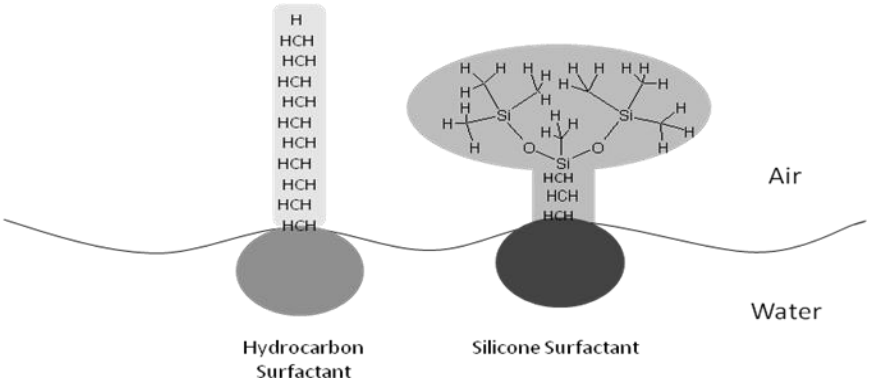

Figure 2-15: Hydrocarbon surfactant vs. silicone surfactant at the water-air interface. Hydrocarbon surfactants produce a methylene film on the surface. Silicone surfactant produces a methyl film on the surface.[67]

Flexible Poly Dimethyl Siloxane chain

De Jaeger, et al. [68] described the differences in bond lengths when four elements (silicon, carbon, oxygen and hydrogen) are i) bonded to carbon and ii) bonded to silicon. In all cases the bond lengths of elements bonded to silicon was larger than that of carbon. The length of the silicon-oxygen and silicon-carbon bonds, along with the weak interaction forces between the methyl pendant groups, results in a flexible PDMS backbone. The greater bond lengths also reduce barriers to rotation along the bond axis. The PDMS backbone can conform to the lowest possible energy configuration, giving the lowest possible surface tension at the water-air interface for silicone surfactants.

Molecular Structure of the Silicone Surfactant

Surface activity and solubility of the silicone surfactant can be carefully controlled by the ratio of PDMS units to polyether units and the ratio between PEO and PPO units. These two ratios determine the hydrophobicity and solubility of the silicone surfactant. Hill, et al. has extensively reported on this subject.[67]

Both hydrocarbon and silicone surfactants are used in this study to stabilise bubbles during bubble-electrospinning.

2.6.3 Deformation of Charged Stable Bubbles in an Electric Field

Air bubbles behave similar to droplets in an electric field. Hilton and van der Net [69] describe the influence of an electric field on a charged bubble. In the presence of a charged interface, droplets and bubbles will undergo similar deformations, only bubbles undergo these deformations on a much larger scale. Due to a larger surface area of the bubble, in comparison to a polymer solution droplet, a larger applied voltage is required to acquire

enough charge density at the bubble surface and to overcome the surface tension of the bubble.

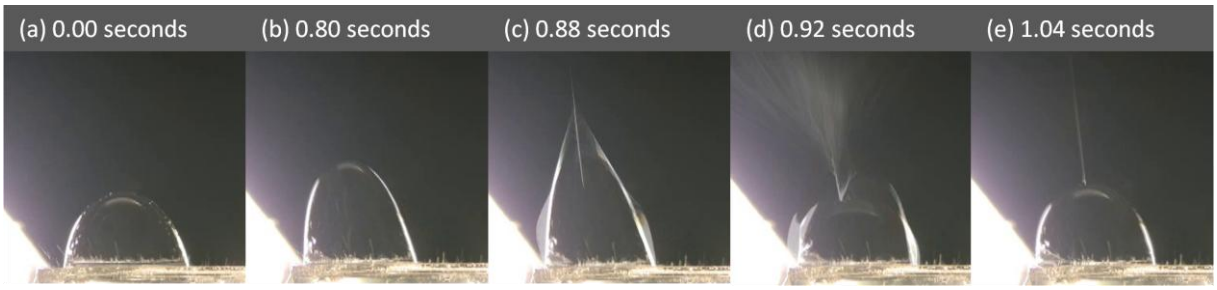

Figure 2-16: Influence of increasing charge density at the bubble surface. (a) Hemispherical bubble with a small charge build-up at the bubble wall; (b) The bubble takes on an egg shape as charge density increases. (c) Charge repelling forces overcome the bubble wall surface tension and a jet of fluid travels towards a grounded or oppositely charged surface (d-e) Bubble relaxes as charge is carried away from the bubble wall.

In an electric field the bubble wall experiences the same conflicting forces between charge repulsion and surface tension as a droplet in needle-electrospinning. The bubble elongates with increasing electric field strength (increasing charge density at the bubble wall) and takes on an egg shape (Figure 2-16 (b)). The increasing charge repulsion forces the bubble shape into a Taylor cone shape.[69] Eventually charge repulsion forces dominate the surface tension of the bubble. A jet of fluid shoots out of the Taylor cone and travels towards a grounded or oppositely charged surface (Figure 2-16 (c)).[15,70]

In the case of the mentioned fluid being a polymer solution, with sufficient polymer molecule entanglements, the ejected solution illustrated in Figure 2-16 (c) will result in a continuous jet of entangled polymer molecules as in Figure 2-16 (e). This process is similar to that of conventional electrospinning of a polymer solution.

In a bubble electrospinning process, a continuous polymer solution jet ejects from the highest point on the bubble surface, also referred to as the bubble cap.[1] Refer to Figure 2-16 (e) and Figure 2-17. The jet carries charge away from the bubble and therefore the bubble relaxes back into a hemispherical shape whilst jetting continues.

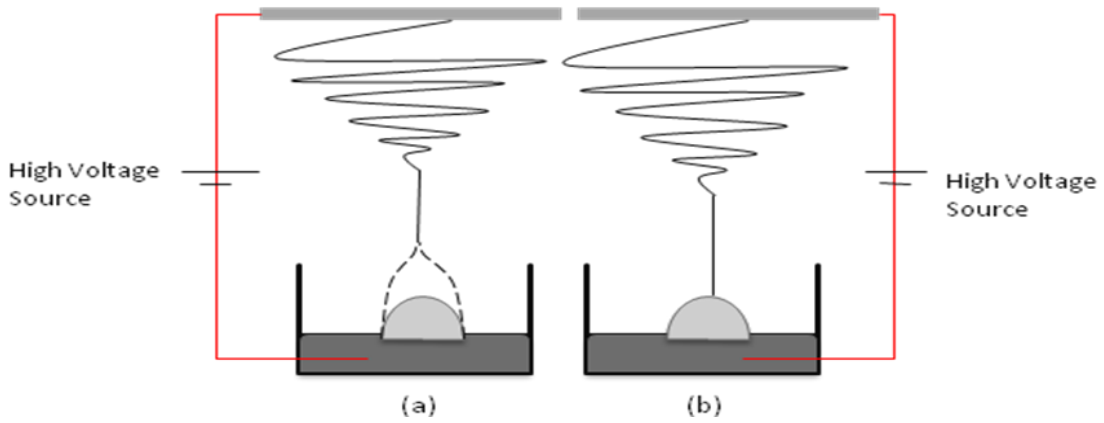

Figure 2-17: (a) Jet formation from the taylor cone and (b) bubble immediately returns back to hemispherical shape whilst jetting.

Similar to electrospinning from a small droplet, the jet ejects from the bubble and elongates along a straight segment. The jet becomes destabilised and undergoes rapid bending instability. Dry nanofibers collect on a grounded or oppositely charged surface.

2.6.4 Multiple Jets

Multiple jet formation is sometimes observed during conventional electrospraying at high electric field strengths and high flow rates of solution. Jaworek, *et al*. [45] described nine forms of liquid emission from a needle tip in an electric field. One such form was multi-jet formation.

Multi-jet formation during electrospinning often occurs from a cone-jet that is slightly skewed (Figure 2-18 (b)). The skewed jet moves to an unstable position at the needle rim, causing two or three more jets to form at the rim of the needle, distributed uniformly. The meniscus of the droplet becomes flat (Figure 2-18 (b-d)).

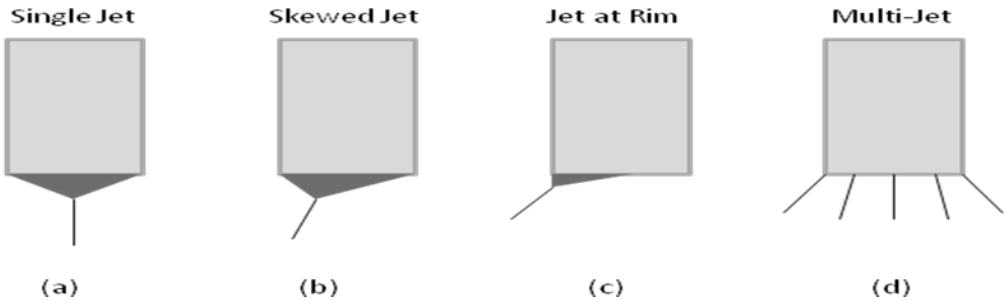

Figure 2-18: Multi-jet formation during electrospinning. (a) A stable single jet formation. (b) Skewed Jet. (c) Jet moves to the rim of the needle. (d) Multi-jet formation.[45]

Smit, *et al*. [1] studied multi-jet formation during bubble-electrospinning from a polymer solution. It was mentioned earlier that droplets and bubbles operate similarly in an electric field but that bubbles operate on a much larger scale. Bubbles used in bubble-electrospinning have a greater surface area than a droplet in conventional electrospinning, and thus more available space for multiple jets to form.

Polymer jets formed from a bubble surface undergo similar instabilities to jets formed from a polymer solution droplet in conventional electrospinning: A bubble surface becomes highly charged with increasing electric field strength, a Taylor cone forms, a continuous jet travels along a straight path (straight segment), the jet starts to whip rapidly (bending instability), fibers elongate and dry fibers deposit on the collector.

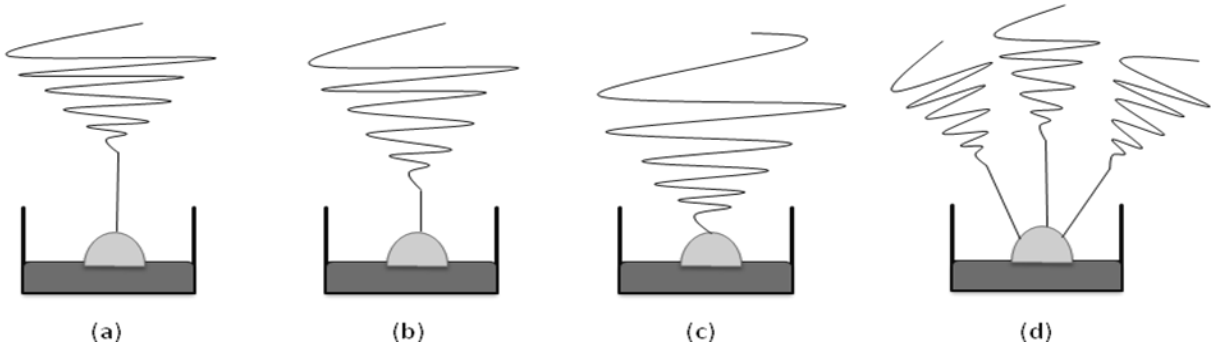

Figure 2-19: Multi-jet formation during bubble-electrospinning. (a) Single jet with a long straight segment prior to the bending instability phase. (b) Straight segment of jet shortens. (c) Bending instability starts on the bubble surface. (d) Multiple jet formation occurs immediately to distribute charge.

With increasing charge on the jet surface (Figure 2-19 (b)) the whipping instability will start sooner than in a jet with low charge density (Figure 2-19 (a)). In cases of increasingly high electric field strengths, the straight segment of the jet decreases in length until the bending instability appears to start directly on the bubble surface (Figure 2-19 (c)). When this happens, the jet splits and multiple jets form. Each jet carries a lower concentration of charge than that of a single jet (Figure 2-19 (d)).[1]

During multiple jet formation, the jets generally form on, or closely surrounding, the bubble cap. A single jet forms right at the centre of the bubble cap (Refer to Figure 2-20 (a)). As the number of jets increase, the jets repel other charged jets and so distribute themselves evenly over the bubble cap area (Refer to Figure 2-20 (b-e)). Larger numbers of jets pack even tighter, primarily forming on the bubble cap. The cap becomes overcrowded by the large number of jets causing jets to move out of the cap area into closely surrounding areas (refer to Figure 2-20 (f)).[1]

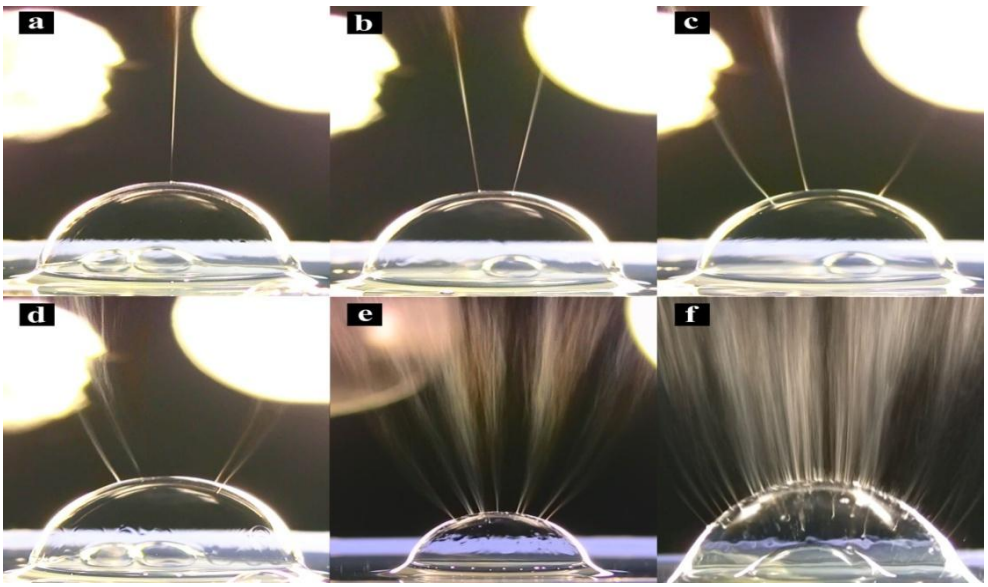

Figure 2-20: Images (a) - (f) illustrate a bubble surface with one to several Jets. The number of jets increase from (a) to (f).[1]

2.6.5 Bubble-Electrospinning Parameters

Detailed research has been done on the influence of solution-, process-, and ambient-parameters in conventional needle-electrospinning but there is only a small number of articles regarding the influence of these parameters in bubble-electrospinning.

In bubble-electrospinning, the applied voltage is shown to have a significant effect on both fiber diameters, similar to that in needle-electrospinning, and the number of jets per bubble. With increasing applied voltage, the charge density at the bubble cap increases and more jets are required to carry charge away from the bubble.[1,16,33]

Increasing polymer concentration, and hence increasing solution viscosity, has also been shown to have significant effect on bubble-electrospun fiber diameter. Average fiber diameters increase with increasing polymer concentration, similar to that of needle-electrospinning. [1,14]

Smit [1] has also shown that the number of jets per bubble increase with increasing solution conductivity.

2.7 Polymer, Solvent and Surfactant Interactions and the Resultant Effect on Solution Properties

The bubble-electrospinning process requires an appropriate polymer solution, and a surfactant that can significantly lower the surface tension of the solution. Each polymer-surfactant-solvent system interacts differently to another. The type of molecule (net molecular charges, molecular structures), and the interactions between molecules, has a significant effect on solution properties.

There are two specific polymers of interest in this study, each with a specific surfactant that is compatible with the solvent system. It is necessary to understand how these polymers behave within a specific solvent and in the presence of a specific surfactant.

2.7.1 Polyvinyl alcohol and Sodium Lauryl Ether Sulphate

Polyvinyl alcohol (PVOH) is a water-soluble polymer used to spin synthetic fibers (fiber cross-section diameter of 10 - 300µm) in the textile industry.[53,71-73] The polymer is produced from the hydrolysis of polyvinyl acetate, a process that converts acetate groups on the polymer backbone into alcohol groups. The chemical structure of the PVOH is shown in

Figure 2-21:

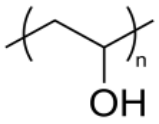

Figure 2-21: Molecular structure of polyvinyl alcohol

PVOH is also a polymer commonly used to produce nonwoven nanofiber mats. The fineness of the PVOH fiber mats are of interest in the filtration industry simply due to the high packing density of nanofibers and the good chemical and thermal properties of PVOH. PVOH nanofibers are also used in biomedical applications such as artificial organs, drug delivery and membranes for its good mechanical properties in its cross-linked form, and biocompatibility. [72,74]

It is well known that PVOH form gels in aqueous solution.[73,75,76] Gelling, common in a range of polymer solutions, can be described as a network of associated polymer chains. Gelling is caused by phase separation and partial crystallisation of polymer chains in solution.[75] The presence of gel directly influences the homogenous character, as well as

the viscosity, of the solution. The gelling rate of these polymer solutions is accelerated by lowering the polymer solution temperature, increasing the polymer concentration and/or polymer molecular weight, and also by selecting a poor solvent for a specific polymer.[75,77]

In PVOH solutions, polymer chains associate via hydrogen bonding with the same/other polymer molecules, as well as with water molecules and possibly with surfactants.[77] The surfactant of interest for this study, and specific to PVOH solutions, is an anionic surfactant, namely Sodium Lauryl Ether Sulphate (SLES).

Ionic surfactant molecules interact with the PVOH molecules via hydrophobic and/or electrostatic associations. At high surfactant concentrations (above the critical micelle concentration of the surfactant), the surfactant forms clusters along the PVOH polymer chain in the form of a pearl necklace.[53,75] The increased association between surfactant molecules and PVOH chains increases the viscosity of the solution and enhances the rate of phase separation and gelling.

PVOH polymer solutions were successfully bubble-electrospun by Smit [1] and Yang [15]. Smit used polymer solutions containing three different polymer and sodium lauryl sulphate (SLS) surfactant concentrations. Yang [15] used a single polymer concentration whilst varying the applied voltage.

2.7.2 Polyacrylonitrile and Silicone Surfactant

Polyacrylonitrile (PAN) has been electrospun in numerous studies and processing parameters have been investigated to a large extent.[78-80] PAN is soluble in organic solvents such as N,N-dimethyl formamide (DMF). The molecular structure of PAN is given below in Figure 2-22.

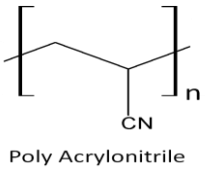

Figure 2-22: Molecular structure of polyacrylonitrile.

PAN is primarily electrospun as a precursor for carbon nanofibers used as composite material reinforcement, transportation, construction and electronics technology. Carbonization of PAN fibers is referenced but not discussed here. [79,81-83]

Smit, et al. [1] successfully bubble electrospun PAN/DMF polymer solution as an exploratory study. Polymer solutions at three different polymer concentrations, all containing JSYK 580 silicone surfactant, were bubble electrospun. Solvation of PAN in DMF solvent is brought about by polymer-solvent Interactions between the DMF dimethyl amino group and the PAN carbonyl groups.[84] The cyano group on the PAN repeat unit is a highly polar group and tends to also interact with surrounding cyano groups over time, eventually leading to gelling. [85,86] As mentioned before, gelling is a non-homogeneous distribution of polymer within solution which affects the solution properties of the solution.

To our knowledge there is thus far no published work that documents the interactions between PAN polymer and silicone surfactant and/or DMF solvent and silicone surfactant. It is expected that hydrophobic/hydrophilic interactions will occur between polymer-surfactant and solvent-surfactant molecules, similar to that of polymer-solvent interactions. Silicone surfactant, consisting of high molecular weight polymer chains, is expected to increase solution viscosity significantly with increasing interactions.

Chapter 3: Experimental Procedures

The solution properties (solution viscosity, conductivity and surface tension), the bubble-electrospinability (bubble size, bubble lifetime, number of jets per bubble), and the resultant fiber diameters of polyvinyl alcohol and polyacrylonitrile solutions was measured to gain understanding with regards to bubble-electrospinning. The details of materials used, solution preparations, procedures of i) solution property measurements; ii) needle-electrospinning; iii) bubble-electrospinning; and iv) average fiber diameter measurements; are all described in this chapter.

3.1 Materials

All chemicals were used as received from the supplier.

The two polymers used were Polyvinyl Alcohol (PVOH), M_w = 89 000 – 98 000 g/mol, 99% hydrolysed (Sigma Aldrich), and Polyacrylonitrile (PAN), M_w = 210 000 g/mol (Dolanit®, Acordis Kelheim GmbH). Distilled water was used as a solvent for PVOH and N,N-Dimethylformamide (DMF) (Chemically Pure, Kimix Chemical Supply) as a solvent for PAN. 25% Sodium Lauryl Ether Sulphate (SLES, 3 mole EO) surfactant (donated by Akulu Marchon) was used in the PVOH aqueous system whilst industrial Grade JSYK 580 (L580) Silicone surfactant (SouthernChem, Johannesburg) was used in the PAN organic system.

3.2 Preparations of polymer solutions

3.2.1 Polyvinyl Alcohol Solutions

PVOH was added to distilled water at room temperature and stirred for 5 minutes. The mixture was then stirred at 80 ˚C for 1 hour. SLES surfactant was added after cooling the solution. The new polymer solution containing surfactant was stirred for another 30 minutes at 80 ˚C to ensure homogeneity of the solution. The solution was cooled to room temperature whilst stirring.

3.2.1.1 Selection of Polymer and Surfactant Concentration Range

A large number of polymer and surfactant concentrations were bubble-electrospun as a pilot study (detailed description in Addendum A) to define a small polymer and surfactant concentration range within which PVOH solutions bubble-electrospun optimally. The

following polymer and surfactant concentrations were selected for further experiments, based on results found in the pilot study (refer to Table 3-1). All solutions were made in triplicate.

Table 3-1: PVOH solutions: List of polymer and surfactant concentrations selected for experiments.

PVOH Concentration (wt %)	SLES surfactant Concentration (x cmc*)
8	0.5
8	1
8	2
10	0.5
10	1
10	2
12	0.5
12	1
12	2

**cmc (SLES) = 0.0008 M*

3.2.1.2 Experimental Procedure

Pilot studies were done on the influence of time on the PVOH solution properties (described in Addendum C) to investigate the possibility of performing bubble-electrospinning experiments and solution property measurements at different time intervals.

It was concluded that the solution viscosity and conductivity could be measured at any point between 3.5 and 9.6 h after the solution was made. The surface tension had to be measured soon after the solution was bubble- and needle-electrospun. The solution preparation and measurement procedure for future experiments were based on the results from the pilot study in Addendum C. The procedure was as follows:

Solutions were prepared, as described in section 3.2.1, and allowed to cool. The bulk solution (100 ml) was separated into two containers of 80 ml and 20 ml. Each solution was heated to 80˚C for 30 minutes prior to any measurements.

Surface tension measurements, needle-electrospinning and bubble-electrospinning of PVOH solutions were done at 24 hours after making the solution (80 ml solution). Solution conductivity and viscosity was measured at any time between 3.5 and 96 hours after the

solution was made (20 ml solutions). All measurements took place within 3 hours after the solution was removed from the heated stirrer.

The solution viscosity and conductivity of all three solution sets (one set containing three polymer and surfactant concentrations) was measured. The surface tension of only one solution set was measured due equipment not being readily available.

3.2.2 Polyacrylonitrile Solutions

The preparation procedure of PAN/DMF/Silicone Surfactant solutions were as follows:

PAN was slowly added to stirring DMF at room temperature and stirred for 30 min. The polymer-solvent mixture was then stirred in a 50˚C oil bath for 1 hour. Silicone surfactant was added to the homogeneous polymer solution and stirred at 50˚C for a further 30 minutes. The solution was cooled to room temperature whilst stirring.

3.2.2.1 Selection of PAN and Silicone Surfactant Concentration Range

A wide range of polymer and surfactant concentrations were bubble-electrospun to select a small concentration range for future experiments within which PAN solutions spun optimally (pilot study described in detail in Addendum B). The following polymer and surfactant concentrations were used for experiments based on this pilot study (refer to Table 3-2).

Table 3-2: PAN solutions: List of polymer and surfactant concentrations selected for experiments.

PAN Concentration (wt%)	SLES surfactant Concentration (wt%)
5	0.5
5	1
5	2
6	0.5
6	1
6	2
7	0.5
7	1
7	2

3.2.2.2 Experimental Procedure

A similar pilot study to that referred to in section 3.2.2.1 was done on PAN solutions to investigate the influence of time on the solution properties (refer to Addendum D). Based on the results, it was concluded that the experimental procedure for future experiments should be as follows:

The prepared PAN solutions were used for solution property measurements, needle- and bubble- electrospinning 1h after the solution was made. No PAN solutions were reheated for measurements. All measurements and electrospinning took place within 3.5 hours after the solution was removed from the heated stirrer.

The surface tension of one solution set (one set containing 3 polymer and surfactant concentrations) was measured due to equipment not being readily available.

3.3 Solution property measurements

This section describes the equipment and procedures used for all solution viscosity, electrical conductivity and surface tension measurements. All solutions from both polymer systems were measured at 25 ˚C (± 1 ˚C).

3.3.1 Solution Viscosity Measurements

A Brookfield RVTD Viscometer, fitted with a small sample adapter, and a cylindrical spindle (nr.21) was used for viscosity measurements. Approximately 10 ml of solution was transferred to the small sample adapter, controlled at a temperature of 25 ˚C (± 1 ˚C).

The rotation speed of the spindle was varied according to the viscosity of the polymer solution. Solutions of the same polymer concentrations were measured at the same rotation speeds. Where possible, the rotation speed was kept constant for more than one polymer concentrations to improve the accuracy of viscosity comparisons. The viscosity reading was taken after remaining constant for approximately 1 minute. This is the reading recorded in data.

3.3.2 Surface Tension Measurements

A GBX Digital Droplet Contact Angle Analyzer (Digidrop) was used to measure the surface tension from solution pendant drops.

Figure 3-1 is a GBX Digital Droplet Contact Angle Analyzer. A syringe pump was used to place pressure on the syringe (containing solution) at a steady rate.

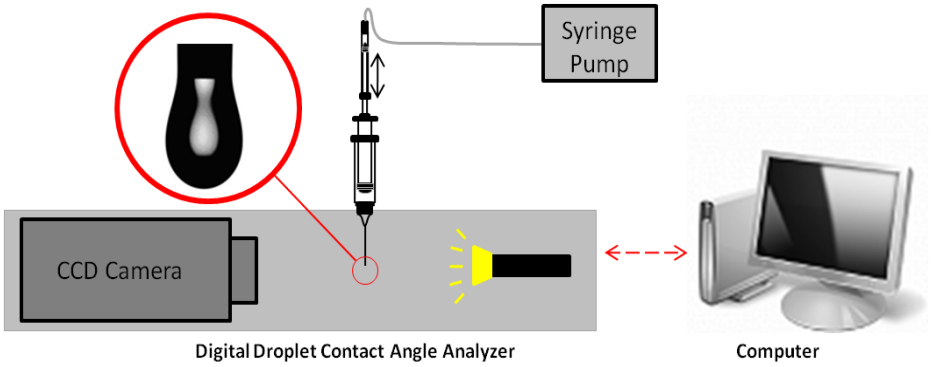

Figure 3-1: Digital Droplet Contact Angle Analyzer

A steady pump rate of 0.005 ml/min (PVOH solutions) and 0.0045 ml/min (PAN Solutions) was used to exert pressure on the syringe (containing solution). A 20 Ga blunt metal needle (Outer diameter: 0.96 mm) was used for surface tension measurements of PVOH solutions. A 20 Ga blunt Teflon needle (Outer diameter: 1.25 mm) was used for surface tension measurements of PAN solutions. The outer diameters of the needles were used for calibration purposes.

Polymer solution was carefully placed in the syringe (refer to Figure 3-1) preventing the formation of air bubbles in solution. The camera was then focused on a solution droplet at the tip of the syringe needle. The piston/syringe pump was switched on, allowing a minimum of 3 drops to form and break. Video recording of solution droplets commenced afterwards.

Five droplets per solution were recorded and analysed using GBX Digital Drop Contact Angle Analyzer Windrop++ software. The surface tension vs. time data was then exported to and analysed in Excel. Details on analysis procedures are described in Addendum E.

3.4 Conductivity Measurements

A Hanna Instruments, EC 215 Conductivity meter was used for electrical conductivity measurements. The calibration solutions were supplied by SPRAYTECH, EC84.

Calibration solutions were kept in a 25 ˚C bath prior to calibration. All residual water from washing was removed from the conductivity meter prior to every measurement. Solutions

were placed in a 25 ˚C (± 1 ˚C) water bath 15 minutes prior to measurements. A minimum of three conductivity measurements were taken per solution.

3.5 Needle-Electrospinning

A typical needle-electrospinning set-up requires a high voltage supply, a needle containing polymer solution, and a conductive collector. The needle-electrospinning set-up used in our experiments is shown in Figure 3-2. A Pump 33 Harvard Apparatus syringe pump was used for all needle-electrospinning experiments:

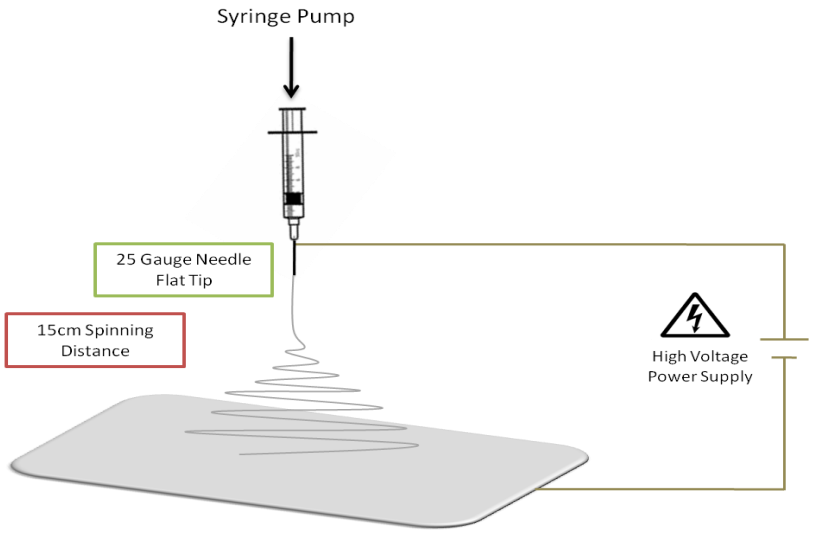

Figure 3-2: Needle-electrospinning set-up

The field strength between the needle (blunt tip, 25 Ga) and the collector was set at +10 kV/15 cm. The pump rate was controlled at constant 0.0035 ml/min for all solutions. The collector was a stationary sheet of foil.

All solutions were needle-electrospun at a room temperature of approximately 23 ˚C. The relative humidity was controlled between 41 and 49%.

3.6 Bubble-electrospinning of polymer solutions

Bubble-electrospinning requires a high voltage supply, a polymer solution bath with an air inlet, and a conducting collector. Figure 3-3 illustrates the small sample bubble-electrospinning bowl used as a solution bath for laboratory scale bubble-electrospinning. The air inlet is referred to on the right.

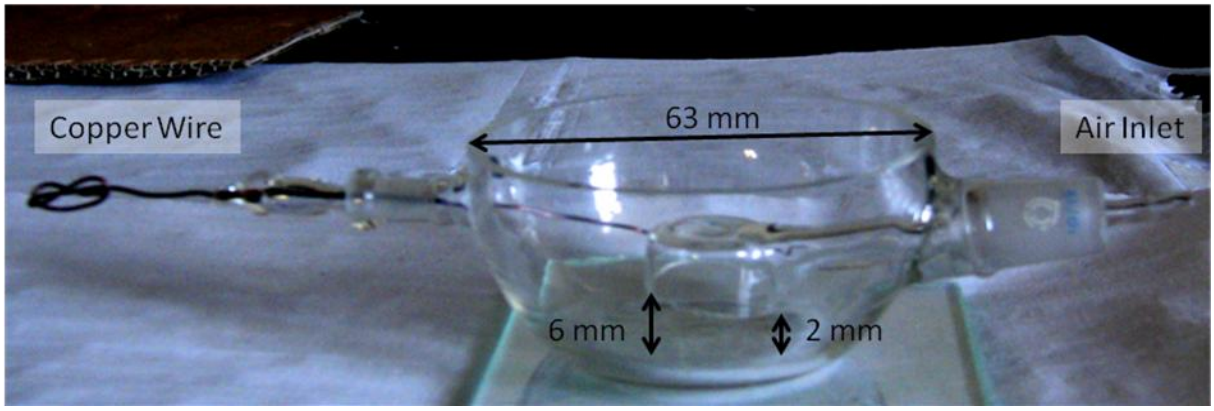

Figure 3-3: Small sample bubble-electrospinning bowl.

A positive voltage supply was attached to the copper wire. Tubing was attached to the air inlet of the small sample bubble-electrospinning bowl. The bowl was filled with polymer solution to the brim (approximately 80 ml solution).

Figure 3-4 illustrates the conductive drum collector used in bubble-electrospinning experiments.

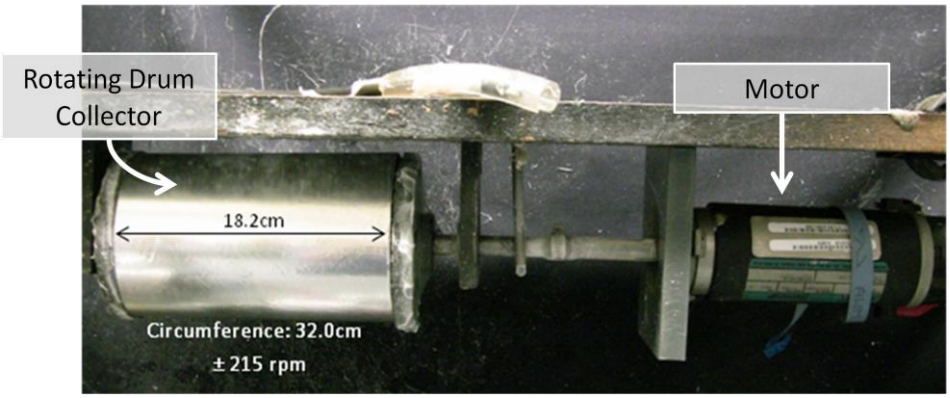

Figure 3-4: Rotating drum collector with a smooth layer of foil as collector material.

During bubble-electrospinning the rotating drum was attached to a negative voltage supply and rotated at approximately 215 rpm. The collecting material was a smooth sheet of foil. The bowl containing polymer solution was placed 15 cm below the rotating drum collector.

A clean sheet of foil was placed on the collector prior to bubble-spinning. At the beginning of the bubble-electrospinning experiments, voltage was applied between the small sample bubble-electrospinning bowl and the collector. The voltage applied during the bubble-electrospinning of PVOH solutions was 40 kV (22.5+ kV (bath); 17.5- kV (collector)), where as for PAN solutions the voltage applied was 35 kV (25+ kV (bath); 10- kV (collector)).

Afterwards 10 - 15 ml of air was pumped into the solution and a single bubble formed on the solution surface. Video footage was taken of 5 to 30 stable bubbles at constant spinning conditions. A second sheet of foil was placed on the collector. Fibers from a minimum of 5 bubbles were collected and imaged under a scanning electron microscope (refer to section 3.9).

Fibers collected were dried and weighed according to the procedure described in section 3.8. All solutions were bubble-electrospun at room temperature. The room temperature was controlled at approximately 23 ˚C. The room relative humidity was controlled between 41 and 49%.

3.7 Video Editing and Analysis: Bubble Lifetimes, Bubble Size and Average Number of Jets per Bubble.

A Canon HG 10 high definition digital video camera was used to record bubble-electrospinning experiments. Corel Ulead VideoStudio 11.5 Plus software was used for video analysis.

Bubble lifetimes were measured from the frame where the first jet ejects from a bubble Taylor cone up to the frame where the bubble ruptured. During the bubble-electrospinning of more viscous solutions, it was observed that the bubble would extend under the strong electric field and part of a stable bubble would break off from the rest of the bubble and travel towards the collector. The remaining bubble on the solution surface had a smaller diameter. The smaller remaining bubbles were immediately suppressed using a glass rod. Hence the bubble lifetime of the bigger bubble was measured between the point of Taylor cone formation and the partial breaking off of the bubble.

The bubble-electrospinning videos, cut into frames of 0.04 s each, were analyzed afterwards using the video analysing program. The bubble size was measured from a bubble in its stable hemispherical-shape state. The diameter of the bubble-electrospinning bowl was used as a reference. The average number of jets was calculated from an average of 10 video frames per bubble. The average number of jets per bubble was calculated from 5 bubbles or more.

3.8 Drying of fibers

Fibers were dried to determine the dry weight of fibers produced per single bubble in bubble-electrospinning. PVOH fibers were dried at room temperature for 24 hours. The room was conditioned at 18.6 ˚C and 53% relative humidity.

PAN fibers were soaked in distilled water for 10 minutes to remove residual solvent. The PAN samples were then allowed to drip-dry over night and dried at room temperature for a further 48 hours. The room was conditioned at 16.8 °C and 57% relative humidity.

3.9 Scanning Electron Microscopy (SEM)

A Leo® 1430VP Scanning Electron Microscope (SEM) – Central Analytical Facility, Stellenbosch University, was used to take SEM images of nanofibers.

Fiber samples were deposited onto a foil sheet during bubble electrospinning. The sample fibers and foil were cut out into 1 cm x 1 cm squares. The fibers on the foil backing were joined onto the SEM stub and sputter coated with gold prior to imaging. Each sample was imaged as follows: One image at 1500 times magnification and 3 to 5 images at 5000 times magnification.

3.10 Fiber diameter measurements

An imaging analysis program, SEM Image Studio, was used to measure the diameters of fibers. Approximately 100 fiber diameters were measured per sample. Bead diameters were measured where present. The average of the bead diameters were calculated separately from the average fiber diameters and listed where applicable.

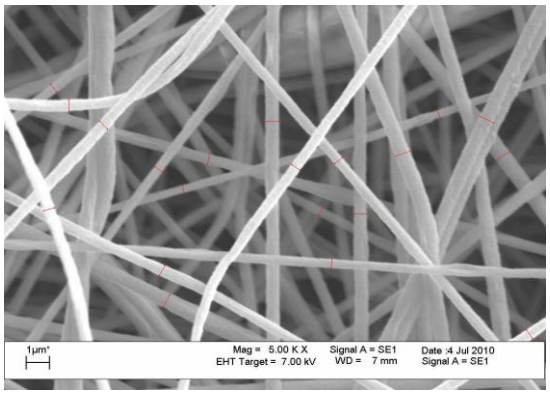

Figure 3-5: SEM image and fiber diameter measurements of a fiber sample. Fiber diameters were measured with SEM Image Studio to determine the average fiber diameter of the sample.

Chapter 4: Results and Discussion

The first aim of this study was to define a set of solution properties within which PVOH and PAN solutions bubble-electrospun. This aim was partially achieved in pilot studies in which solutions with a range of polymer and surfactant concentrations were bubble-electrospun and their properties measured. Narrower polymer and surfactant concentration ranges were then selected based on the ease of bubble-electrospinning and the resultant fiber qualities (Refer to Addendum A and B). These smaller ranges were used for more in-depth analysis on the bubble-electrospinning process.

A second aim was to better understand the comparison of bubble-electrospinability between two solutions with regards to their solution properties. The solution properties, needle- and bubble-electrospinning results related to the smaller polymer and surfactant concentration ranges are discussed in this chapter.

For the sake of comparison, this chapter is divided into four sections. The first two sections include solution properties (viscosity, conductivity and surface tension), needle-electrospinning results and discussions for PVOH and PAN solutions, respectively. The last two sections give bubble-electrospinning results and discussions for both PVOH and PAN solutions. The bubble-electrospinning results of both polymers are then compared in Chapter 5.

4.1 Polyvinyl Alcohol Solution Property and Needle-Electrospinning Results and Discussion

The solution properties are illustrated in sections 4.1.1 to 4.1.3. Section 4.1.4 illustrates needle-electrospinning results and results are then discussed in section 4.1.5.

4.1.1 Solution Properties: Viscosity

Figure 4-1 illustrates the influence of polymer and surfactant concentration on the viscosity of PVOH solutions used for bubble-electrospinning experiments.

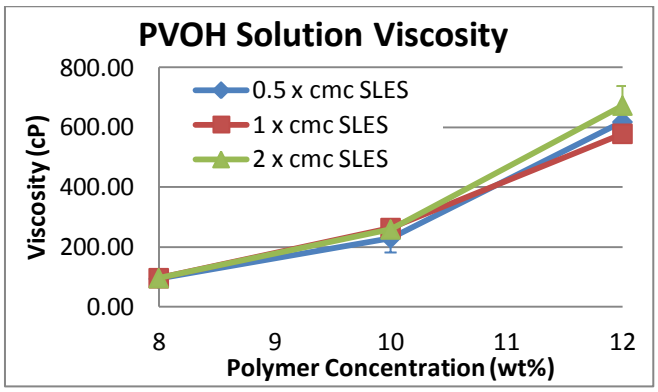

Figure 4-1: PVOH solution viscosity with increasing polymer and surfactant concentration.

From Figure 4-1 it was observed that the solution viscosity increased to a large extent with increasing polymer concentration, whilst only showing small increases (8 wt% PVOH solution showed no increase) with increasing surfactant concentration. Increasing solution viscosity with increasing concentration is a general trend found in electrospinning solutions.[57,87,88]

4.1.2 Solution Properties: Conductivity

The solution conductivity of the solutions is displayed in Figure 4-2.

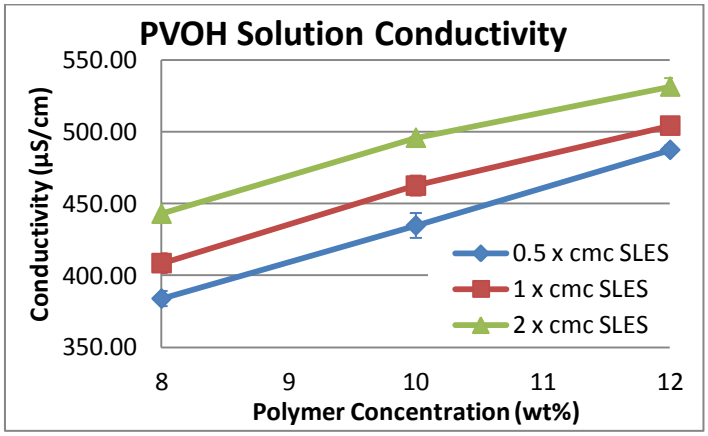

Figure 4-2: PVOH solution conductivity of bubble-electrospun solutions.

The solution conductivity showed larger increases with increasing polymer concentration than with increasing surfactant concentration. PVOH is a non-ionic polymer and the solvent used was deionised water. Thus, the increase in conductivity was largely attributed to an increase in impurities in solution carried by the bulk polymer. Impurities generally originate during the bulk polymer production process.[38] SLES is an anionic surfactant, increasing the solution conductivity with increasing concentration.

4.1.3 Solution Properties: Surface Tension

Figure 4-3 shows the solution surface tension of bubble-electrospun solutions.

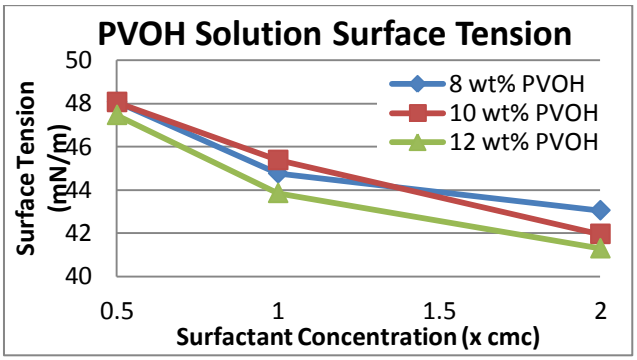

Figure 4-3: PVOH solution surface tension of bubble-electrospun solutions.

Figure 4-3 illustrates how the solution surface tension decreased with increasing surfactant concentration. The graph also shows that the polymer concentration appeared to have no apparent effect on the surface tension.

4.1.4 Needle-Electrospinning

All solutions were needle-electrospun at a field strength of +10 kV/ 15 cm. SEM images of fibers, average fiber diameters and the fiber diameter distribution are illustrated in sections 4.1.4.1 and 4.1.4.2. The results are then discussed in section 4.1.5.

4.1.4.1 SEM Images

As-spun PVOH fibers were imaged at 1500 x (left) and 5000 x (right) magnification. Images within a single set of figures are arranged by increasing surfactant concentration. Three separate figures (Figure 4-4 to Figure 4-6) are arranged by increasing polymer concentration.

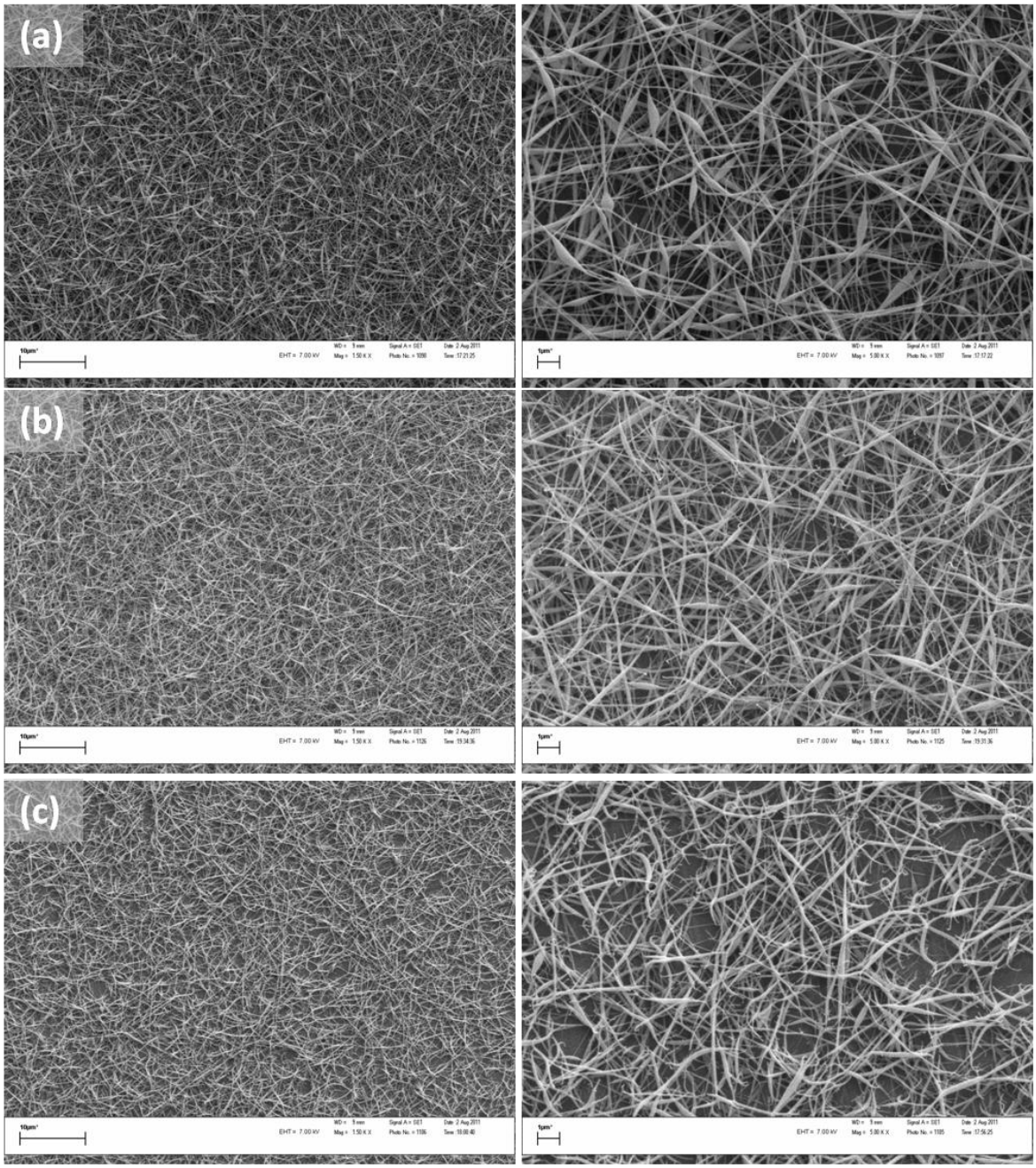

Figure 4-4: SEM images of needle-electrospun PVOH fibers at 1500x (left) and 5000x (right) magnification. Fibers spun from solutions containing 8 wt% PVOH and (a) 0.5 x cmc, (b) 1 x cmc, and (c) 2 x cmc SLES.

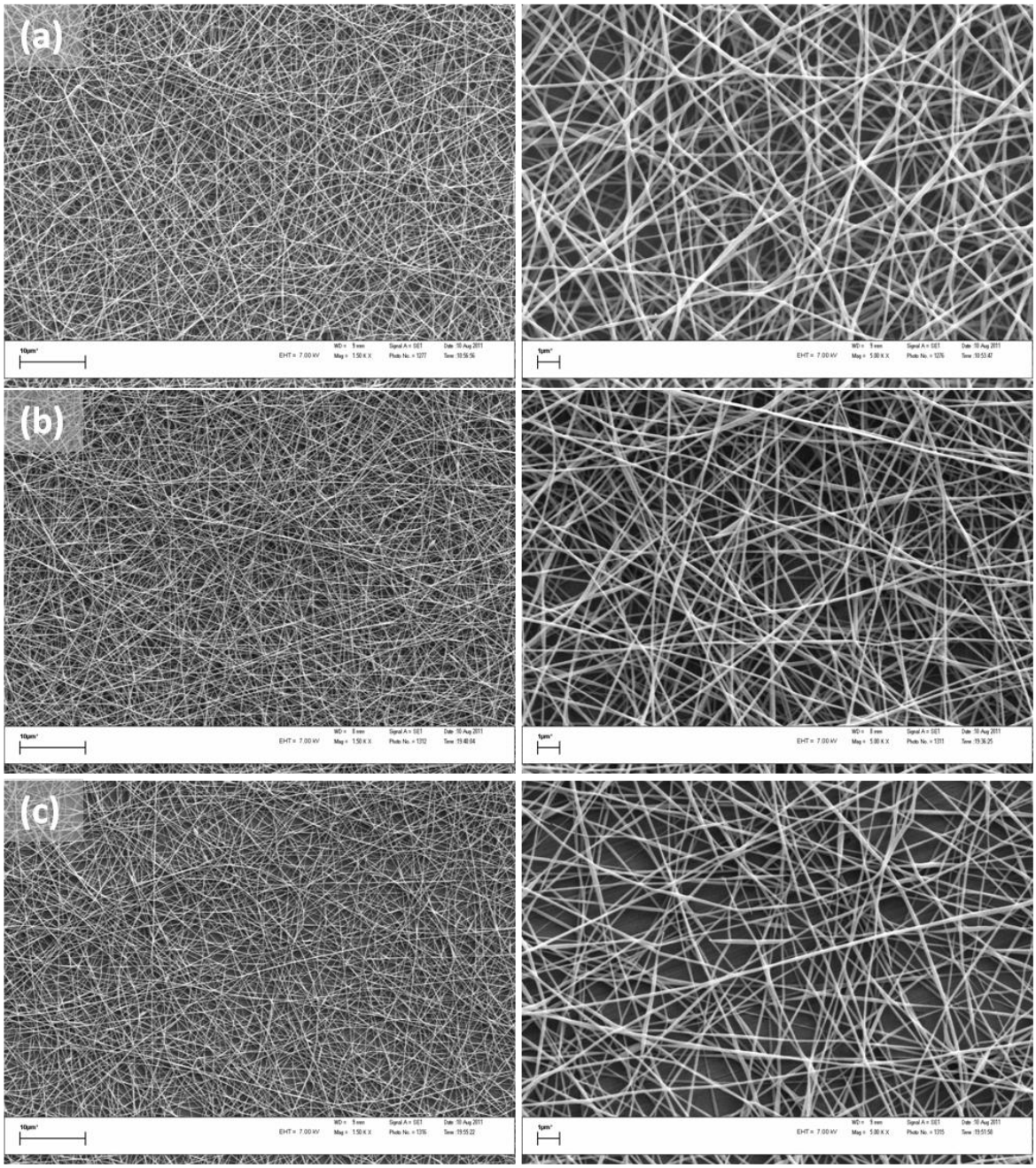

Figure 4-5: SEM images of needle-electrospun PVOH fibers at 1500x (left) and 5000x (right) magnification. Fibers spun from solutions containing 10 wt% PVOH and (a) 0.5 x cmc, (b) 1 x cmc, and (c) 2 x cmc SLES.

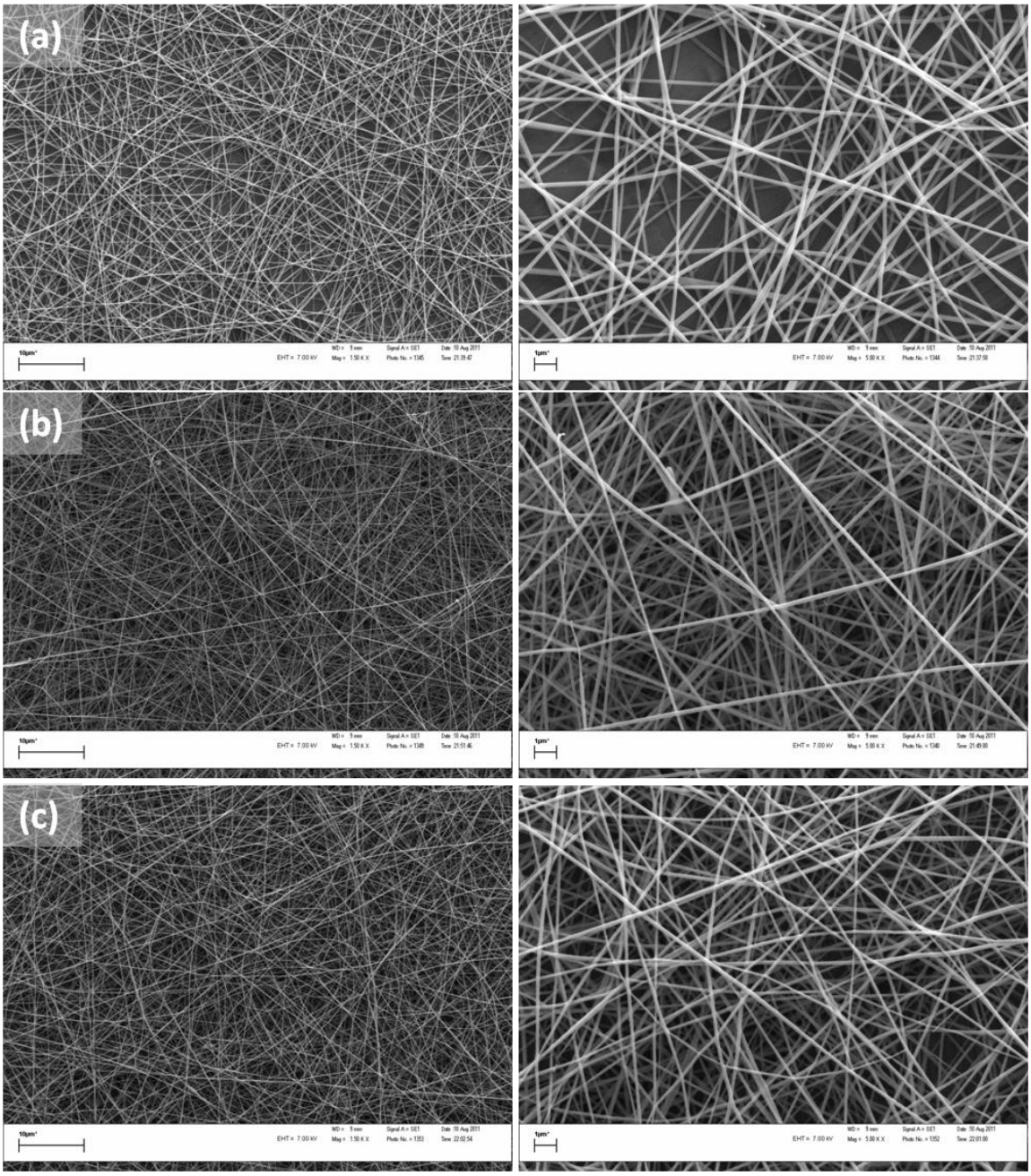

Figure 4-6: SEM images of needle-electrospun PVOH fibers at 1500x (left) and 5000x (right) magnification. Fibers spun from solutions containing 12 wt% PVOH and (a) 0.5 x cmc, (b) 1 x cmc, and (c) 2 x cmc SLES.

4.1.4.2 Average Fiber Diameters and Fiber Diameter Distribution

Figure 4-7 illustrates the average fiber and bead diameters from needle-electrospun PVOH solutions.

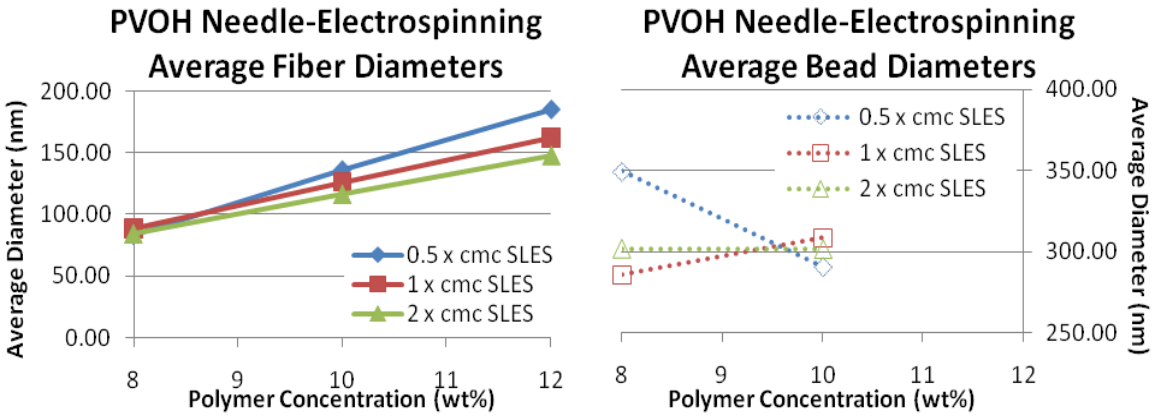

Figure 4-7: PVOH needle-electrospinning average fiber (left) and bead (right) diameters.

Figure 4-8 illustrates the fiber diameter distribution of needle-electrospun fibers.

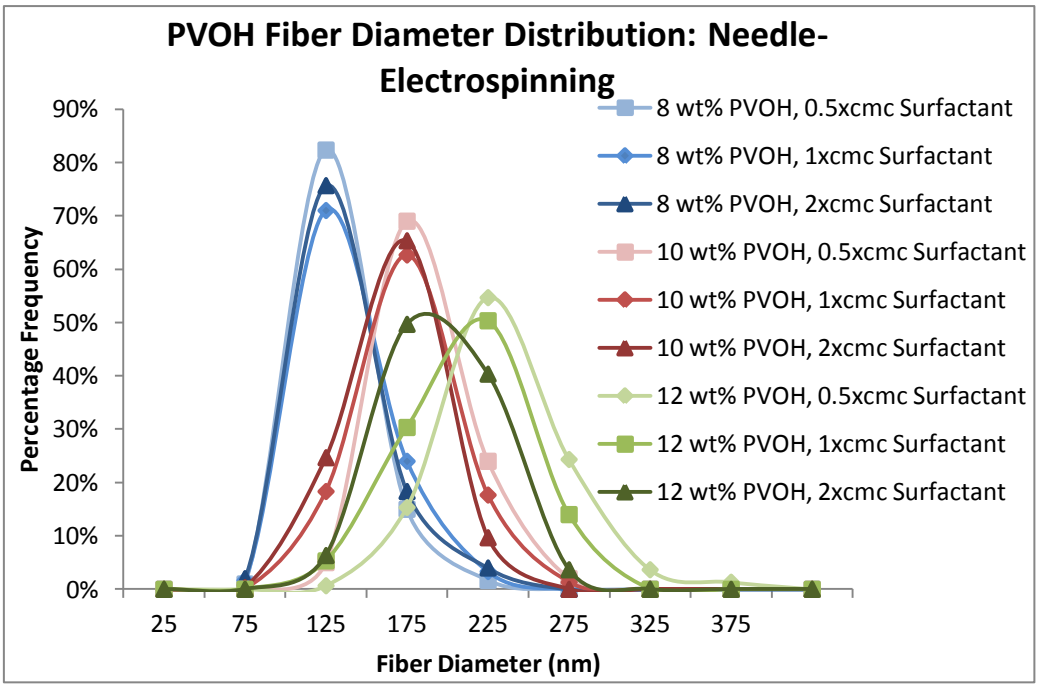

Figure 4-8: PVOH fiber diameter distribution: Needle-electrospinning.

4.1.5 Solution Properties and Needle-Electrospinning Results Discussion

The results illustrated in section 4.1.4.1 and 4.1.4.2 show trends with regards to the influence of solution properties on resultant needle-electrospun fibers. The SEM images indicated that the fiber diameter increased with increasing polymer concentration. The observation was confirmed by Figure 4-7 that shows that the fiber diameters increased with increasing polymer concentration. Based on solution properties described in section 4.1.1 it was expected that the fiber diameter would increase with increasing polymer concentration (increased solution viscosity).

It was also expected that low viscosity solutions would show a larger number of beads in comparison to solutions with a high viscosity. The expectation was confirmed in Figure 4-4 through to Figure 4-6, which shows that the number of beads was reduced with increasing polymer concentration. Figure 4-6 showed that no beads formed during needle-electrospinning solution containing 12 wt% PVOH.

It was also expected that solutions with high viscosities and high conductivities would form more uniform fibers. Although 10 and 12 wt% PVOH samples showed a reduction in the number of beads per sample, it was observed from Figure 4-8 that the fiber diameter distribution increased with increasing polymer concentration. The solution viscosity and conductivity increased with increasing polymer concentration. The two solution properties have opposing effects on the solution jet and hence, it was possible that the fibers showed an increase (viscosity has a larger effect) or decrease (charge repulsion has a larger effect) in fiber diameter depending on the distribution of charges and/or molecules within solution.

Figure 4-7 showed that the average fiber diameter decreased with increasing surfactant concentration. From section 4.1 results indicated that the solution viscosity increased slightly whilst the surface tension decreased with increasing surfactant concentration. Solution jets that have weaker surface tensions undergo more rapid whipping (charge repulsion forces dominate over the surface tension forces with more ease). The resultant fibers would have small fiber diameters, which was the case in Figure 4-7.

Figure 4-4 showed an interesting trend with regards to surfactant concentration. Fibers produced from solutions containing 0.5 x cmc surfactant, appeared to be continuous beaded fibers. As the surfactant concentration increased, the fine uniform fiber segments between cylindrical beads showed increasing amounts of breakage. Figure 4-4 (b) shows that the fiber breakage occurred after the fiber deposited on the collector. Refer to Figure 4-9. The arrows indicate some areas of fiber breakage.

From section 4.1.3 it was shown that the solution surface tension was reduced with increasing surfactant concentration. It is also shown that 8 wt% PVOH solution conductivity increased with increasing surfactant concentration, but the solution viscosity remained a constant low. It was expected that the number of beads would be reduced with increasing surfactant concentration due to a decrease in surface tension.

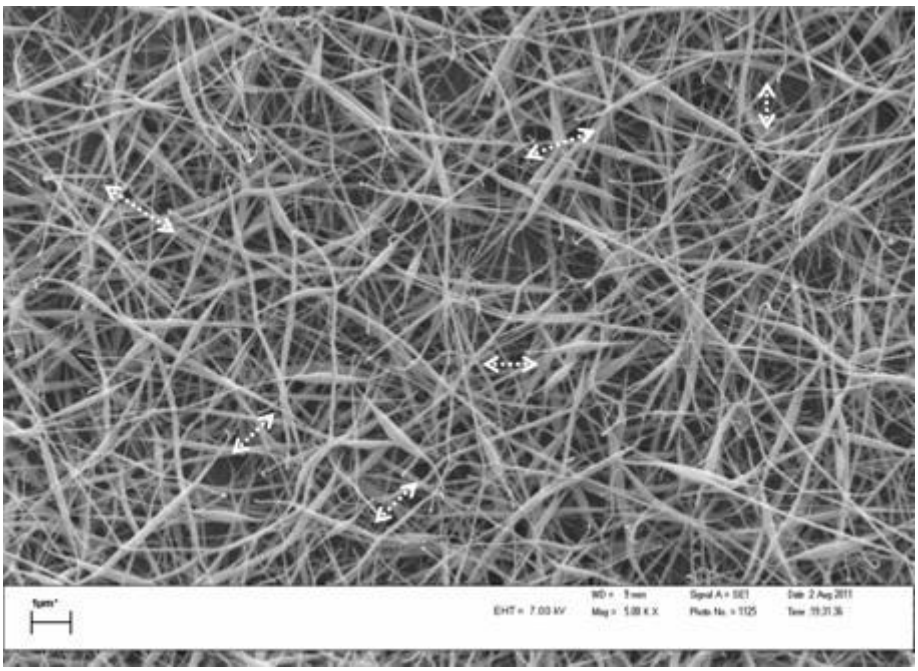

Figure 4-9: PVOH needle-electrospinning fibers containing 8 wt% PVOH and 1 x cmc SLES. The image illustrates cases of fiber breakage along fiber length.

It was found that the average bead diameter was reduced from fibers spun from solutions containing 0.5 to 1 x cmc surfactant. In addition, it appeared that charge repulsion forces had increasing dominance over the solution jet surface tension with increasing ionic surfactant concentration (surface tension decreased and the solution conductivity increased). As a result, the dominating charge repulsion forces stretched the solution jet so that the fine uniform fiber segments thinned (~60 nm fiber diameter). It was mentioned that the fibers appeared to only break after landing on the target. It was also observed that the underlying fibers remained intact. One possible explanation for this observation is that electrostatic repulsion between the residual charges on the already-spun fibers on the target, and the charges on the incoming electrospinning jet, could be sufficient to lead to breakage of the extremely fine fibers suspended across small gaps formed by underlying fibers.

4.2 Polyacrylonitrile Solution Property and Needle-Electrospinning Results and Discussion

4.2.1 Solution Properties: Viscosity

Figure 4-10 illustrates the influence of polymer and surfactant concentration on the solution viscosity.

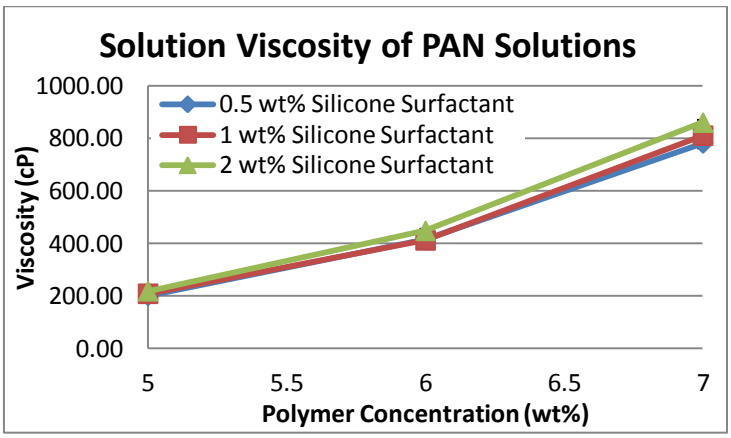

Figure 4-10: PAN solution viscosity with increasing polymer and surfactant concentration.

From Figure 4-10 it was observed that the solution viscosity increased with increasing polymer concentration. The solution viscosity also increases slightly with increasing surfactant concentration. The silicone surfactant molecules have a bulky molecular structure and so it was understandable that the surfactant concentration had a noticeable effect on the solution viscosity.

4.2.2 Solution Properties: Conductivity

Figure 4-11 shows the solution conductivity increased with increasing polymer and surfactant concentration.

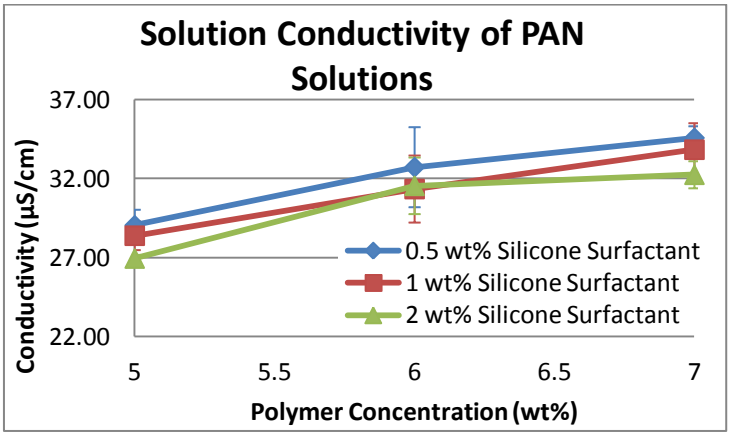

Figure 4-11: PAN solution conductivity with increasing polymer and surfactant concentration.

A general trend was observed in Figure 4-11 with regards to polymer concentration. The solution conductivity decreased insignificantly with increasing surfactant concentration. Both PAN and the silicone surfactants are non-ionic. The small increases in solution conductivity with increasing polymer concentration were possibly due to an increase in impurities carried by the polymer into solution.[38]

4.2.3 Solution Properties: Surface Tension

Figure 4-12 illustrates the trends in surface tension of PAN solutions in relation to increasing polymer and surfactant concentration.

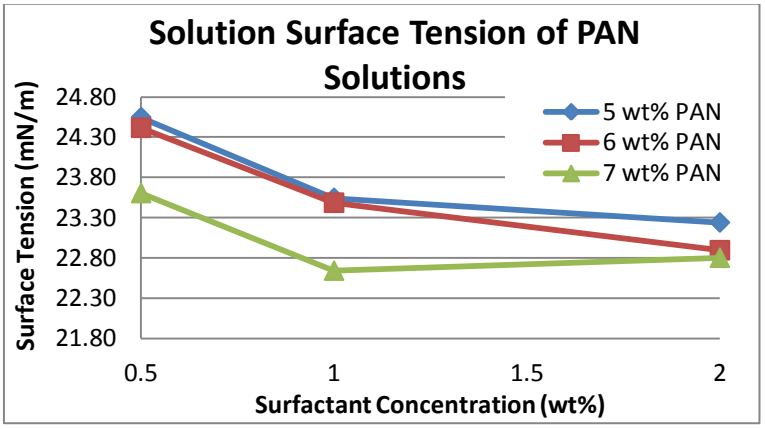

Figure 4-12: PAN solution surface tension with increasing polymer and surfactant concentration.

Figure 4-12 shows that the surface tension decreased with increasing surfactant concentration. Figure B-6 and Figure D-4 (addendum B and D, respectively) are additional graphs also illustrating the surface tension of PAN solutions with increasing surfactant concentration. These graphs also illustrate a decrease in surface tension with increasing surfactant concentration, confirming the above mentioned observations.

4.2.4 Needle-Electrospinning

PAN solutions were needle-electrospun at 10+ kV/15 cm onto a stationary sheet of foil. The fibers were imaged and fiber diameters measured. The fiber images, average fiber and bead diameters, as well as fiber diameter distributions, are shown (section 4.2.4.1and 4.2.4.2) and discussed (section 4.2.5) here.

4.2.4.1 SEM Images

SEM images of as-spun PAN fibers were taken at 1500x (left) and 5000x (right) magnifications and are illustrated in Figure 4-13 through to Figure 4-15.

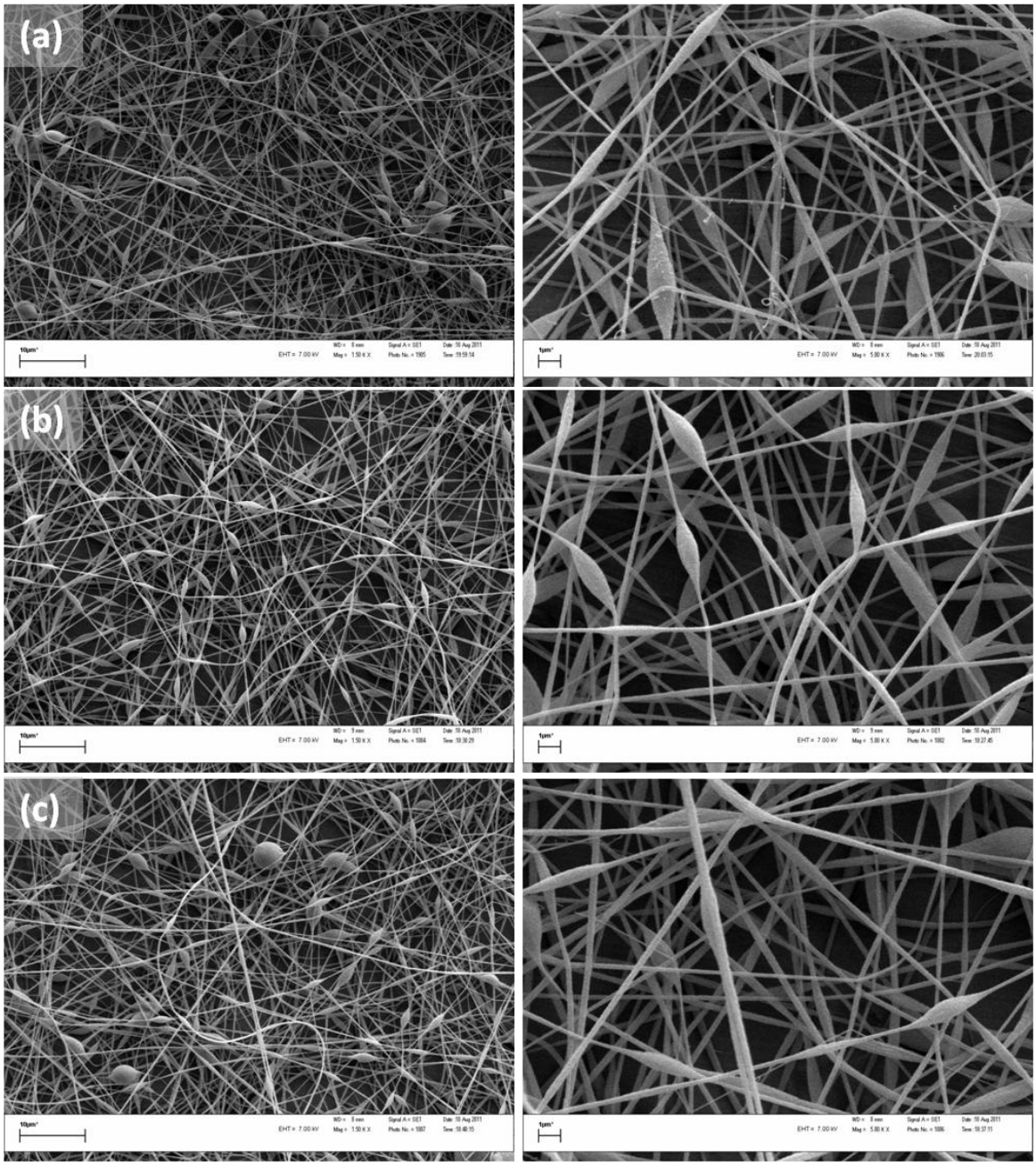

Figure 4-13: SEM images of needle-electrospun PAN fibers at 1500x (left) and 5000x (right) magnification. Fibers spun from solutions containing 5 wt% PAN and (a) 0.5 wt%, (b) 1 wt%, and (c) 2 wt% silicone surfactant.

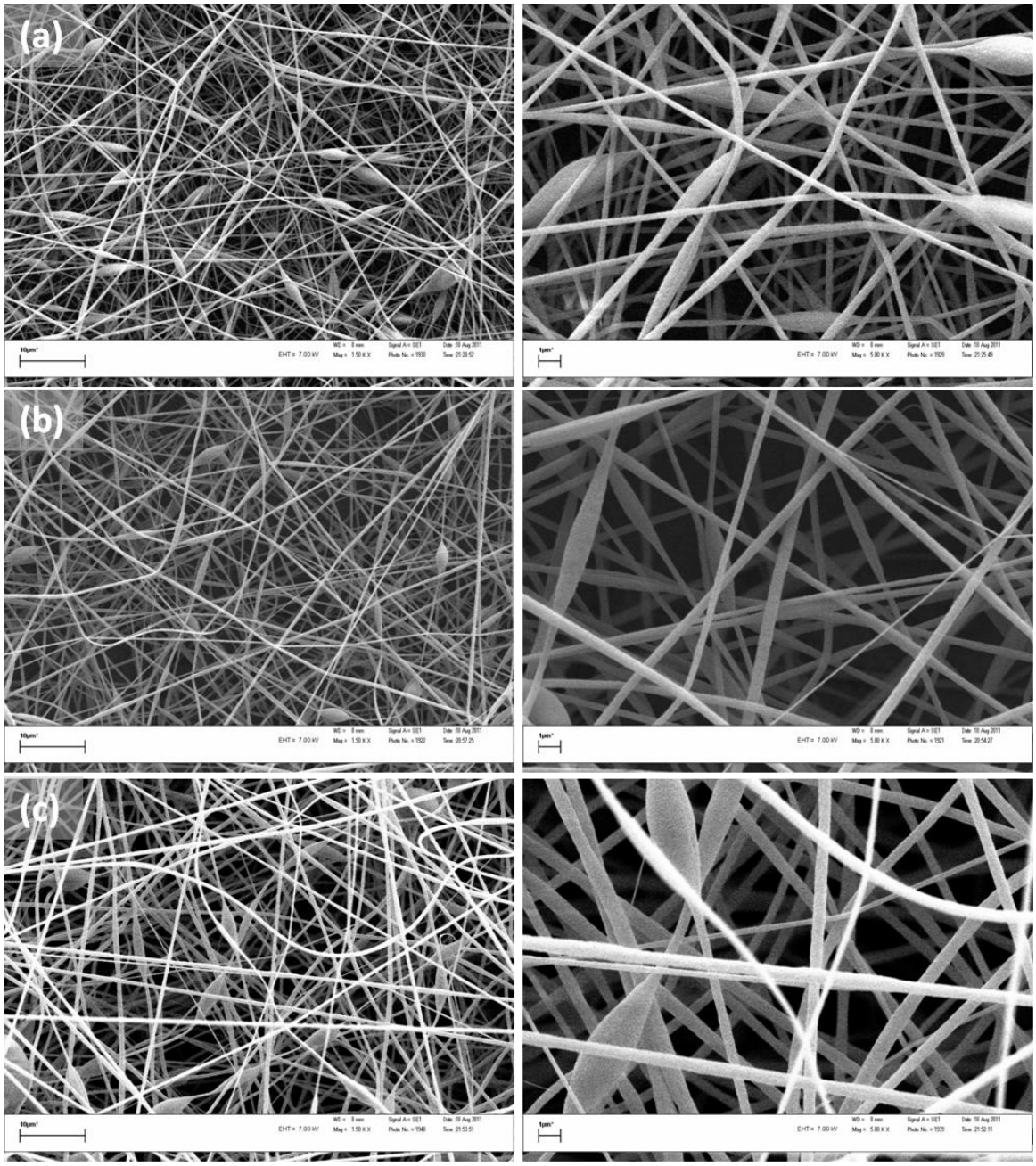

Figure 4-14: SEM images of needle-electrospun PAN fibers at 1500x (left) and 5000x (right) magnification. Fibers spun from solutions containing 6 wt% PAN and (a) 0.5 wt%, (b) 1 wt%, and (c) 2 wt% silicone surfactant.

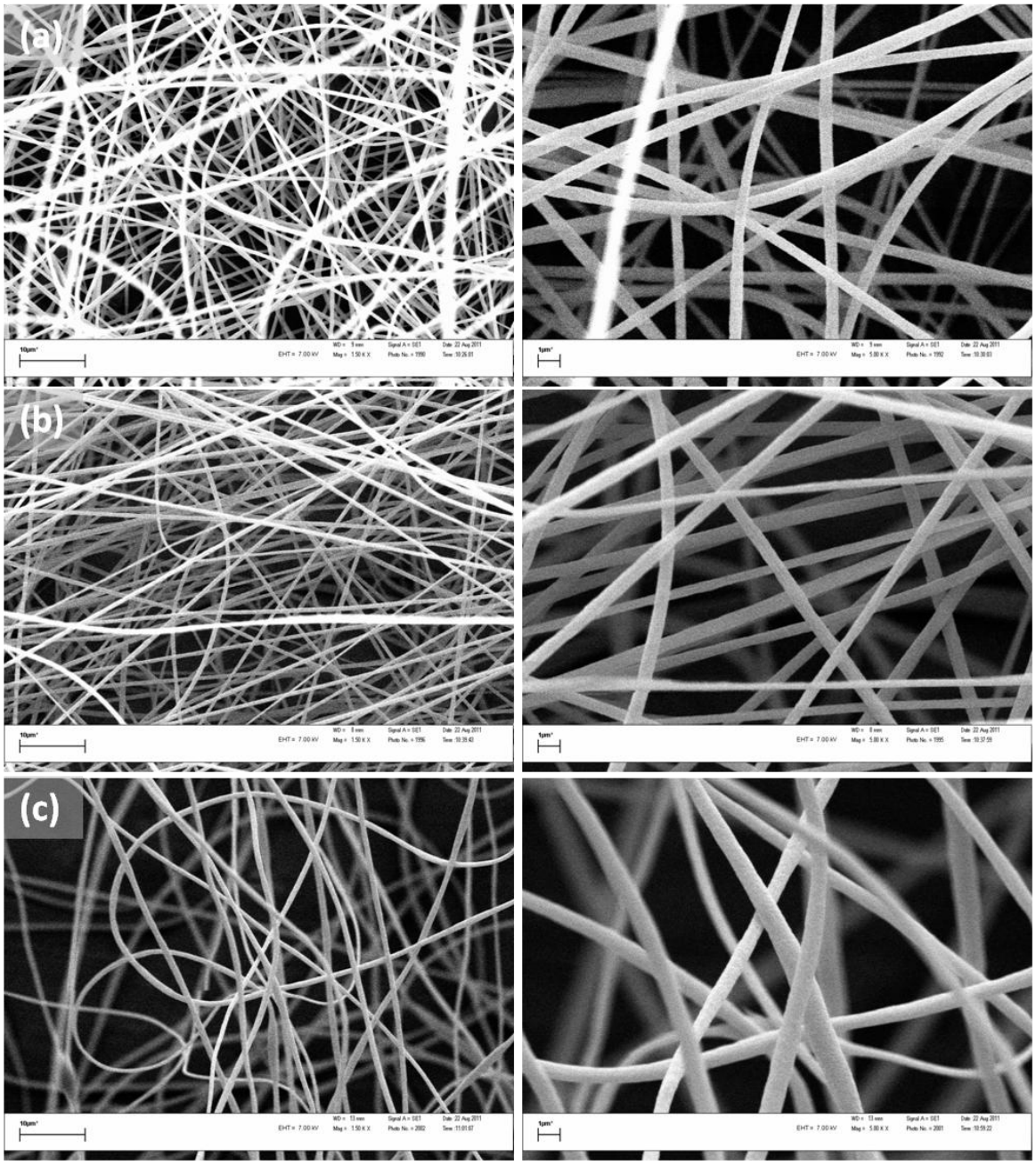

Figure 4-15: SEM images of needle-electrospun PAN fibers at 1500x (left) and 5000x (right) magnification. Fibers spun from solutions containing 7wt% PAN and (a) 0.5 wt%, (b) 1 wt%, and (c) 2 wt% silicone surfactant.

4.2.4.2 Average Fiber Diameters and Fiber Diameter Distributions

For most PAN fiber samples, 100 fiber diameters were measured. The exceptions were PAN fibers spun from 7 wt% PAN solutions where a minimum of 70 fiber diameters were measured. Figure 4-16 illustrates the average fiber diameters of needle-electrospun fibers.

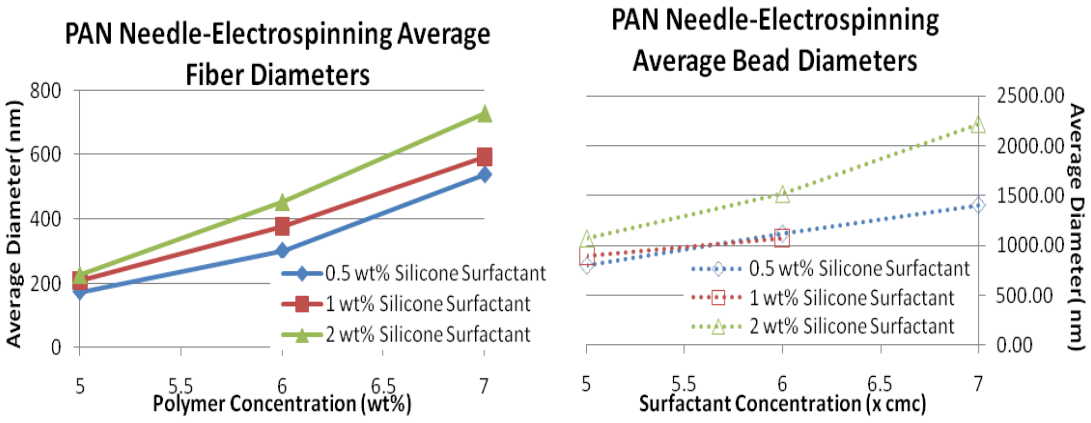

Figure 4-16: PAN needle-electrospinning average fiber (left) and bead (right) diameters.

Figure 4-17 shows fiber diameter distributions of the same.

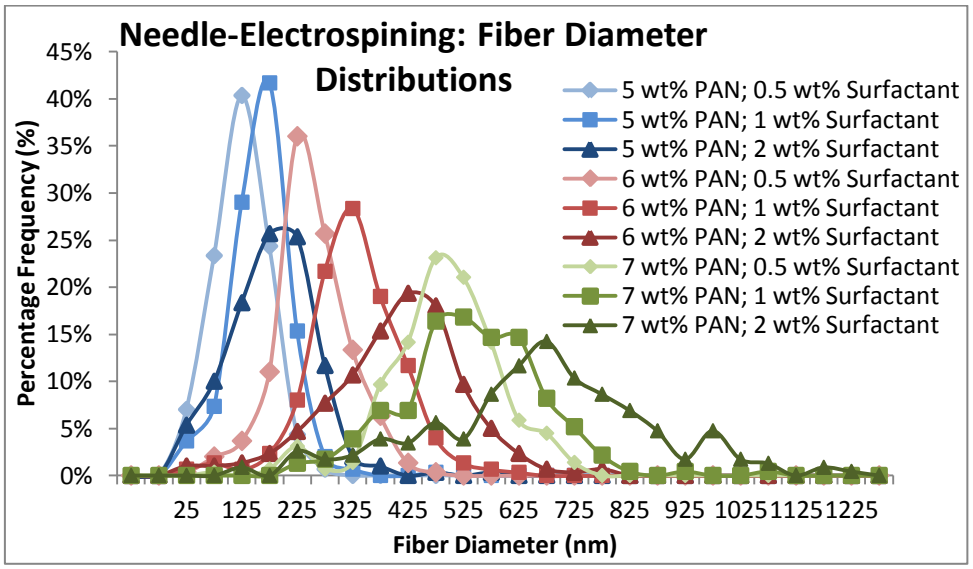

Figure 4-17: PAN needle-electrospun fiber diameter distribution.

4.2.5 Needle-electrospinning Discussion

Figure 4-13 to Figure 4-15 illustrates visually how the fiber diameters increased and the amount of beads decreased with increasing polymer concentration. The increase in fiber diameters with increasing polymer concentration was also evident in Figure 4-17. It was discussed in section 4.2 that the solution viscosity and conductivity increased with increasing polymer concentration. Concerning the 5 wt% PAN solution fibers, it was evident that the surface tension dominated charge repulsion forces during fiber formation which resulted in beaded fibers. One possible explanation for the increase in fiber uniformity, i.e. decreasing number of beads, with increasing polymer concentration was an increase in solution viscosity. The solution conductivity and surface tension decreased only slightly with

increasing polymer concentration, but very large increases were observed in the solution viscosity. High solution viscosity has high resistance to change brought about by forces such as charge repulsion and surface tension on the solution jet. Solution viscosity was thus believed to be the primary influence on the resultant fibers.

The average fiber diameters increased and fiber diameter distributions broadened with increasing surfactant concentration. The increase in fiber diameter was attributed to the increasing viscosity of the solutions since the solution flow resists change brought about by other forces.

Fibers in most fiber samples were also observed to have an uneven fiber shape, which resulted in wide fiber diameter distributions (refer to Figure 4-18).

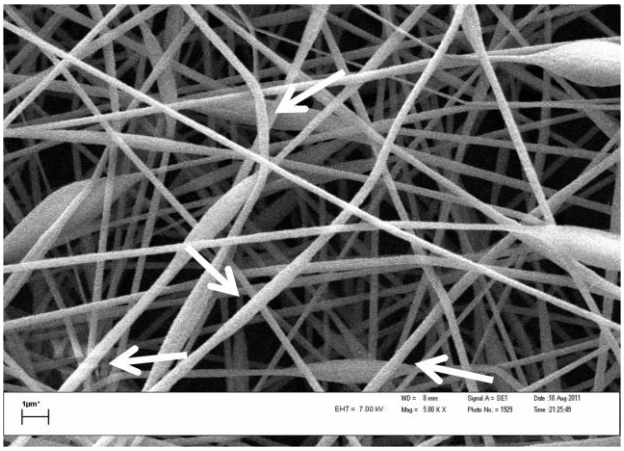

Figure 4-18: Needle-electrospun fibers from a solution containing 6 wt% PAN, 0.5 wt% surfactant. Fibers with uneven fiber shape are pointed out by arrows.

4.3 PVOH Bubble-Electrospinning Results and Discussion

The solution properties of PVOH and PAN solutions have been discussed. The same PVOH solutions were bubble-electrospun at room temperature. The bubble lifetime, bubble size, and the average number of jets per bubble were recorded and analysed to obtain information regarding the bubble-electrospinning of PVOH solutions for the sake of comparison.

4.3.1 Bubble Lifetime

Figure 4-19 illustrates the relationship between bubble lifetime, polymer- and surfactant concentration.

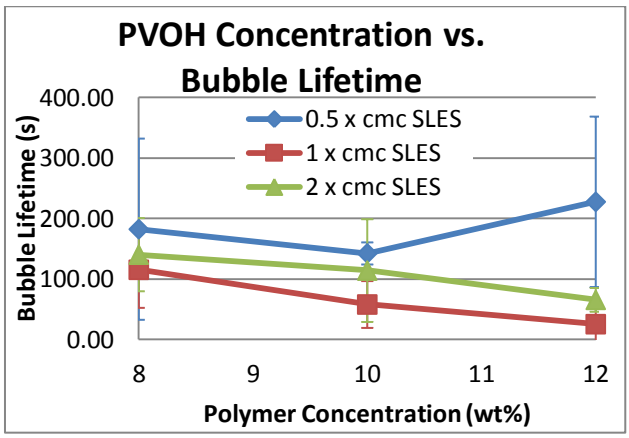

Figure 4-19: Bubble-electrospinning of PVOH solutions: Bubble lifetime

PVOH solutions formed bubbles with longer bubble lifetimes than PAN solutions (refer to section 4.4). A PVOH solution that does not contain surfactant has a surface tension around that of water (72.8 mN/m).[89] In this study the surface tension of a 10 wt% PVOH solution was measured to be 73.8 mN/m. A PVOH solution containing surfactant, on the other hand, has a surface tension between 40 and 48 mN/m (refer to Figure 4-3 for surface tension values of PVOH solutions containing surfactant). Long bubble lifetimes was possibly due to the strong surface tension gradient created between areas of low (weak spots) and high surfactant concentrations along the bubble wall, known as the Gibbs-Marangoni effect.

The general trend observed from Figure 4-19 was that that bubble lifetime decreased with increasing polymer concentration. The solution viscosity was expected to have a large effect on the bubble lifetime. In bubble-electrospinning, polymer solution continuously flows from the bath, along the bubble wall, and away from the bubble along the solution jet. The flow rate into the bubble must match the flow rate of solution out of the bubble, similar to needle-electrospinning, to sustain a continuous solution jet. Solutions with higher viscosities can be expected to have a slower solution flow along the bubble wall and would not be able to sustain the solution jet(s) for long periods of time. As a result, the bubble would rupture earlier due to the strong pulling force applied by the electric field. The hypothesis was supported by the results in Figure 4-19 which indicated that the bubble lifetime decreased with increasing polymer concentration, i.e. increasing solution viscosity.

4.3.2 Bubble Size

Figure 4-20 illustrates the influence of polymer and surfactant concentration on bubble size.

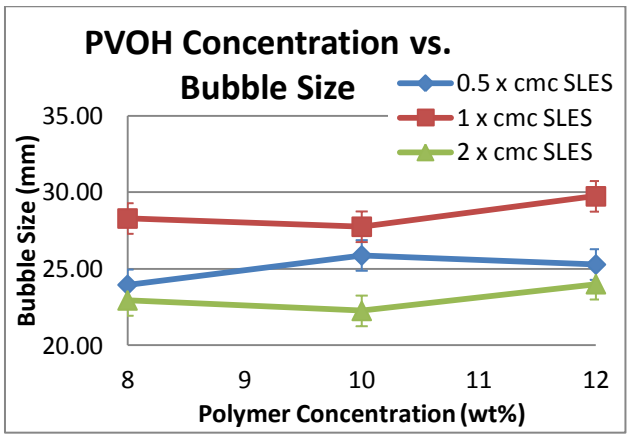

Figure 4-20: Bubble-electrospinning of PVOH solutions: Bubble size.

From Figure 4-20, it is observed that the polymer concentration had no noticeable influence on the bubble size. Concerning surfactant concentration, there was an insignificant increase in bubble size as the surfactant concentration increased from 0.5 to 1 x cmc SLES. A significant decrease in bubble size was then observed when increasing the surfactant concentration from 1 to 2 x cmc SLES. This was supported with statistical data listed in Table 4-1.

Table 4-1: p-Values from a Nonparamatics Kruskal-Wallis test to test significance of variations in bubble size as a function of PVOH and SLES concentration. Significance level is p=0.05.

Polymer Concentration (wt%)	8 R:12.722	10 R:11.938	12 R:14.375
8		1.000000	1.000000
10	1.000000		1.000000
12	1.000000	1.000000	

Surfactant Concentration (x cmc)	0.5 R:13.222	1 R:21.000	2 R:6.5556
0.5		0.107979	0.163992
1	0.107979		**0.000295**
2	0.163992	**0.000295**	

Below is an equation explaining the relationship between normal bubble size (no electric field present) and surface tension (Young-Laplace equation):

$$\Delta P = -\frac{2\gamma}{r}$$

Where r is the bubble curvature radius; ΔP is the difference in external and internal pressure; and γ is the surface tension of the solution. From the equation, it is understood that bubble

size would be smaller with decreasing surface tension.[90] The implication of the equation was confirmed by Table 4-1 which shows that the bubble size significantly decreased with decreases in surface tension (surface tension decreased with increases in surfactant concentration from 1 to 2 x cmc). It is not clear, from the parameters investigated in this study, why the bubble size actually increased when going from 0.5 to 1 x cmc SLES.

4.3.3 Average Number of Jets per Bubble

Figure 4-21 illustrates the relationship between polymer concentration, surfactant concentration and the average number of jets per bubble. The field strength was held constant at 40 kV/ 15cm.

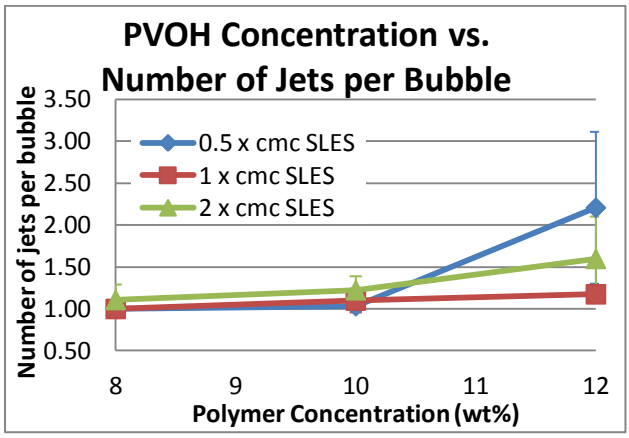

Figure 4-21: Bubble-electrospinning of PVOH solutions: Average number of jets per bubble.

Figure 4-21 shows the following: The number of jets increased from 10 to 12 wt% PVOH concentration but was not significantly influenced by the surfactant concentration. The 12 wt% PVOH solution had a large standard deviation and scarcely followed the trend set out by the 8 and 10 wt% solutions. The same statistical analysis was done on the data as before and is described in Table 4-2.

Table 4-2 shows that there was significant change in the average number of jets from solutions containing 8 wt% PVOH to 12 wt% PVOH. The surfactant concentration did not significantly influence the average number of jets per bubble.

Table 4-2: p-Values from a Nonparamatics Kruskal-Wallis test to test significance of variations in average number of jets per bubble as a function of PVOH and SLES concentration. Significance level is p=0.05.

Polymer Concentration (wt%)	8 R:7.5556	10 R:12.375	12 R:19.750
8		0.533326	**0.001950**
10	0.533326		0.135168
12	**0.001950**	0.135168	

Surfactant Concentration (x cmc)	0.5 R:12.444	1 R:10.571	2 R:15.444
0.5		1.000000	1.000000
1	1.000000		0.566701
2	1.000000	0.566701	

Results described in section 4.1 showed that the solution viscosity and conductivity increased with increasing polymer concentration. Solutions with higher conductivity should have a faster charge build-up at the bubble wall surface. Lukas [91] described the influence of field strength on the average number of jets produced in free surface electrospinning. Although the field strength remained constant throughout these experiments, the principle remains the same in that charge builds up either by increasing the solution conductivity or increasing the field strength. Hence, Lukas's research supports this statement. The more charge density at the surface, the more jets would be required to carry charge away from the bubble surface and stabilise the bubble.

During experiments it was observed that the 12 wt% PVOH solutions formed multiple jets but the number of jets varied on a continuous basis. It appeared as if the jets formed and scattered vigorously across the bubble surface. Solutions with a higher viscosity would have more solution flow resistance and would carry charge away from the charged bubble surface at a slower pace than low viscosity solutions. Hence, a larger number of jets are required to stabilise the bubble. The continuous varying number of jets could be due to the high viscosity and low mobility of the solution.

Although it was initially assumed that the number of jets observed per bubble could be a useful measure in characterising the process, the observations clearly show that the number of jets continually changes in a highly dynamic fashion. The results obtained in this regard therefore do not lead to any specific insights into the process. In future work, high speed photography could possibly be used in evaluating the average number of jets at a specific moment as a function of the amount of electrical current that is measured to flow through the system at that instant. These results could then possibly correlate with the solution properties in some way.

4.3.4 SEM images of PVOH Bubble-Electrospun Fibers

Figure 4-24 to Figure 4-26 are SEM images of bubble-electrospun fibers. The figures are arranged in the same manner as before: three figures showing fibers from solutions with increasing polymer concentrations and each figure set showing fibers from solutions with increasing surfactant concentrations. All solutions were bubble-electrospun at a field strength of 40 kV/15cm. The as-spun fibers were imaged at 1500 x (left) and 5000 x (right) magnifications. Average fiber diameters and fiber diameter distributions of bubble-electrospun fibers are illustrated in section 4.3.5.

4.3.5 Average PVOH Bubble-Electrospun Fiber Diameters and Fiber Distributions

Figure 4-22 illustrates the average fiber and bead diameters of bubble-electrospun PVOH fibers.

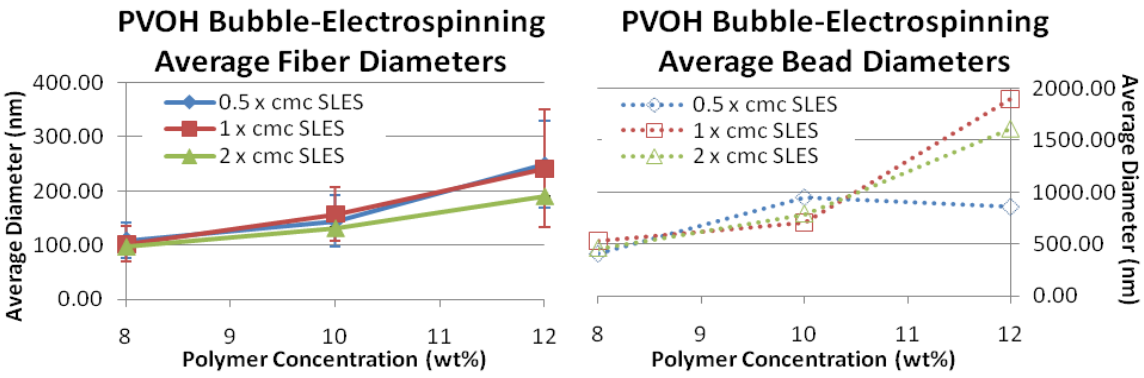

Figure 4-22: Bubble-electrospinning average PVOH fiber and bead diameters.

Figure 4-23 illustrates the fiber diameter distribution of bubble-electrospun PVOH fibers.

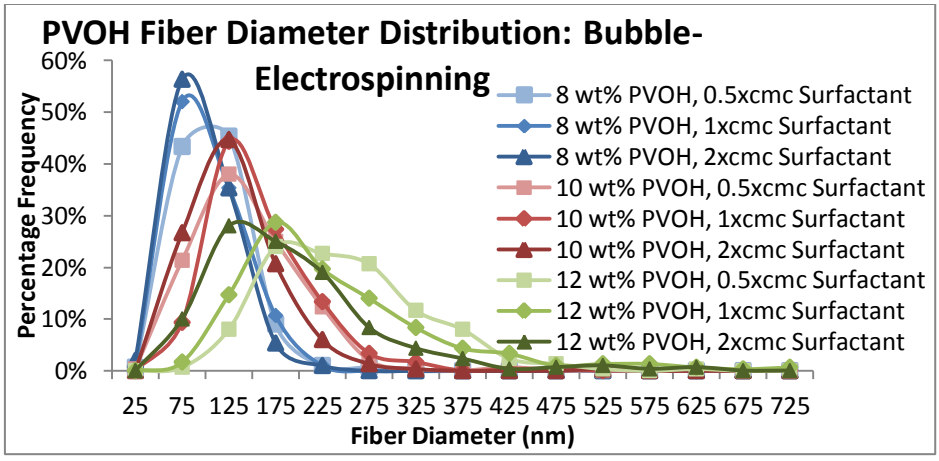

Figure 4-23: PVOH fiber diameter distribution: Bubble-electrospinning.

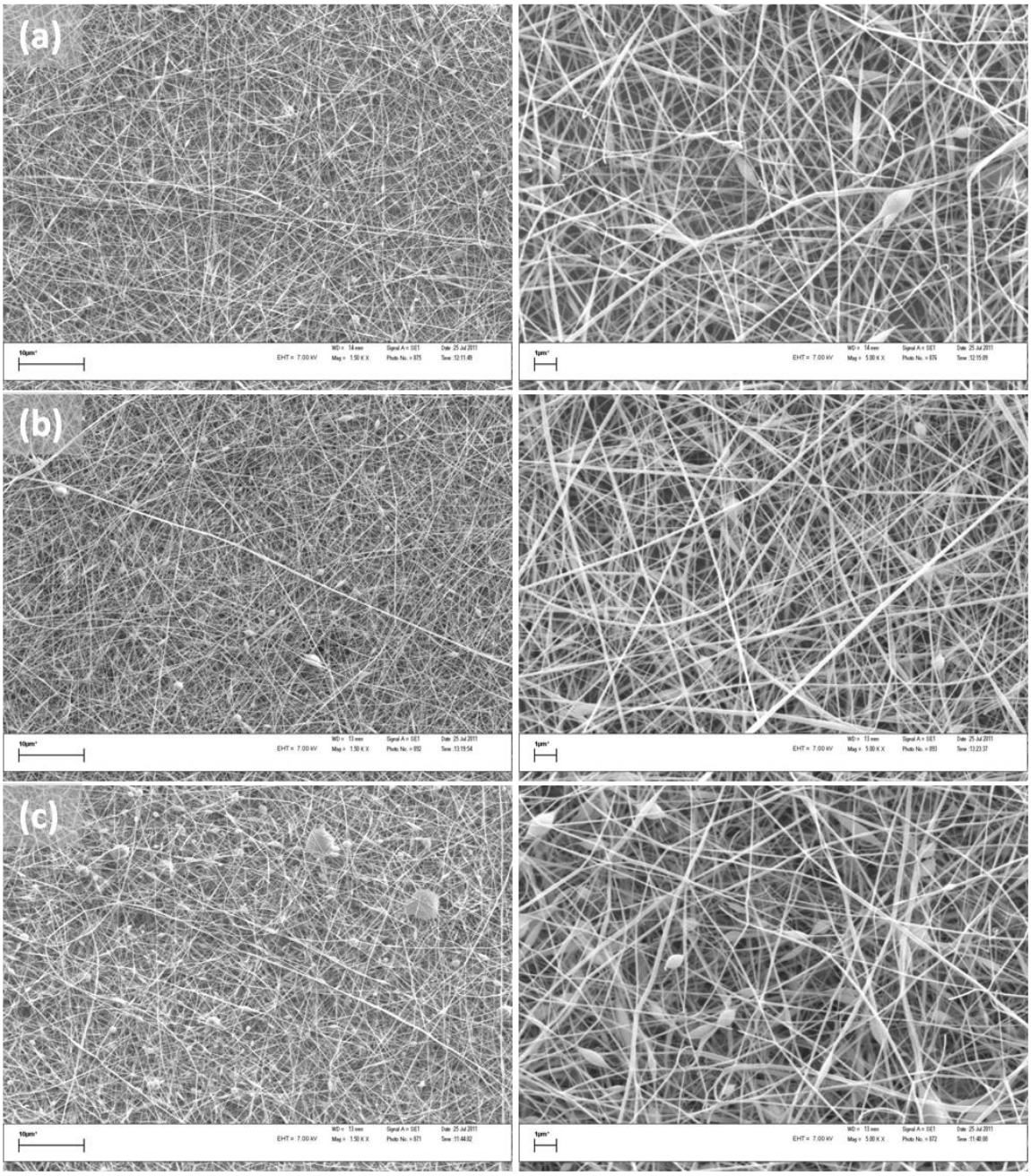

Figure 4-24: SEM images of bubble-electrospun PVOH fibers at 1500x (left) and 5000x (right) magnification. Fibers spun from solutions containing 8 wt% PVOH and (a) 0.5 x cmc, (b) 1 x cmc, and (c) 2 x cmc SLES.

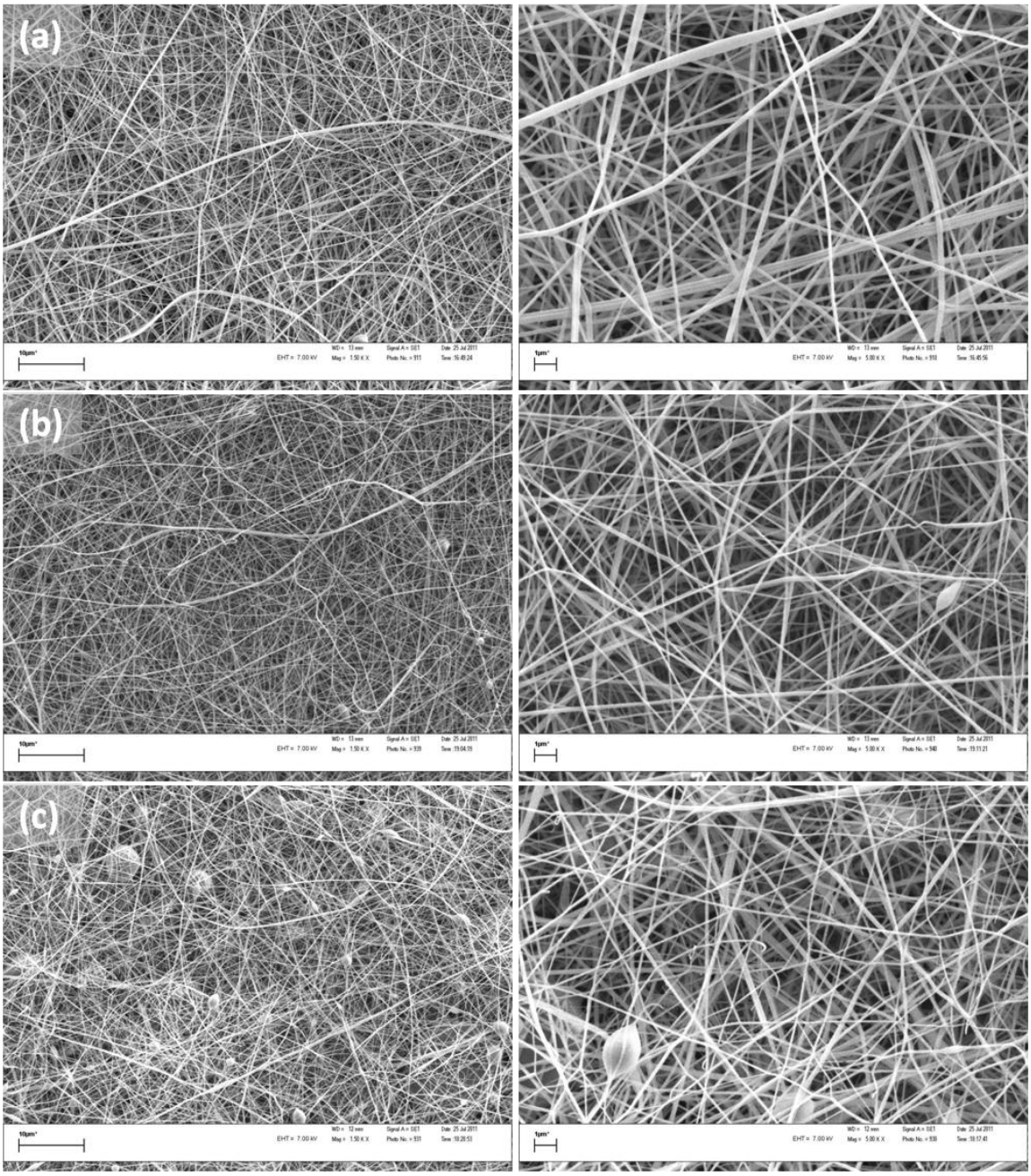

Figure 4-25: SEM images of bubble-electrospun PVOH fibers at 1500x (left) and 5000x (right) magnification. Fibers spun from solutions containing 10 wt% PVOH and (a) 0.5 x cmc, (b) 1 x cmc, and (c) 2 x cmc SLES.

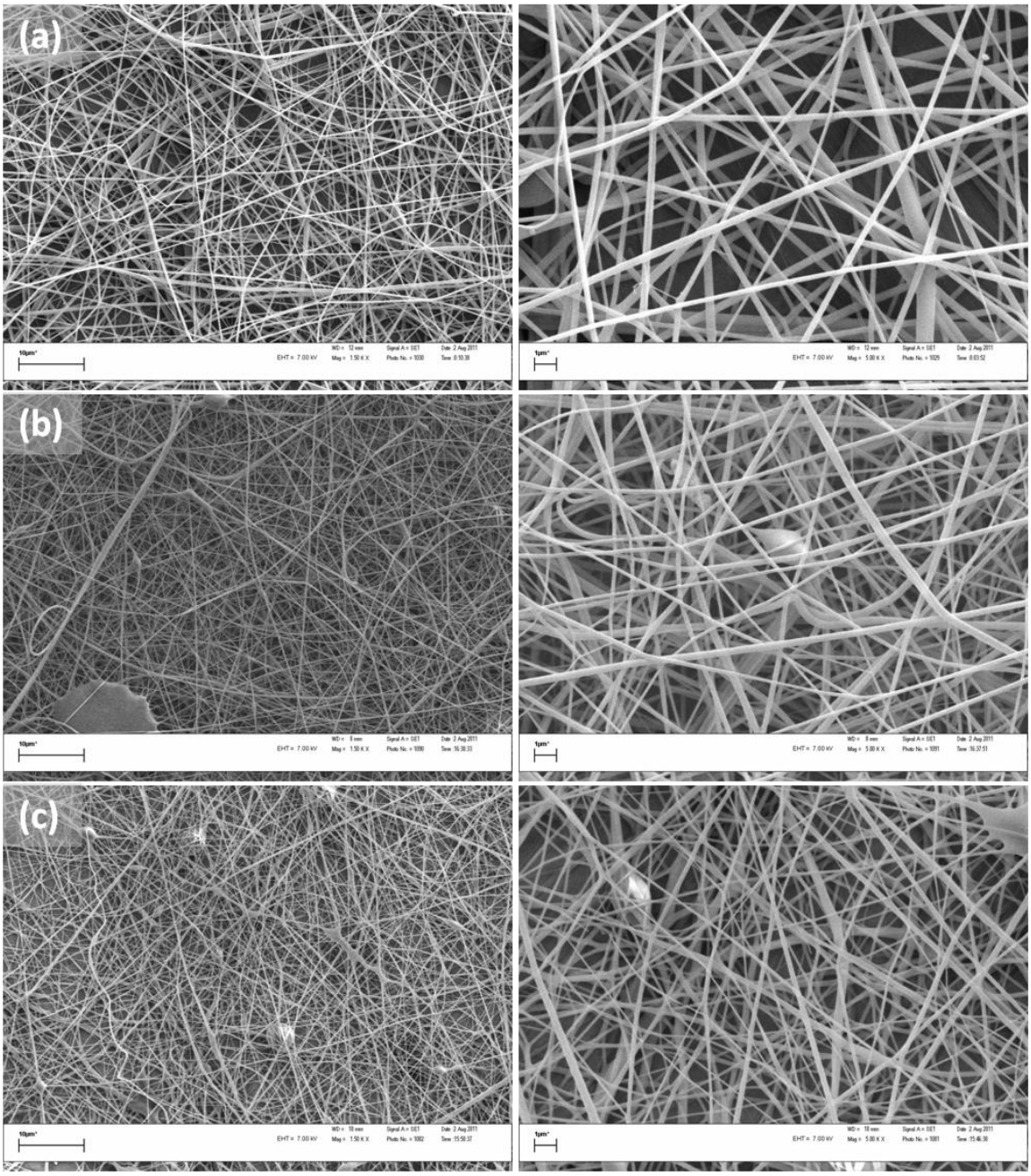

Figure 4-26: SEM images of bubble-electrospun PVOH fibers at 1500x (left) and 5000x (right) magnification. Fibers spun from solutions containing 12 wt% PVOH and (a) 0.5 x cmc, (b) 1 x cmc, and (c) 2 x cmc SLES.

4.3.6 Discussion on Resultant Bubble-Electrospun PVOH Fibers

From the SEM images of bubble-electrospun fibers it was observed that the fiber diameters increased with increasing polymer concentration. The solution viscosity increased to a large degree with increasing polymer concentration and so the fiber diameters were expected to increase with increasing polymer concentration which is the case in Figure 4-22.

A second observation was that the fiber diameters were not significantly influenced by the surfactant concentration. The decrease in surface tension, and increase in solution conductivity showed to have no noticeable effect on the resultant fibers.

A third observation was that fibers spun from 8 wt% PVOH solution formed a smaller number of beaded fibers than that observed in needle-electrospun fibers. The number of beads was reduced with increasing polymer concentration although beads were observed in all samples. Fewer beaded fibers can possibly be attributed to the stronger applied field strength in bubble-electrospinning (2.67 kV/cm), in comparison to needle-electrospinning (0.67 kV/cm). The strong field strength results in a larger charge build-up at the jet surface. As a result, the jet undergoes more rapid whipping and stretching. The surface tension has a weaker effect on the jet in comparison to the charge repulsion forces and so less beaded fibers form.

The high field strength in bubble-electrospinning, compared to needle-electrospinning, results in a higher charge build-up at the bubble surface and in the solution jet and applies a stronger pulling force on the solution jets. It was therefore expected that the fiber diameters would be reduced and that the fibers would be more uniform (less bead formation). Instead, it was observed that the fibers had large fiber diameter distributions (refer to Figure 4-23). In addition, the bubble-electrospun fiber diameters were slightly higher than fibers produced in needle-electrospinning from the same polymer solution concentrations.

A much larger charge density is required to overcome the surface tension of a larger surface area, i.e. a bubble in comparison to a droplet in needle-electrospinning. When a jet ejects from the bubble surface, charge is carried away along with the jet. With increasing amounts of charge carried away by the jet, bending instability occurs earlier and earlier along the jet path (closer to the bubble surface) and then, suddenly, the jet separates into two or more jets simultaneously. Multiple jets eject from the bubble to distribute the charge more evenly amongst the jets, instead of one jet carrying all the charge.[1] Refer to Figure 4-27.

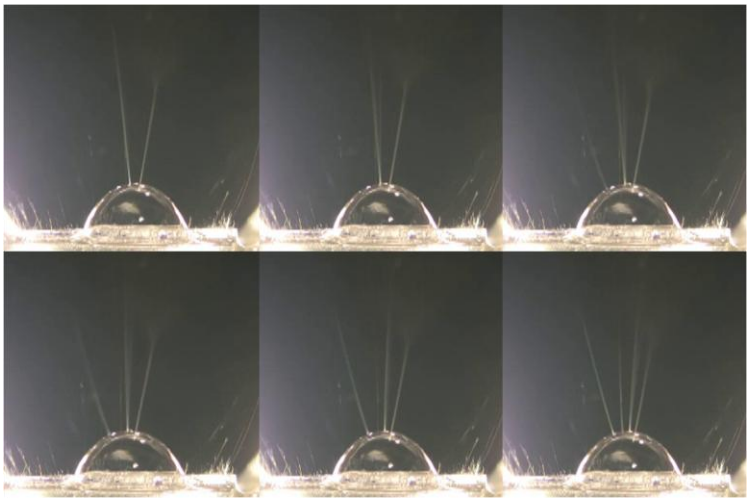

Figure 4-27: Bubble-electrospinning of a PVOH solution. The images captured from a single bubble, illustrates how the number of jets varies throughout the lifetime of the bubble.

During these bubble-electrospinning experiments the small number of simultaneous jets per bubble varied slightly within a single bubble lifetime, possibly having a large impact on fiber diameters. Jets carrying a large amount of charge will undergo more rapid whipping and produce thinner fibers in comparison to jets carrying only a small amount of the charge. The ever-changing number of jets for single bubbles in a strong electric field could then produce nanofibers with a broad range of fiber diameters as was the case with the bubble-electrospun samples.

In addition, the larger percentage charge carried by jets for bubble-electrospinning, in comparison to needle-electrospinning, also contributes to less beading (charge repulsion overcomes surface tension forces) and more uniform fibers at lower polymer concentrations. However, beaded fibers were observed in all fiber images. As jets multiply in to two or more jets, the pulling force applied to the charged jet is reduced due to a lower charge density carried by the jet.

The fiber diameters were not significantly reduced with increasing surfactant concentration (refer to Figure 4-22 and Figure 4-23). The decrease in solution surface tension and a slight increase in solution conductivity was not sufficient to influence fiber morphology.

4.3.7 Calculated PVOH Fiber Production Rates

Figure 4-28 illustrates the calculated production rates of fibers per solution with increasing polymer and surfactant concentration. The production rates were calculated from the fiber mass produced per bubble. Refer to Table 4-3.

Table 4-3: Average PVOH fiber production per bubble.

Polymer (wt%)	Surfactant (xcmc)	Ave. Fiber Mass per Bubble (mg)
8	0.5	4.79
10	0.5	3.70
12	0.5	6.14
8	1	11.12
10	1	9.03
12	1	7.49
8	2	23.67
10	2	6.13
12	2	7.32

The production rates were calculated with the following assumptions: (i) bubbles are fitted directly next to each other within a meter squared bath; (ii) a new bubble replaces a ruptured bubble immediately. Refer to addendum F.4 for fiber production rate calculations.

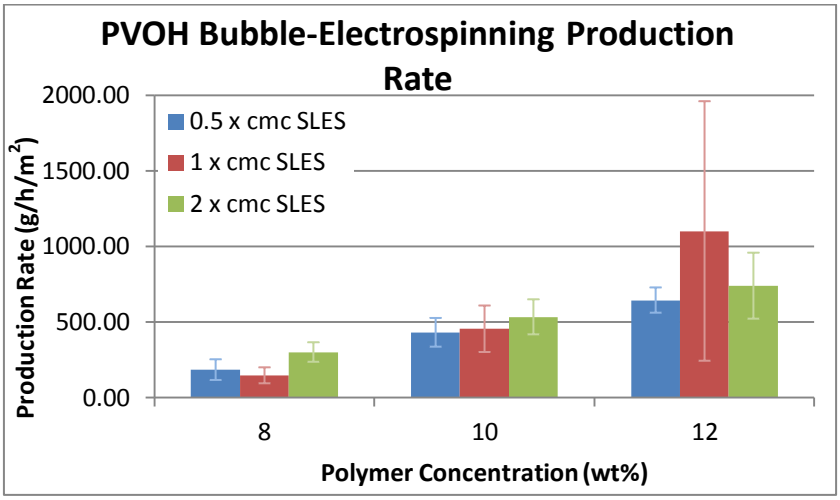

Figure 4-28: Total fiber production rates during bubble-electrospinning of PVOH solutions within a meter squared bath of solution over 1 hour of spinning.

The first observation from Figure 4-28 was that the production rate increased with increasing polymer concentration. The number of jets and the average fiber diameters increased with increasing polymer concentration due to a large increase in solution viscosity. It was not possible within this study to predict the percentage mass increase contributed by i) fiber diameter and ii) number of jets. The production rate appears to follow no trend with regards to surfactant concentration. The number of jets generally increased with increasing surfactant

concentration due to a decrease in surface tension but the number of jets remained relatively low in comparison to work done by Smit [1].

Solutions containing 12 wt% PVOH and 1 x cmc surfactant have a large standard deviation concerning production rates. Viscous solutions formed bubbles that would partially break off during bubble-electrospinning (refer to Figure 4-29). The flow rate of viscous solution within the bubble wall was too slow, and the surface tension too high, to maintain a continuous solution jet or a sufficient flow of charge. To counteract the slow flow of charge from the bubble to the collector, the bubble began to elongate and eventually broke off, leaving a small fraction of the spinning bubble behind. The remaining bubble was destroyed to prevent fiber formation from bubbles with very small bubble sizes (< 15mm). Not all bubbles experienced this process, hence the large standard deviations for production rates.

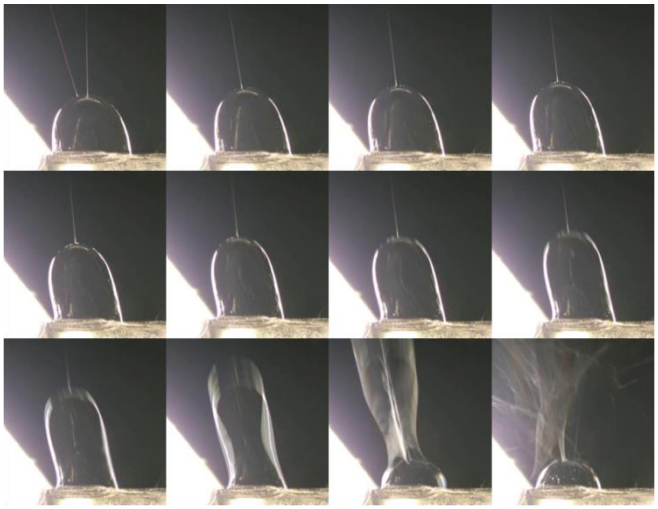

Figure 4-29: Partial break-off of bubble: 12 wt% PVOH solutions during bubble-electrospinning.

4.4 PAN Bubble-Electrospinning Results and Discussions

All PAN solutions were bubble-electrospun with a field strength of 35 kV/ 15 cm. The average bubble lifetime, bubble size and number of jets were measured. The graphs illustrate trends with regards to polymer and surfactant concentrations.

4.4.1 Bubble Lifetime

Figure 4-30 shows the influence of polymer and surfactant concentration on the average bubble lifetime. Bubbles formed from PAN solutions had very short lifetimes relative to PVOH solution bubbles.

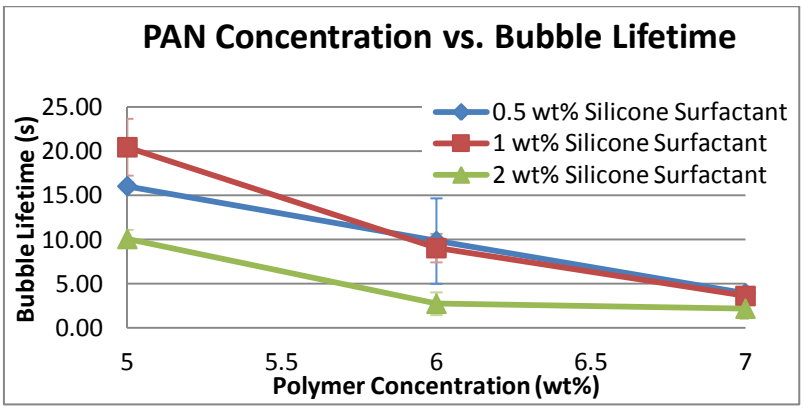

Figure 4-30: Bubble-electrospinning of PAN solutions: Average bubble lifetime.

The data from Figure 4-30 shows that the bubble lifetime decreased with increasing polymer concentration. No significant trend was observed with regards to surfactant concentration. The observations were confirmed by statistical analysis. Refer to Table 4-4.

Table 4-4: p-Values from a Nonparamatics Kruskal-Wallis test to test significance of variations in bubble lifetimes as a function of PAN and silicone surfactant concentration. Significance level is p=0.05.

Polymer Concentration (wt%)	5 R:22.444	6 R:12.667	7 R:6.8889
5		0.026908	0.000097
6	0.026908		0.367637
7	0.000097	0.367637	

Surfactant Concentration (wt%)	0.5 R:16.778	1 R:16.444	2 R:8.7778
0.5		1.000000	0.097528
1	1.000000		0.121386
2	0.097528	0.121386	

Table 4-4 shows that there was no significant change in bubble lifetime with increases in surfactant concentration but the bubble lifetime significantly decreased with increasing polymer concentration.

From section 4.2, solution viscosity and conductivity increased with increasing polymer concentration. Looking at Figure 4-30, the bubble lifetime decreased as the solution viscosity increased (increased resistance to solution flow) and the conductivity decreased (smaller pulling force). The increase in solution viscosity (increase in polymer and surfactant concentration) reduces the flow rate of solution within the bubble wall. The bubble is less able to sustain out-flowing solution jets for long periods of time and, as a result, the bubble ruptures under the applied stress.

4.4.2 Bubble Size

Figure 4-31 illustrates the relationship between bubble size, polymer and surfactant concentration.

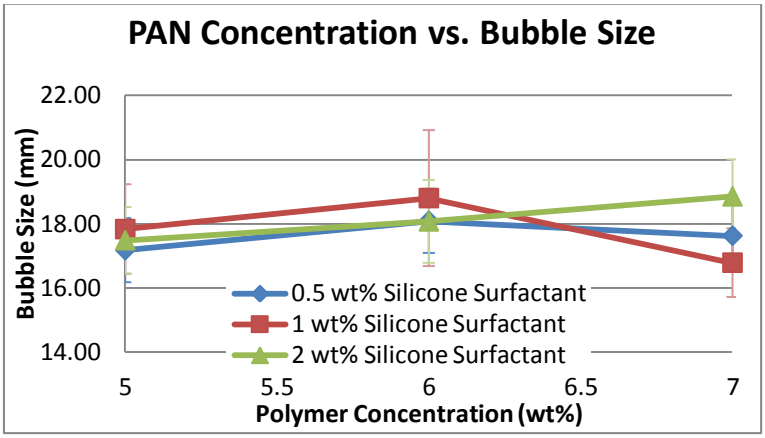

Figure 4-31: Bubble-electrospinning of PAN solutions: Average bubble size.

No evident trends with regards to polymer and surfactant concentration were observed in Figure 4-31.

Bubble size is generally influenced by the surface tension and the viscosity of the solution (assuming all else remains constant). The surface tension was not noticeably changed by polymer concentration and changed very little with increasing surfactant concentration. It is therefore understandable that the bubble size appears to be affected by other parameters not represented here.

4.4.3 Average Number of Jets per Bubble

Figure 4-32 shows the relationship between average number of jets per bubble, polymer and surfactant concentrations.

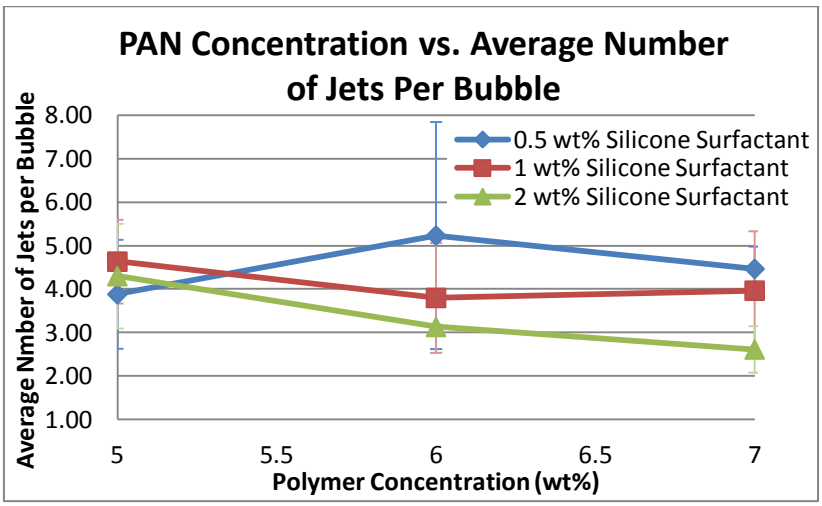

Figure 4-32: Bubble-electrospinning of PAN solutions: Average number of jets per bubble.

Data from Figure 4-32 appears to not be influenced by either polymer or surfactant concentration. Statistical analysis also showed that all variances were insignificant.

Table 4-5: p-Values from a Nonparamatics Kruskal-Wallis test to test significance of variations in average number of jets per bubble as a function of PAN and silicone surfactant concentration. Significance level is p=0.05.

Polymer Concentration (wt%)	5 R:16.056	6 R:14.500	7 R:11.444
5		1.000000	0.653431
6	1.000000		1.000000
7	0.653431	1.000000	

Surfactant Concentration (wt%)	0.5 R:15.778	1 R:16.611	2 R:9.6111
0.5		1.000000	0.297990
1	1.000000		0.184106
2	0.297990	0.184106	

From section 4.2 it was observed that the solution conductivity and the viscosity increased slightly with increasing polymer concentration. Concerning jet formation, solutions with higher conductivity were expected to form a larger number of jets. Solutions with high viscosity were expected to require a larger number of jets to carry sufficient charge away from the bubble. For PAN solutions, the solution conductivity was exceedingly low in comparison to PVOH solutions. Due to the low conductivity of the solution there was only a small charge build-up at the bubble wall and so the number of jets that could form was limited and hence no significant trend can be observed.

4.4.4 SEM Images of PAN Bubble-Electrospun Fibers

This section includes SEM images of bubble-electrospun PAN fibers. All images are arranged as before, imaged at 1500x and 5000x magnification (Refer to Figure 4-33 through to Figure 4-35).

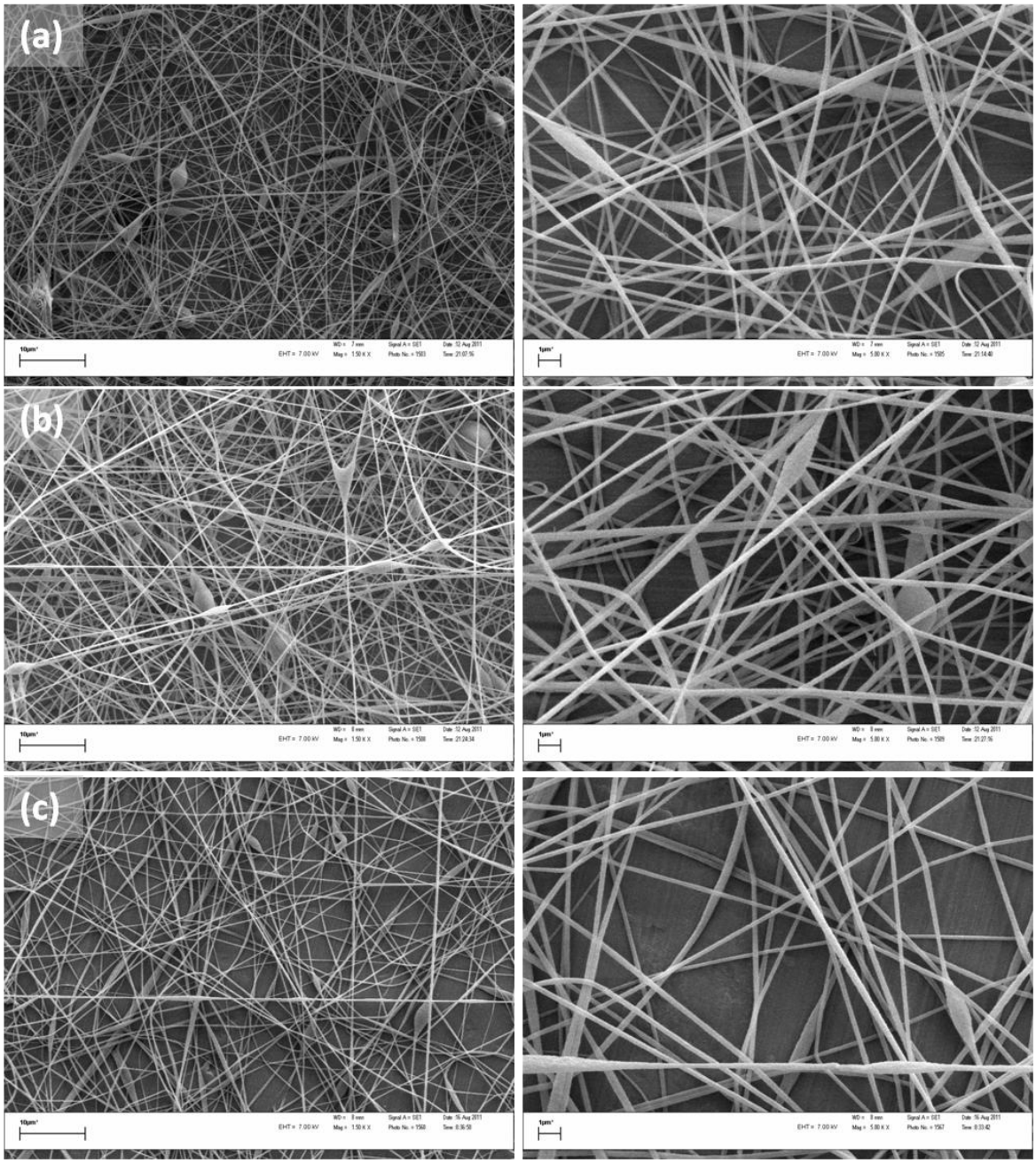

Figure 4-33: SEM images of bubble-electrospun PAN fibers at 1500x (left) and 5000x (right) magnification. Fibers spun from solutions containing 5 wt% PAN and (a) 0.5 wt%, (b) 1 wt%, and (c) 2 wt% silicone surfactant.

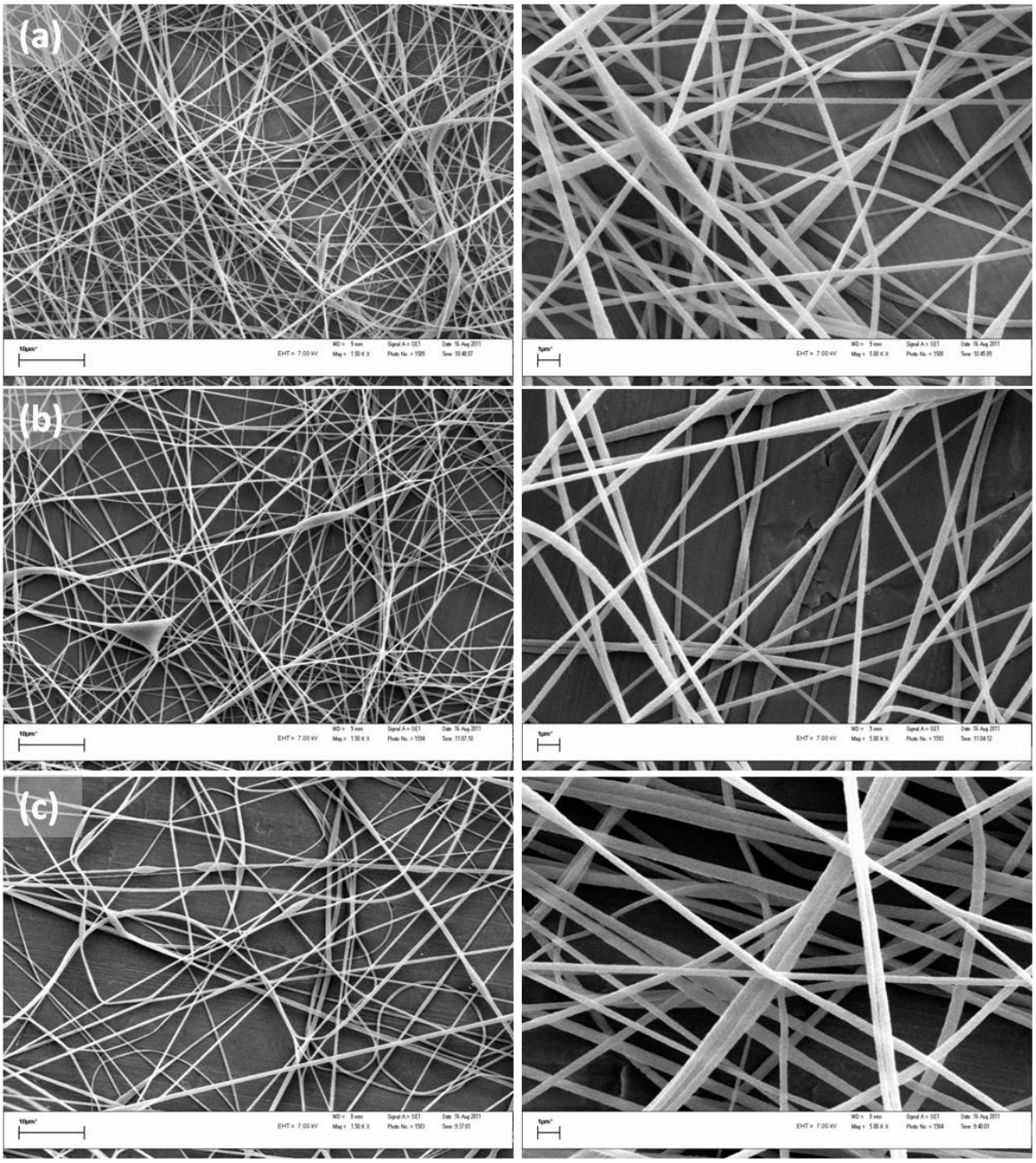

Figure 4-34: SEM images of bubble-electrospun PAN fibers at 1500x (left) and 5000x (right) magnification. Fibers spun from solutions containing 6 wt% PAN and (a) 0.5 wt%, (b) 1 wt%, and (c) 2 wt% silicone surfactant.

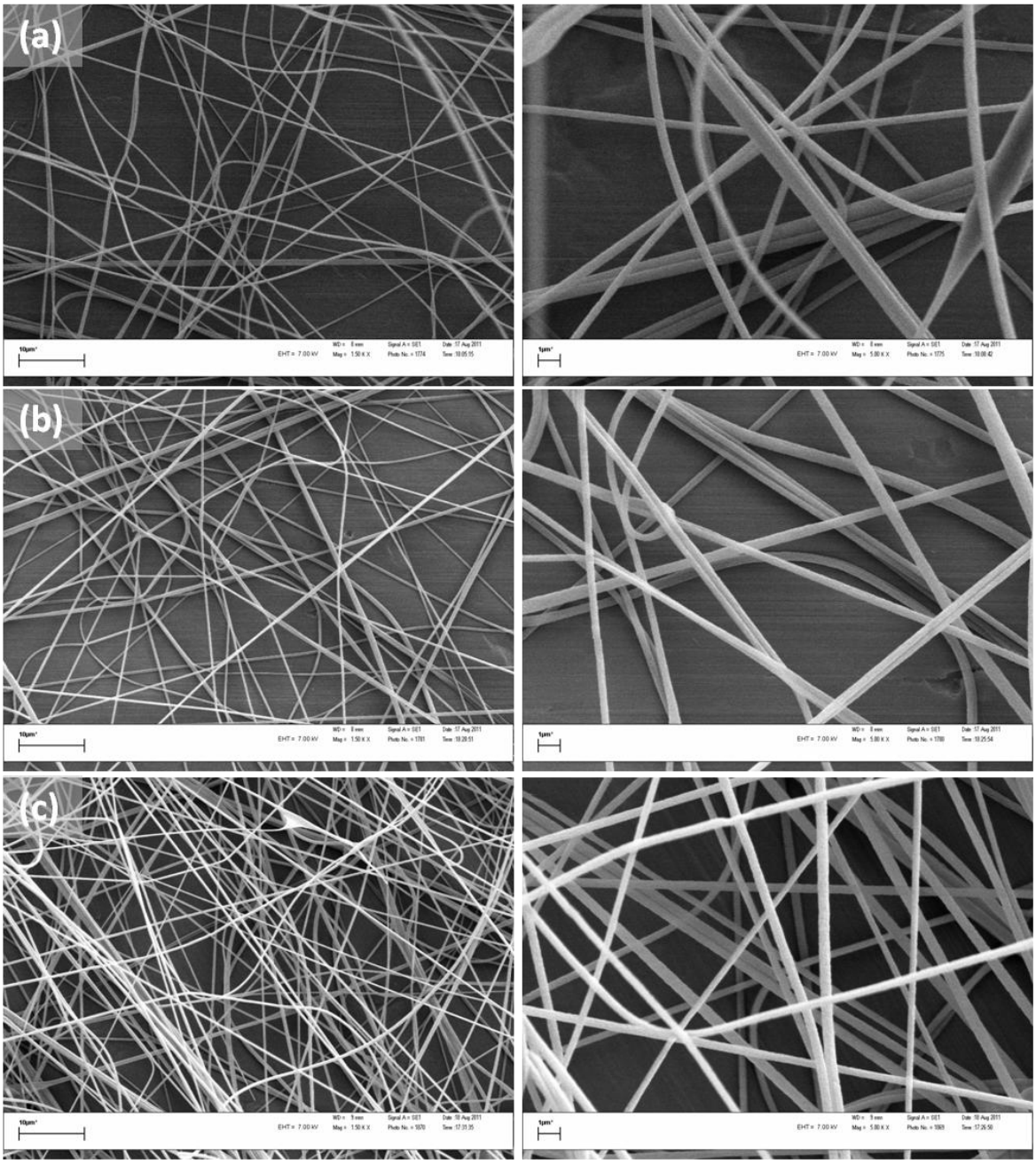

Figure 4-35: SEM images of bubble-electrospun PAN fibers at 1500x (left) and 5000x (right) magnification. Fibers spun from solutions containing 7 wt% PAN and (a) 0.5 wt%, (b) 1 wt%, and (c) 2 wt% silicone surfactant.

4.4.4.1 Fiber Diameters and Fiber Diameter Distributions

Figure 4-36 illustrates the average fiber and bead diameters for bubble-electrospun PAN fibers.

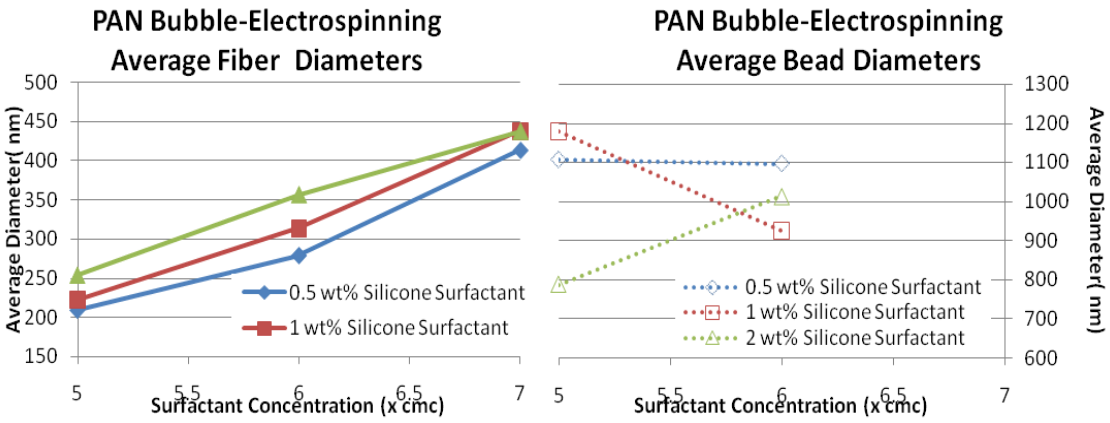

Figure 4-36: Bubble-electrospun average PAN fiber (left) and bead (right) diameters.

Figure 4-37 shows fiber diameter distributions of bubble-electrospun PAN fibers.

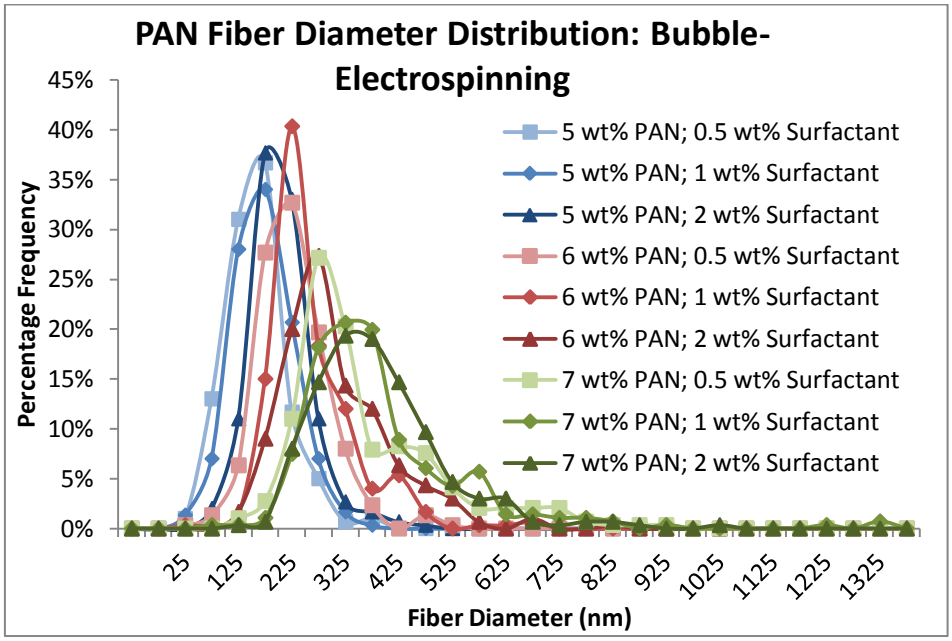

Figure 4-37: Bubble-electrospun PAN fiber diameter distributions.

4.4.5 Discussion on Resultant PAN Bubble-electrospun Fibers

From the SEM images it was observed that 5 wt% PAN solutions formed only a small number of beaded fibers in comparison to that of needle-electrospinning (refer to Figure 4-33). Solutions containing 6 wt% PAN also formed beaded fibers, but a smaller number of beads than that of 5 wt% PAN solutions. 7 wt% PAN solutions formed no beads, except for random traces.

As before, and as expected, solutions with increasing polymer concentration, i.e. increasing resistance to flow, tend to dominate over surface tension and charge repulsion forces and

consequently reduce jet stretching and/or bead formation. At low polymer concentrations the surface tension dominates over the charge repulsion forces in the jet and forms beads, but as the polymer concentration increases, the fibers become more uniform.

The average fiber diameters increased with increasing polymer and surfactant concentrations. This was as expected. The increase in solution viscosity resists stretching by the applied field strength. The molecules also have less ability to disentangle and align with the pulling force. As a result, the fiber diameters increase with increasing polymer and surfactant concentrations.

The bubble-electrospun fiber diameter distributions generally increase with increasing polymer concentration, but show no significant trend with regards to surfactant concentrations. The results in Figure 4-37 indicate that the fiber diameter distributions were slightly narrower for bubble-electrospinning in comparison to needle-electrospinning.

4.4.6 Calculated Production Rates

The fiber production rates were calculated based on the same assumptions described in section 4.3.7. The average fiber production rates per bubble are given in Table 4-6.

Table 4-6: Average PAN fiber production per bubble.

Polymer (wt%)	Surfactant (xcmc)	Fiber Weight per bubble (mg)
5	0.5	1.84
5	1	2.40
5	2	1.16
6	0.5	1.64
6	1	1.17
6	2	0.69
7	0.5	1.16
7	1	1.03
7	2	0.72

Figure 4-38 illustrates the calculated PAN fiber production rate ($g/m^2/h$). Refer to addendum F.4 for fiber production rate calculations.

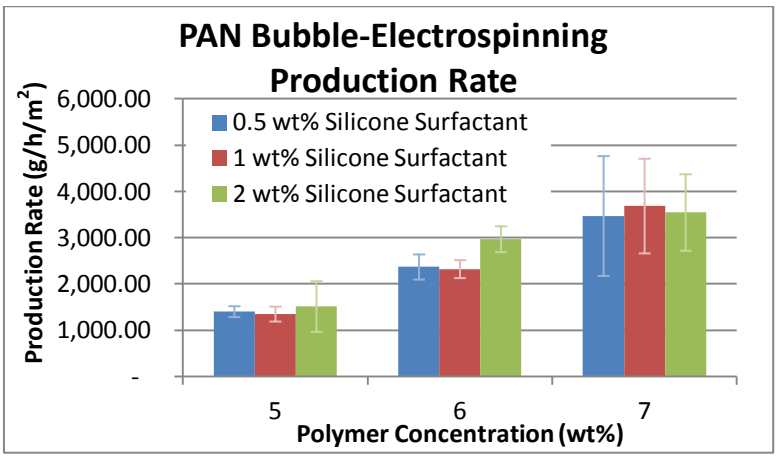

Figure 4-38: Total production rates of PAN bubble-electrospun fibers.

Fiber mass generally increased with increasing polymer concentrations due to larger fiber diameters, similar to that of PVOH fibers. Therefore, one cannot determine the most productive system without considering fiber diameter. Results Figure 4-38 indicates that no evident trends formed in fiber production rates with regards to surfactant concentrations.

4.5 Bubble-electrospinning Comparison between PVOH and PAN Solutions

Solutions of two polymers, namely, polyvinyl alcohol (PVOH) and polyacrylonitrile (PAN) solutions were investigated in this study with regards to solution properties, needle- and bubble-electrospinning, resultant fiber quality and average fiber diameters. Table 4-7 and Table 4-8 is a summary of solution properties for both polymer solutions.

Table 4-7: Summary of PVOH solution properties and trends with regards to polymer and surfactant concentrations.

PVOH Solutions	**Minimum Value**	**Maximum Value**	**Effect of Polymer Concentration**	**Effect of Surfactant Concentration**
Viscosity	90 cP	700 cP	Increased	Increased
Conductivity	380 µs/cm	540 µs/cm	Increased	Increased
Surface tension	40 mN/m	48 mN/m	-	Decreased

Table 4-8: Summary of PAN solution properties and trends with regards to polymer and surfactant concentrations.

PAN Solutions	**Minimum Value**	**Maximum Value**	**Effect of Polymer Concentration**	**Effect of Surfactant Concentration**
Viscosity	200 cP	860 cP	Increased	Increased
Conductivity	29 µs/cm	35 µs/cm	Increased	-
Surface tension	23 mN/m	24 mN/m	-	Decreased

An aim in this study was to compare the bubble-electrospinning (Bubble lifetimes, bubble size and average number of jets per bubble) of the two polymer solutions in terms of their solution properties. Both polymer solutions could be bubble-electrospun although they had very different solution properties.

The bubble lifetimes of PVOH solutions decreased with increasing surfactant concentration whilst PAN bubble lifetimes decreased with increasing polymer concentration. Refer to sections 4.3.1 and 4.4.1. There was thus no common trend between the two solutions in terms of bubble lifetime and the measured solution properties.

Results showed that there was no trend with regards to bubble size and polymer concentration for either polymer solution. The average bubble size of PVOH solutions increased and then decreased with increasing surfactant concentration however, PAN solution bubble size remained unaffected. Refer to sections 4.3.2 and 4.4.2 for detailed results.

The average number of jets per bubble increased with increasing polymer concentration for PVOH solutions. Polymer and surfactant concentration had no significant effect on PAN solutions and their average number of jets per bubble. Refer to 4.3.3 and 4.4.3. It was interesting that the PAN solutions formed a larger number of jets than PVOH solutions. PVOH solutions produced 1 to 2 jets per bubble on average. PAN solutions produced 4 to 5 jets per bubble on average. PAN solutions had a smaller conductivity and surface tension than PVOH solutions. It was possible that the surface tension of PAN solutions was small enough for jets to form from a solution with such low conductivity. On the other hand, the larger surface tension of PVOH solutions resisted jetting, even at higher solution conductivities and thus only 1 or 2 jets could form simultaneously.

In addition to the bubble-electrospinnability of the two solutions, it was of interest to compare the calculated fiber production rates of the two polymer solutions. Figure 4-39 illustrates the

same production rate graphs for both polymer systems for the sake of comparison. Figure 4-39 shows that PAN fiber production rates were significantly higher than PVOH fiber production rates. PAN solutions formed smaller bubbles with a larger number jets per bubble in comparison to PVOH solutions which resulted in higher production rates per meter squared bath per hour. Refer to addendum F.4 for fiber production rate calculations.

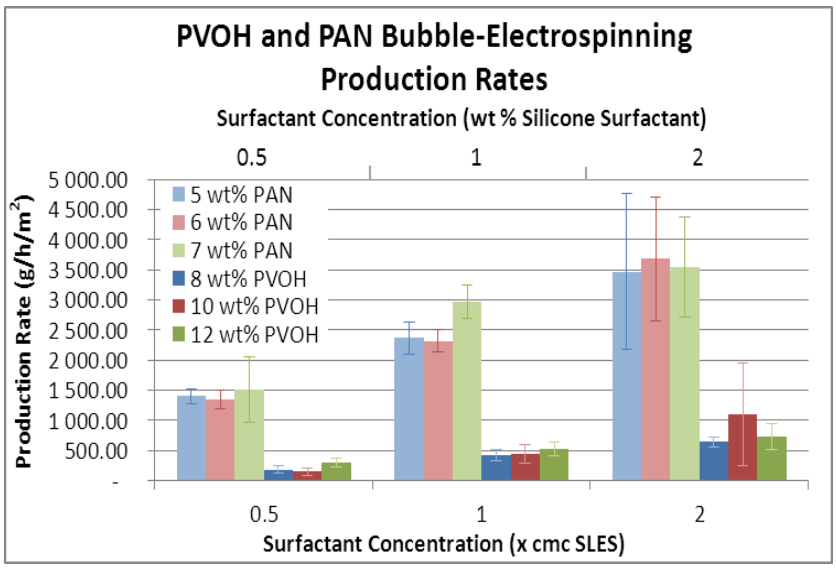

Figure 4-39: PVOH and PAN bubble-electrospinning fiber production rates for comparison.

Fiber production rates increased with increasing polymer concentrations. The average fiber diameters increased from 97 to 249nm and 208 to 438 nm with increasing PVOH and PAN concentration, respectively. (Refer to addendum F.4) It was understandable that the fiber diameter influenced the dry fiber weight and hence the calculated fiber production rates.

The aim of this study was to define operating windows within which both polymer systems bubble-electrospun. It would have been ideal, as a concluding result, to identify a single viscosity, conductivity and surface tension range within which both polymer systems produced the best bubble-electrospinning results. Based on the above discussion, the ideal solution properties do not exist for either of the polymer systems. The bubble lifetime, bubble size, average number of jets per bubble, resultant fibers and the various production rates all showed different trends with regards to polymer and surfactant concentrations i.e. different solution properties. No common trend was found between the two polymer solutions in relation to their bubble lifetimes, bubble sizes, and/or average number of jets per bubble. As a conclusion, it was not possible to identify common trends with regards to the bubble-electrospinning of two different polymer systems in terms of solution viscosity, surface tension and conductivity but the differences in solution properties supported the different

behaviours during the bubble-electrospinning process. This then illustrates the significant influence of solution properties on the bubble-electrospinning process.

The most important factors in nanofiber production, especially when using a mass-production technique such as bubble-electrospinning, are the final production rates and the resultant fibers. PVOH solutions containing 12 wt% PVOH and 1 x cmc SLES showed highest average production rates of 1100 g/m^2/h (Solution viscosity = 579 cP; Conductivity = 504 µS/cm; Surface tension = 44 mN/m). PAN solutions containing 7 wt% PAN and 1 wt% silicone surfactant had the highest average fiber production rate (3685 g/m^2/h) (Solution viscosity = 811 cP; Conductivity = 34 µS/cm; Surface tension = 23 mN/m).

With regards to the resultant fibers, PVOH solutions produced uniform fibers from 10 and 12 wt% PVOH solutions. The fiber uniformity increased with increasing surfactant concentration. 10 wt% PVOH solutions produced smaller diameter fibers, with smaller diameter distributions in comparison to 12 wt% PVOH solutions. 8 wt% solutions formed a large concentration of beaded fibers, reducing fiber quality. Based on the size and uniformity of fiber diameters, 10 wt% PVOH, 2 x cmc SLES solutions was seen as the solution that produced the best bubble-electrospun fiber quality (production rate of 10 wt% PVOH, 2 x cmc surfactant solutions was 533 g/m^2/h) (Solution viscosity = 259 cP; Conductivity = 496 µS/cm; Surface tension = 42 mN/m).

PAN solutions containing 7 wt% PAN concentration formed uniform fibers, but the fibers had large fiber diameters. It would rather be said that 6 wt% solutions was the optimum solution for bubble-electrospinning with regards to fiber quality. The fibers did form a few beads but the fiber diameters were much smaller than 7 wt% PAN solutions. 5 wt% PAN solutions formed a large concentration of beaded fibers, reducing the fiber quality. Although the surfactant concentration did not affect the resultant fibers as much as polymer concentration, it can be seen in Figure 4-39 that solutions containing 1 wt% surfactant had the largest fiber production for the 6 wt% PAN solutions. Consequently, the 6 wt% PAN solution, containing 1 wt% surfactant, formed the best quality fibers (production rate of 6 wt% PAN, 1 wt% surfactant solutions was 2324 g/m^2/h) (Solution viscosity = 412 cP; Conductivity = 31 µS/cm; Surface tension = 23 mN/m).

Chapter 5: Conclusions

A study was done to gain understanding on the influence of specific solution properties, namely viscosity, conductivity and surface tension, on the bubble-electrospinning process. The bubble-electrospinability of a solution was characterized in this study by average bubble lifetime, bubble size and average number of jets per bubble. A second aim of this study was to compare two different polymer systems in terms of their bubble-electrospinability in relation to their solution properties.

The first two objectives were to define trends between solution properties, polymer and surfactant concentrations as well as to investigate the influence of solution properties on the needle-electrospinning process of both polymer systems. This first objective was achieved and results are summarized in Table 4-7 and Table 4-8. Common trends found in literature were observed with regards to the needle-electrospun fibers. The fiber diameter increased with increasing polymer concentration and beaded fibers formed at low polymer concentrations. PVOH fiber diameters decreased with increasing anionic SLES concentration whilst PAN fiber diameters increased with increasing silicone surfactant concentration.

A third objective was to bubble-electrospin both polymer solutions and analyse the average bubble lifetime, bubble size and average number of jets per bubble in relation to their solution properties. Results showed that PVOH solutions bubble lifetime increased significantly with increasing surfactant concentration (decreasing surface tension; increasing viscosity and conductivity). PAN solutions bubble lifetime decreased with increasing polymer concentration Increasing viscosity and conductivity). Concerning bubble size, PVOH solution bubble size increased and then decreased with increasing surfactant concentration, however, PAN solution bubble size remained unaffected by increasing polymer and surfactant concentrations. The average number of jets per bubble increased with increasing polymer concentration but PAN solutions remained unaffected by increasing polymer and surfactant concentrations.

A fourth objective was to evaluate the influence of solution properties on the resultant bubble-electrospun fiber morphologies. Similar trends to that of needle-electrospinning were observed here. Fiber diameters increased with increasing polymer concentration and beaded fibers formed at low polymer concentrations (low solution viscosities). PVOH fiber diameters was insignificantly influenced whilst PAN fiber diameters increased with increasing surfactant concentration.

A fifth objective was then to draw a comparison between the bubble-electrospinnability of the two polymer solutions. There was no common trend found between the bubble-electrospinnability of the two solutions in relation to the solution properties measured in this study but the differences could be explained by the different solution properties. The different effects as a result of different solution properties show that these three solution properties play a significant role in the bubble-electrospinning process but are not the only significant contributing parameters to the bubble-electrospinning process. In other words, a polymer solution should not be expected to bubble-electrospin solely based on the three solution properties investigated in this study.

The drawn conclusions show that there is still much required research regarding bubble-electrospinning and the influence of solution properties that could not be covered in this study. For this reason recommended future work is listed below:

- Based on the work of this study, it would now be possible to do a more quantitative investigation on the influence of specific solution properties. As an example, it would be possible to reduce the surface tension of PVOH solutions further by simply using a silicone surfactant instead of SLES. Other possibilities could be to vary the polymer but use the same solvent system, vary the solvent using the same polymer, etc. As a result, the solution conductivity and viscosity would remain similar but the surface tension would be reduced. It would then be possible to determine the influence of surface tension in relation to the other solution properties such as conductivity and viscosity.
- Investigate other possible influences (solution, process and ambient parameters) on the bubble-electrospinning process, e.g. the electric field shape and its effect on fiber formation; humidity and air pressure, air and solution purity.
- A small pilot study was done in this work to investigate the influence of bubble size on the resultant fibers. It was observed that the fiber diameters appeared increasingly non-uniform with decreasing bubble size. This work fell outside the scope of this study and it would be interesting to investigate this matter further in future work.

Chapter 6: References

(1) Smit, AE, Sanderson, RD. Studies Towards High-Throughput Production of Nanofiber Yarns. University of Stellenbosch; 2008.

(2) Fan J, Hunter L. Engineering apparel fabrics and garments. 1st ed. Cambridge: Woodhead Publishing Ltd.; 2009.

(3) NUSNNI (NUS Nanoscience and Nanotechnology Initiative). Polymer Nanofibers - An overview of applications and current research into processing techniques. 2007; Available at: http://www.azonano.com/article.aspx?ArticleID=1280. Accessed 09/19, 2011.

(4) Cooley JF, inventor. Apparatus for Electrically Dispersing Fluids USA patent 692,631. 1902 February 4, 1902.

(5) Beachley V, Wen X. Effect of electrospinning parameters on the nanofiber diameter and length. Mater Sci Eng: C 2009;29(3):663-668.

(6) Yördem OS, Papila M, Menceloğlu YZ. Effects of electrospinning parameters on polyacrylonitrile nanofiber diameter: An investigation by response surface methodology. Mater Des 2008;29(1):34-44.

(7) Thompson CJ, Chase GG, Yarin AL, Reneker DH. Effects of parameters on nanofiber diameter determined from electrospinning model. Polymer 2007;48(23):6913-6922.

(8) Theron SA, Zussman E, Yarin AL. Experimental investigation of the governing parameters in the electrospinning of polymer solutions. Polymer 2004;45(6):2017-2030.

(9) He J. Electrospun nanofibres and their applications. Shawbury, Shrewsbury, Shropshire, U.K.: iSmithers; 2008.

(10) Yoon K, Hsiao BS, Chu B. functional nanofibers for environmental applications. J Mater Chem 2008;18(44):5326-5334.

(11) Zhou F, Gong R, Porat I. Mass production of nanofibre assemblies by electrostatic spinning. Polym Int 2009;58(4):331-342.

(12) Smit AE, Sanderson RD, inventors. A process for the production of fibers. WO 2008/125971 A1. 23 October 2008.

(13) El-Newehy MH, Al-Deyab SS, Kenawy ER, Abdel-Megeed A. Nanospider Technology for the Production of Nylon-6 Nanofibers for Biomedical Applications. J Nanomater 2011.

(14) Ren Z, He J. Single polymeric bubble for the preparation of multiple micro/nano fibers. J Appl Polym Sci 2011;119(2):1161-1165.

(15) Yang R, He J, Xu L, Yu J. Bubble-electrospinning for fabricating nanofibers. Polymer 2009;50(24):5846-5850.

(16) Liu Y, He J, Yu J. Bubble-Electrospinning: A Novel Method for Making Nanofibers. J Phys: Conference Series 2008;96:1-4.

(17) Yarin AL, Zussman E. Upward needleless electrospinning of multiple nanofibers. Polymer 2004 4;45(9):2977-2980.

(18) Yamashita Y. Current State of Nanofiber Produced by Electrospinning and Prospects for Mass Production. J Text Eng 2008;54(6):119-205.

(19) Niu H, Lin T, Wang X. Needleless electrospinning. I. A comparison of cylinder and disk nozzles. J Appl Polym Sci 2009;114(6):3524-3530.

(20) Wang X, Niu H, Lin T, Wang X. Needleless Electrospinning of nanofibers with a conical wire coil. Polym Eng Sci 2009;49(8):1582-1586.

(21) Thoppey NM, Bochinski JR, Clarke LI, Gorga RE. Edge electrospinning for high throughput production of quality nanofibers. Nanotech 2011;22:345301.

(22) Varabhas JS, Chase GG, Reneker DH. Electrospun nanofibers from a porous hollow tube. Polymer 2008;49(19):4226-4229.

(23) Lu B, Wang Y, Liu Y, Duan H, Zhou J, Zhang Z, et al. Superhigh-Throughput Needleless Electrospinning Using a Rotary Cone as Spinneret. Small 2010;6(15):1612-1616.

(24) Reneker DH, Yarin AL. Electrospinning jets and polymer nanofibers. Polymer 2008;49(10):2387-2425.

(25) Greiner A, Wendorff JH. Electrospinning: a fascinating method for the preparation of ultrathin fibers. Angew Chem Int Ed 2007;46(30).

(26) Rutledge GC, Fridrikh SV. Formation of fibers by electrospinning. Adv Drug Deliv Rev 2007;59(14):1384-1391.

(27) Jun HW, Paramonov SE, Hartgerink JD. Biomimetic self-assembled nanofibers. Soft Matter 2006;2(3):177-181.

(28) Wei Z, Zhang Z, Wan M. Formation mechanism of self-assembled polyaniline micro/nanotubes. Langmuir 2002;18(3):917-921.

(29) Ma PX, Zhang R. Synthetic nano-scale fibrous extracellular matrix. J Biomed Mater Res 1999;46(1):60-72.

(30) Tan EPS, Lim CT. Physical properties of a single polymeric nanofiber. Appl Phys Lett 2004;84(9):1603-1605.

(31) McCann JT, Marquez M, Xia Y. Melt coaxial electrospinning: a versatile method for the encapsulation of solid materials and fabrication of phase change nanofibers. Nano Lett 2006;6(12):2868-2872.

(32) Sandler JKW, Pegel S, Cadek M, Gojny F, Van Es M, Lohmar J, et al. A comparative study of melt spun polyamide-12 fibres reinforced with carbon nanotubes and nanofibres. Polymer 2004;45(6):2001-2015.

(33) Liu Y, He J. Bubble electrospinning for mass production of nanofibers. International J Nonlin Sci Num 2007;8(3):393-396.

(34) Taylor GI. Disintegration of water drops in an electric field. Proc Roy Soc 1964;280(A):383-397.

(35) 80 years of electrospinning. International conference on Latest Advances in High-Tech Textiles and Textile-Based Materials, Proceedings; 2009.

(36) Huang Z, Zhang Y-, Kotaki M, Ramakrishna S. A review on polymer nanofibers by electrospinning and their applications in nanocomposites. Composites Sci Technol 2003;63(15):2223-2253.

(37) Schiffman JD, Schauer CL. A Review: Electrospinning of Biopolymer Nanofibers and their Applications. Polym Rev 2008;48(2):317-352.

(38) Andrady AL. Science and Technology of Polymer Nanofibers. 1st ed. Hoboken, New Jersey: John Wiley & Sons, Inc.; 2008.

(39) Gupta P, Elkins C, Long TE, Wilkes GL. Electrospinning of linear homopolymers of poly(methyl methacrylate): exploring relationships between fiber formation, viscosity, molecular weight and concentration in a good solvent. Polymer 2005;46(13):4799-4810.

(40) Deitzel JM, Kleinmeyer J, Harris D, Beck Tan NC. The effect of processing variables on the morphology of electrospun nanofibers and textiles. Polymer 2001;42(1):261-272.

(41) Eda G, Liu J, Shivkumar S. Solvent effects on jet evolution during electrospinning of semi-dilute polystyrene solutions. European Polymer Journal 2007;43(4):1154-1167.

(42) Chen H, Yu D. An elevated temperature electrospinning process for preparing acyclovir-loaded PAN ultrafine fibers. J Mater Process Technol 2010;210(12):1551-1555.

(43) Givens SR, Gardner KH, Rabolt JF, Chase DB. High-temperature electrospinning of polyethylene microfibers from solution. Macromol 2007;40(3):608-610.

(44) Lu C, Chen P, Li J, Zhang Y. Computer simulation of electrospinning. Part I. Effect of solvent in electrospinning. Polymer 2006;47(3):915-921.

(45) Jaworek A. Micro- and nanoparticle production by electrospraying. Powder Technol 2007;176(1):18-35.

(46) Chen DR, Pui DYH, Kaufman SL. Electrospraying of conducting liquids for monodisperse aerosol generation in the 4 nm to 1.8 [mu] m diameter range. J Aerosol Sci 1995;26(6):963-977.

(47) Heikkilä P, Harlin A. Parameter study of electrospinning of polyamide-6. Eur Pol J 2008;44(10):3067-3079.

(48) Hansen CM. 50 Years with solubility parameters—past and future. Prog Org Coat 2004;51(1):77-84.

(49) Iovleva MM, Smirnova VN, Budnitskii GA. The solubility of polyacrylonitrile. Fibre Chem 2001;33(4):262-264.

(50) Dressel M, Gruner G. Electrodynamics of solids: optical properties of electrons in matter. 1st ed. United Kingdom: Cambridge University Press; 2002.

(51) Brown WH, Foote CS, Iverson BL, Anslyn EV. Organic Chemistry: Enhanced. 5th ed. Belmont USA: Brookes/Cole Cengage Learning; 2010.

(52) Rosen MJ. Surfactants and interfacial phenomena. 3rd ed. Hoboken, New Jersey: Wiley-Interscience; c2004.

(53) Jung YH, Kim HY, Lee DR, Park SY, Khil MS. Characterization of PVOH nonwoven mats prepared from surfactant-polymer system via electrospinning. Macromol Res 2005;13(5):385-390.

(54) Manglik RM, Wasekar VM, Zhang J. Dynamic and equilibrium surface tension of aqueous surfactant and polymeric solutions. Exp Therm Fluid Sci 2001;25(1-2):55-64.

(55) Goddard ED, Hannan RB. Cationic polymer/anionic surfactant interactions. J Colloid Interface Sci 1976 4;55(1):73-79.

(56) Ramakrishna S, Fujihara K, Teo W, Yong T, Ma Z, Ramaseshan R. Electrospun nanofibers: solving global issues. Mater Today 2006;9(3):40-50.

(57) Teo W, Ramakrishna S. A review on electrospinning design and nanofibre assemblies. Nanotechnology 2006;17(14):89.

(58) Katta P, Alessandro M, Ramsier RD, Chase GG. Continuous electrospinning of aligned polymer nanofibers onto a wire drum collector. Nano letters 2004;4(11):2215-2218.

(59) Wannatong L, Sirivat A, Supaphol P. Effects of solvents on electrospun polymeric fibers: preliminary study on polystyrene. Polym Int 2004;53(11):1851-1859.

(60) Seo JM, Arumugam GK, Khan S, Heiden PA. Comparison of the Effects of an Ionic Liquid and Triethylbenzylammonium Chloride on the Properties of Electrospun Fibers, 1-Poly(lactic acid). Macromolecular Materials and Engineering 2009;294(1):35-44.

(61) Boys JE, Howells TH. Humidification in anaesthesia. Br J Anaesth 1972;44(8):879.

(62) Ackerman SA, Knox JA. Meteorology: Understanding the Atmosphere. 3rd ed. USA: Jones & Bartlett Publishers; 2011.

(63) Pugh RJ. Foaming, foam films, antifoaming and defoaming. Adv Colloid Interface Sci 1996;64:67-142.

(64) Zhang XD, Macosko CW, Davis HT, Nikolov AD, Wasan DT. Role of Silicone Surfactant in Flexible Polyurethane Foam. J Colloid Interface Sci 1999;215(2):270-279.

(65) Hill RM. Silicone surfactants—new developments. Curr Opin in Colloid Interface Sci 2002;7(5-6):255-261.

(66) Buzzacchi M, Schmiedel P, von Rybinski W. Dynamic surface tension of surfactant systems and its relation to foam formation and liquid film drainage on solid surfaces. Colloids Surf Physicochem Eng Aspects 2006;273(1-3):47-54.

(67) Hill RM editor. Silicone Surfactants. 1st ed. New York: Marcel Dekker; 1999.

(68) De Jaeger R, Gleria M. Inorganic Polymers. 1st ed. Europe: Nova Science Publishers; 2007.

(69) Hilton JE, Van Der Net A. Dynamics of charged hemispherical soap bubbles. Europhys Lett 2009;86(2):24003.

(70) Liu Y, Dong L, Fan J, Wang R, Yu J. Effect of applied voltage on diameter and morphology of ultrafine fibers in bubble electrospinning. J Appl Polym Sci 2011;120(1):592-598.

(71) Qin XH, Wang SY. Filtration properties of electrospinning nanofibers. J Appl Polym Sci 2006;102(2):1285-1290.

(72) Supaphol P, Chuangchote S. On the electrospinning of poly (vinyl alcohol) nanofiber mats: A revisit. J Appl Polym Sci 2008;108(2):969-978.

(73) Yao L, Haas TW, Guiseppi-Elie A, Bowlin GL, Simpson DG, Wnek GE. Electrospinning and stabilization of fully hydrolyzed poly (vinyl alcohol) fibers. Chem Mater 2003;15(9):1860-1864.

(74) Zhang C, Yuan X, Wu L, Han Y, Sheng J. Study on morphology of electrospun poly(vinyl alcohol) mats. Eur Pol J 2005;41(3):423-432.

(75) Hong P, Chou C, He C. Solvent effects on aggregation behavior of polyvinyl alcohol solutions. Polymer 2001;42(14):6105-6112.

(76) Ohkura M, Kanaya T, Kaji K. Gelation rates of poly(vinyl alcohol) solution. Polymer 1992;33(23):5044-5048.

(77) Briscoe B, Luckham P, Zhu S. The effects of hydrogen bonding upon the viscosity of aqueous poly(vinyl alcohol) solutions. Polymer 2000;41(10):3851-3860.

(78) Kostakova E, Meszaros L, Gregr J. Composite nanofibers produced by modified needleless electrospinning. Mater Lett 2009;63(28):2419-2422.

(79) Zhang L, Hsieh Y. Carbon nanofibers with nanoporosity and hollow channels from binary polyacrylonitrile systems. Eur Pol J 2009;45(1):47-56.

(80) GU S, WU Q, REN J. Preparation and surface structures of carbon nanofibers produced from electrospun PAN precursors. New Carbon Mater 2008;23(2):171-176.

(81) Moon S, Farris RJ. Strong electrospun nanometer-diameter polyacrylonitrile carbon fiber yarns. Carbon 2009;47(12):2829-2839.

(82) Zussman E, Chen X, Ding W, Calabri L, Dikin DA, Quintana JP, et al. Mechanical and structural characterization of electrospun PAN-derived carbon nanofibers. Carbon 2005;43(10):2175-2185.

(83) Zhou Z, Lai C, Zhang L, Qian Y, Hou H, Reneker DH, et al. Development of carbon nanofibers from aligned electrospun polyacrylonitrile nanofiber bundles and characterization of their microstructural, electrical, and mechanical properties. Polymer 2009;50(13):2999-3006.

(84) Minagawa M, Takasu T, Morita T, Shirai H, Fujikura Y, Kameda Y. The steric effect of solvent molecules in the dissolution of polyacrylonitrile from five different N,N-dimethylformamide derivatives as studied using Raman spectroscopy. Polymer 1996;37(3):463-467.

(85) Beckmann J, Zenke D. Thermoreversible gelation of polyacrylonitrile/ dimethylformamide-solution. Colloid Pol Sci 1993;271(5):436-445.

(86) Tan L, Pan D, Pan N. Gelation behavior of polyacrylonitrile solution in relation to aging process and gel concentration. Polymer 2008;49(26):5676-5682.

(87) Ramakrishna S. An introduction to electrospinning and nanofibers. Singapore: World Scientific; 2005.

(88) Sill TJ, von Recum HA. Electrospinning: Applications in drug delivery and tissue engineering. Biomater 2008;29(13):1989-2006.

(89) Myers D. Surfactant Science and Techonology. 3rd ed. New Jersey: John Wiley and Sons; 2006.

(90) Schäfer R, Merten C, Eigenberger G. Bubble size distributions in a bubble column reactor under industrial conditions. Exp Therm Fluid Sci 2002;26(6-7):595-604.

(91) Lukas D, Sarkar A, Pokorny P. Self-organization of jets in electrospinning from free liquid surface: A generalized approach . J Appl Phys 2008;103(8):1-7.

Addendum A: Pilot Study on PVOH polymer and surfactant concentration range selection.

A pilot study was conducted to obtain an operating window of polymer and surfactant concentrations within which the PVOH solutions bubble-electrospun and formed uniform fibers. From this operating window it was desirable to select a finer range of concentrations for further and more detailed experiments.

A range of polymer concentrations from 8 wt% to 17 wt% were made up. PVOH solutions containing 16 and 17 wt% PVOH gelled within 1 hour after being removed from the 80˚C oil bath, even though the solution stirred continuously and thoroughly.

A.1 Solution Properties of Solutions

Solutions with polymer concentrations 8 to 15 wt% were measured in terms of viscosity, conductivity and surface tension.

A.1.1 Viscosity

The solution viscosity of different polymer concentrations is shown in the table below. All solutions contained 1 x cmc SLES surfactant concentration. Solutions were measured at a controlled temperature of 25 ˚C using a waterbath.

Table A-1: Viscosity measurements, at 25 ˚C, of polymer solutions at various polymer concentrations and 1xcmc SLES surfactant concentration.

PVOH Solution Viscosity		
Polymer concentration (wt%)	**RPM (Spindle 21)**	**Viscosity (cP)**
8	60	106.7
9	60	163.3
10	60	242.5
12	60	691.7
14	10	1395
15	10	2480

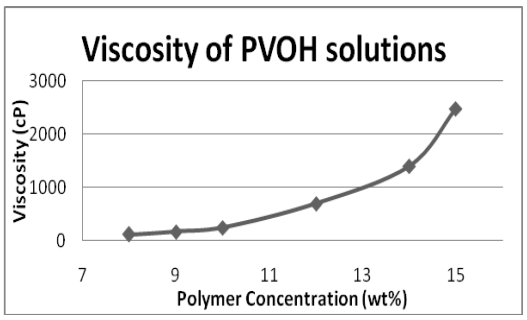

Figure A-1: Viscosity of polymer solutions with increasing PVOH concentration.

It was observed from Figure A-1 that the viscosity increased with increasing polymer concentration.

A.1.2 Conductivity

The conductivity of solutions with different polymer concentrations is shown in the table below. All solutions contained 1xcmc SLES surfactant concentration. Solutions were heated to a temperature of 25˚C and then measured.

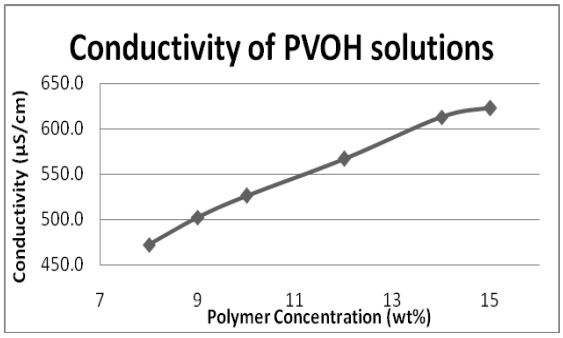

Figure A-2: Conductivity of polymer solutions with increasing PVOH concentration.

It was observed from Figure A-2 that conductivity of the solution increased with increasing polymer concentration.

A.1.3 Surface Tension

The solution surface tension of different polymer concentrations was measured with a De Nöuy Ring Tensiometer. The results are shown in Figure A-3. All solutions contained 1 x cmc SLES. The solutions were corrected using Jordan and Harkins Correction factors. Solutions were heated to a temperature of 25˚C and then measured.

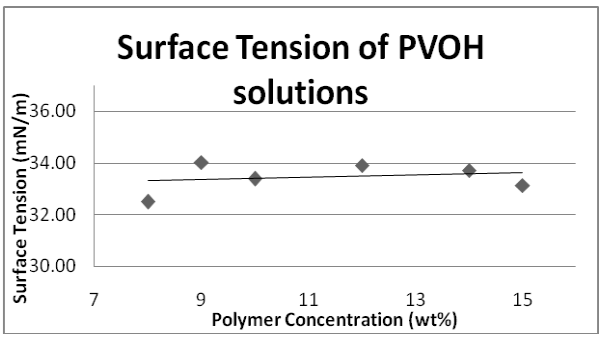

Figure A-3: Surface Tension of PVOH solutions with increasing PVOH concentration.

The first observation from the data is that the data points are very scattered and follow a somewhat linear, barely increasing, trend. It was suspected that the viscosity of the solution had a drastic effect on the ring as it is pulled out of solution, hence distorting the surface tension readings measured. The viscosity counteracts the upward force. It was suggested to investigate another form of tensiometery, called the pendant drop method. The pendant drop method is only dependant on gravitational and surface tension forces, and not influenced by viscosity. Further experimental data for surface tension is described in Addendum E.

A.2 Needle Electrospinning

Solutions were needle-electrospun at room temperature using a syringe pump (0.0022 ml/min). The following fibers and fiber diameters were obtained:

Table A-2: Average fiber diameters for needle-electrospinning samples with increasing PVOH concentration.

Polymer Conc. (wt%)	Ave. Fiber Diameter (nm)	Std. Deviation (nm)
8	64.90	20.08
9	66.45	14.00
10	138.47	21.53
12	147.05	27.71
14	300.35	28.83
15	445.93	105.28

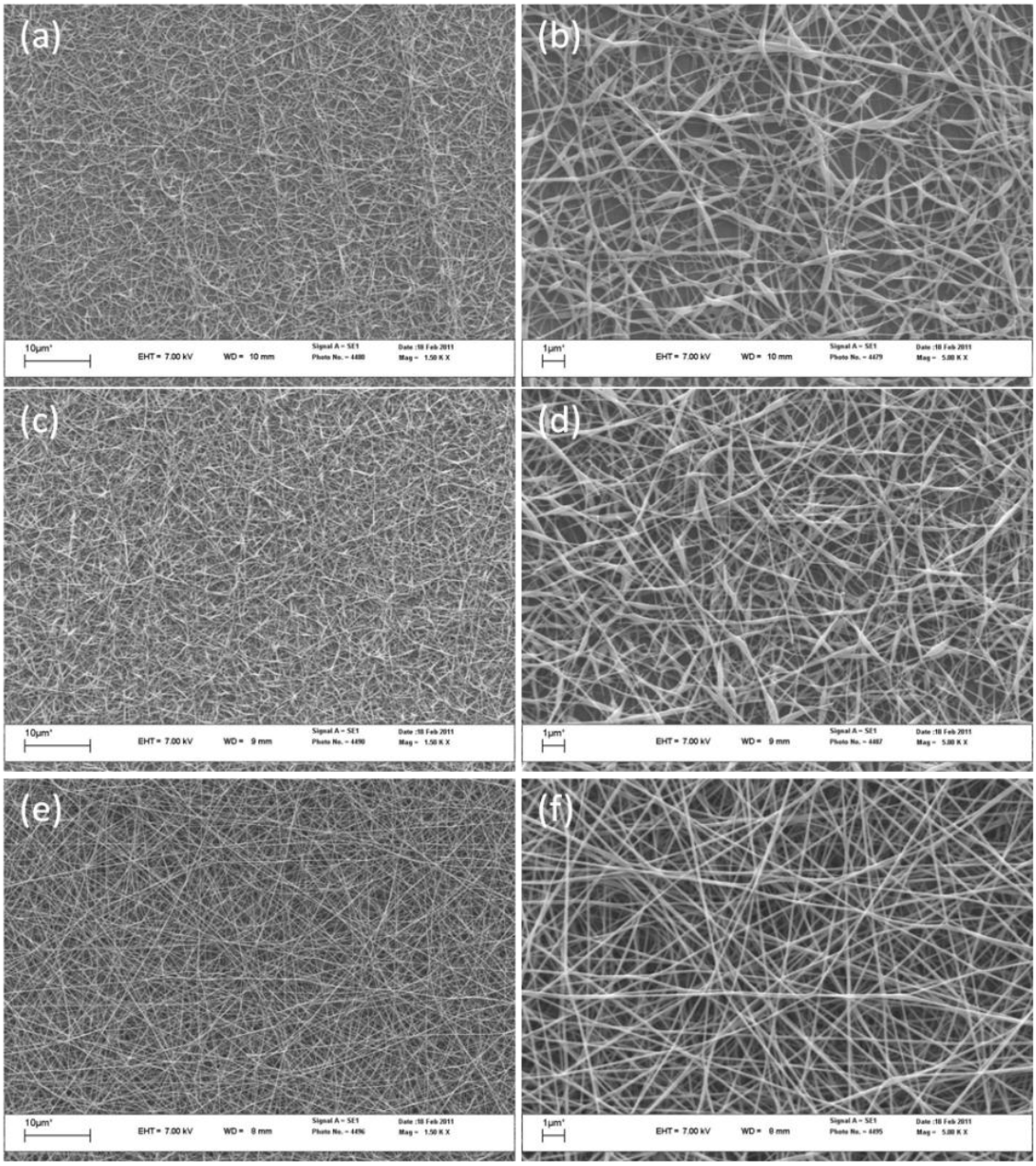

Figure A-4: SEM images of needle-electrospinning fibers at +10 kV/15 cm. (a-b) 8 wt% POVH at 1500 and 5000x magnification, respectively; (c-d) 9 wt% POVH at 1500 and 5000x magnification, respectively; (e-f) 10 wt% POVH at 1500 and 5000x magnification, respectively.

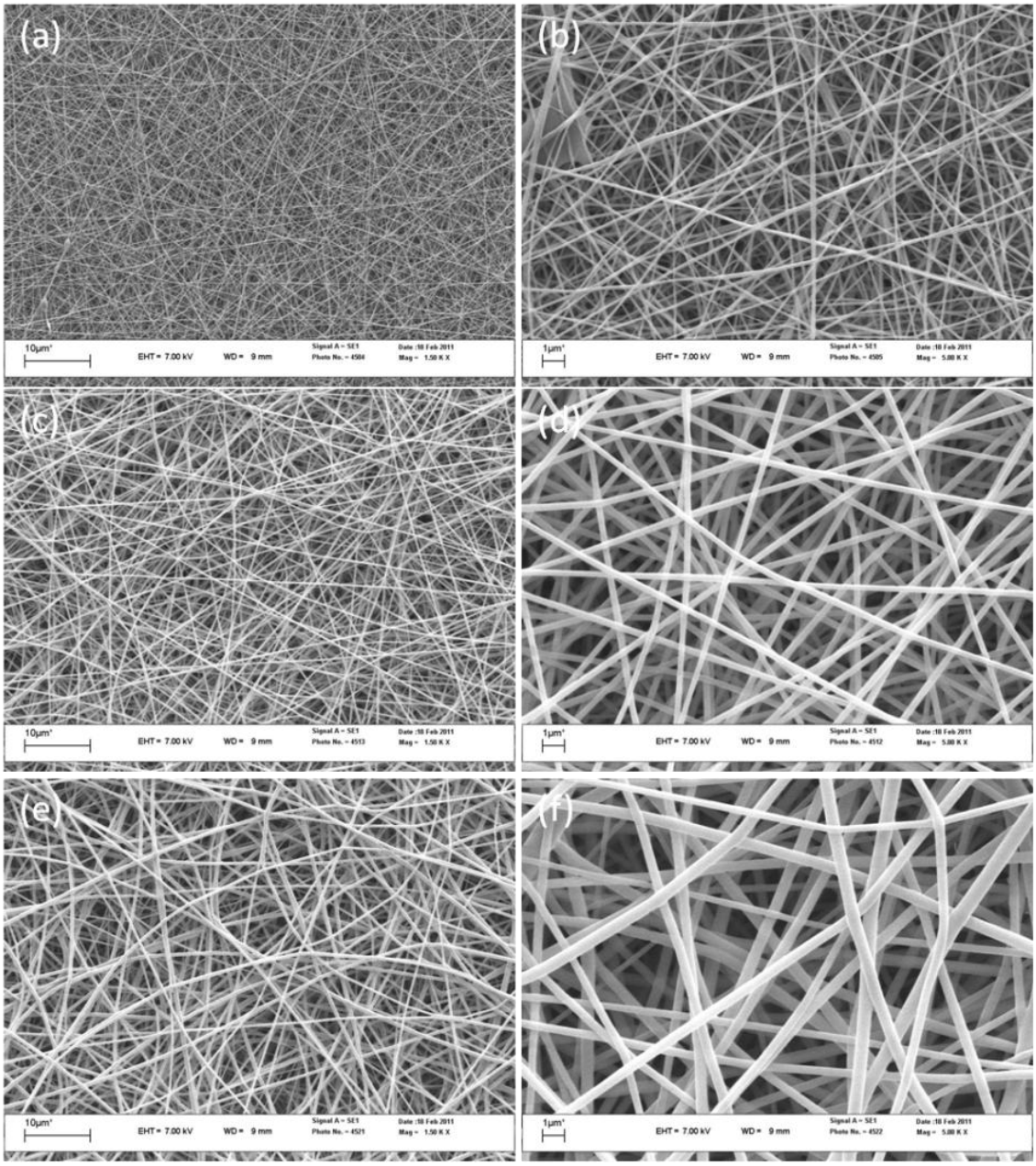

Figure A-5: SEM images of needle-electrospinning fibers at +10 kV/ 15 cm. (a-b) 12 wt% POVH at 1500 and 5000x magnification, respectively; (c-d) 14 wt% POVH at 1500 and 5000x magnification, respectively; (e-f) 15 wt% POVH at 1500 and 5000x magnification, respectively.

In observation, the average fiber diameters of fibers increased with increasing polymer concentration. Only fibers from the 8 and 9 wt% failed to follow this trend simply due to the intense beading that occurred at such low polymer concentrations (refer to Figure A-4 (a-d)). It was observed that the solution conductivity increased with an increase in PVOH concentration. At low polymer concentrations and low field strengths (in this case +10 kV/15 cm), the surface tension forces overcome the charge repulsion forces at the solution jet surface and form ‗beads' along the jet length.

A.3 Bubble-Electrospinning

Solutions were bubble-electrospun at room temperature using a bubble-electrospinning bowl device. The field strength was controlled at 37.5 kV/ 15cm. The following fibers and fiber diameters were obtained:

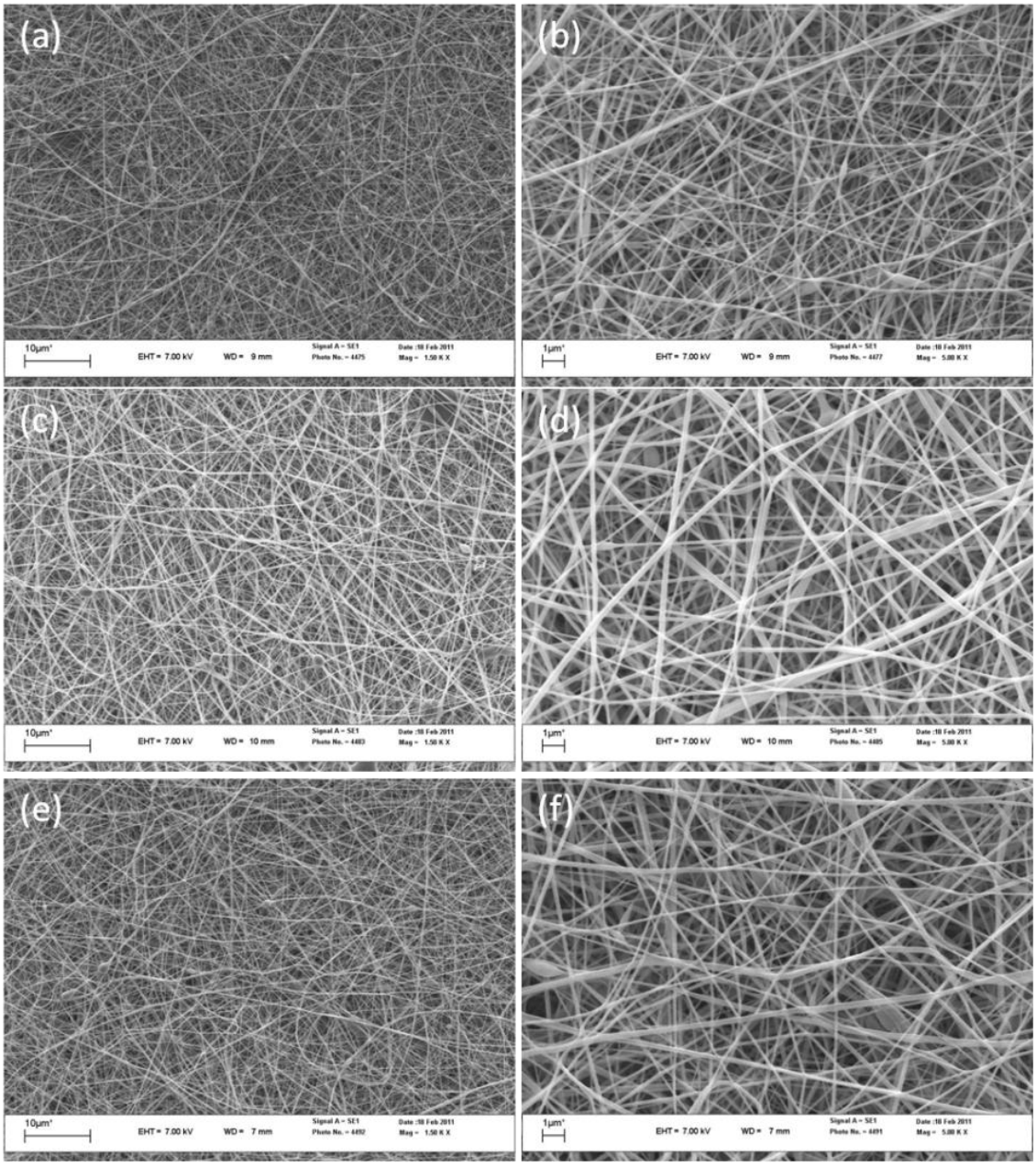

Figure A-6: SEM images of bubble-electrospinning fibers at 37.5kV/15cm. (a-b) 8 wt% POVH at 1500 and 5000x magnification, respectively; (c-d) 9 wt% POVH at 1500 and 5000x magnification, respectively; (e-f) 10 wt% POVH at 1500 and 5000x magnification, respectively.

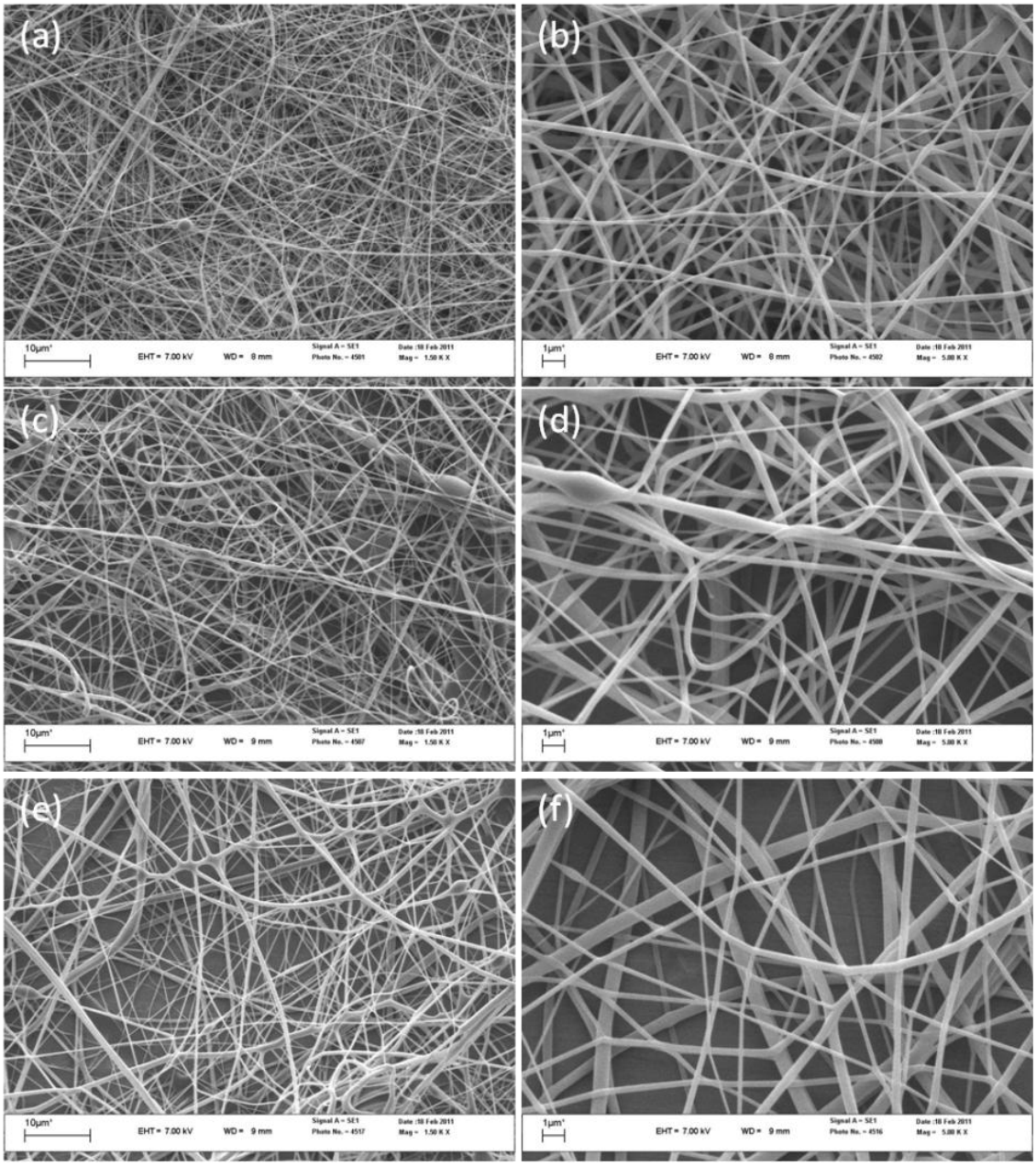

Figure A-7: SEM images of bubble-electrospinning fibers at 37.5kV/15cm. (a-b) 12 wt% POVH at 1500 and 5000x magnification, respectively; (c-d) 14 wt% POVH at 1500 and 5000x magnification, respectively (spun at a field strength of 42.5kV/15cm); (e-f) 15 wt% POVH at 1500 and 5000x magnification, respectively.

Table A-3: Average fiber diameters of bubble-electrospinning solutions with increasing PVOH concentration.

Polymer Conc. (wt%)	Ave. Fiber Diameter (nm)	Std. Deviation (nm)
8	93.85	29.47
9	140.61	41.71
10	152.37	44.25
12	201.07	90.52
14	228.70	75.60
15	300.06	158.21

The average fiber diameter measurements followed the trend of increasing fiber diameters with increasing polymer concentration. It is obvious that there are large differences in the quality of fibers when needle- and bubble-electrospun fiber images are compared. Needle-electrospun fibers appeared uniform with a small standard deviation overall. Bubble-electrospun fibers had a large standard deviation in fiber diameters. Another note was that the nanofibers of 8 and 9 wt% PVOH solutions differ between needle- and bubble-electrospinning in terms of fiber uniformity.

A.4 Conclusion

A range of polymer concentrations were bubble-electrospun to investigate the influence on solution properties, the bubble-electrospinning process and the resultant fibers. Solutions containing between 8 and 12 wt% PVOH concentration gave uniform and dry fibers with small fiber diameters. Polymer concentrations 8, 10 and 12 wt% PVOH was therefore selected for further experiments.

Smit (1) studied the bubble-electrospinning of PVOH solutions and found optimum bubble-electrospinning results for solutions containing 1 x cmc SDS surfactant. Higher surfactant concentrations were not tested. Surfactant concentrations were selected for experiments based on results found in Smit‘s study and to investigate the influence of higher surfactant concentrations. It is for this reason that a surfactant concentration below (0.5 x cmc) and above (2 x cmc) 1 x cmc SLES surfactant were selected for further experiments.

Addendum B: Pilot Study on PAN Polymer and Surfactant Concentration Range Selection

A large number of polymer and surfactant concentrations were tested to define a small range of concentrations for future experiments within which PAN solution bubble-electrospun. The solution properties of all solutions were measured (solution viscosity, -conductivity and –surface tension). The solutions were needle- and bubble- electrospun. The resultant fibers were then imaged using a Scattering Electron Microscope (SEM) and measured to obtain the average fiber diameters. The results are discussed in the sections to follow.

The first set of experiments was done on solutions containing the following PAN concentrations and the same surfactant concentration:

4, 5, 5.5, 6, 6.5, 7 and 8 wt% PAN.

A second set of experiments were done on solutions containing the following silicone surfactant concentrations and 6 wt% PAN:

0.25, 0.50, 0.75, 1.00, 1.25, 1.50, 2.00 and 4.00 wt% silicone surfactant.

The polymer was added to DMF solvent at room temperature and stirred for 30 minutes. The mixture then was heated for 1 hour at 50 °C. Silicone surfactant was added and the solution stirred for another 30 minutes at 50 °C.

B.1 Solution Property Measurements

The viscosity, electrical conductivity and surface tension of the polymer solutions were measured.

B.1.1 Solution Viscosity

The viscosities of the solutions were measured with a Brookfield RVTD Viscometer, fitted with a small sample adapter, and a cylindrical spindle (nr.21). The small sample adapter was controlled at 25˚C (±1.0˚C).

Figure B-1 shows the results of solution viscosities for a range of polymer concentrations.

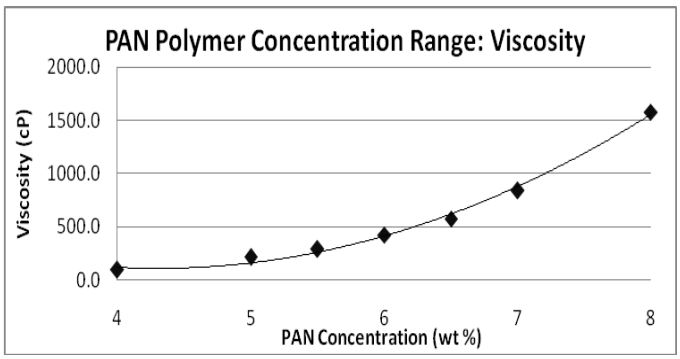

Figure B-1: Viscosity vs. PAN Polymer Concentration

Figure B-2 shows results of solution viscosities for a range of silicone surfactant concentrations.

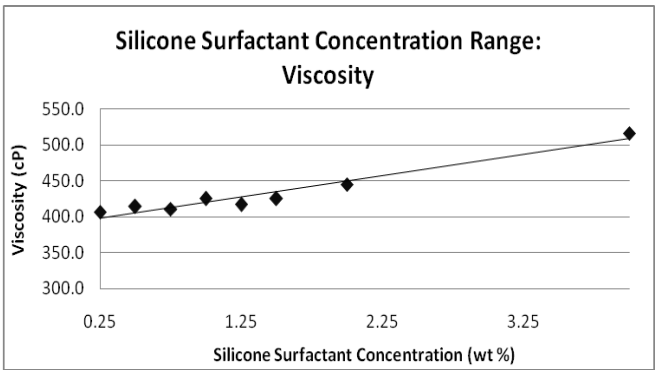

Figure B-2: Solution viscosity of solutions within silicone surfactant concentration range.

Figure B-1 and Figure B-2 shows that the solution viscosity increased with increasing polymer concentrations and slightly increased with increasing silicone surfactant concentration. This is a common trend found in literature, specifically with electrospinning solutions and their range of viscosities.(5,91)

B.1.2 Solution Conductivity

The solution conductivity was measured using a Hanna Instrument, EC 215 Conductivity meter. The calibration solutions were supplied by SPRAYTECH, EC84. All solutions were kept in a 25˚C (±0.5˚C) water bath directly prior to measurements.

Figure B-3 shows the solution conductivities of solutions containing increasing concentrations of polymer:

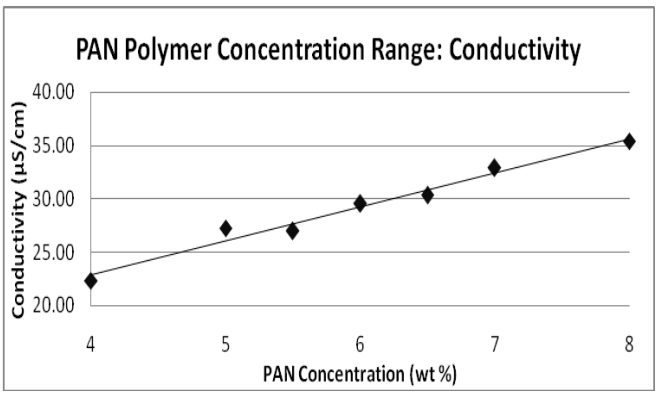

Figure B-3: PAN solution electrical conductivity with increasing polymer concentations.

Figure B-4 shows the solution conductivities of solutions containing increasing concentrations of silicone surfactant:

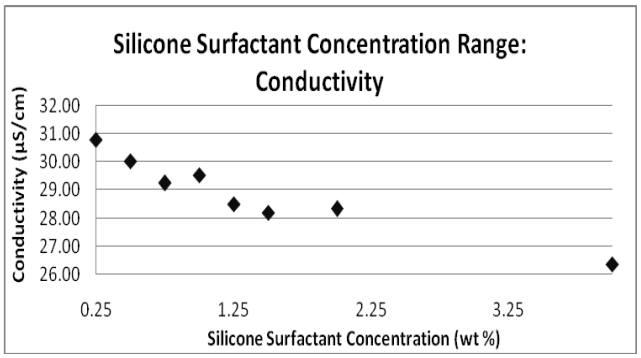

Figure B-4: PAN solution electrical conductivity with increasing silicone surfactant concentrations.

The electrical conductivity of the polymer solutions increase with increasing polymer concentration but decreases with increasing surfactant concentration. The increase in conductivity with increasing polymer concentration could be due to increasing contaminants from polymer and/or a decrease in DMF volume with increasing polymer concentrations (electrical conductivity of DMF: 0.9µS/cm).

The conductivity decreases, on the other hand, with increasing surfactant concentration. The non-ionic silicone surfactant carries no net charge and hence decreases the solution conductivity with increasing concentration.

B.1.3 Solution Surface Tension

A GBX Digital Droplet Contact Angle Analyzer (Didigdrop) was used to measure the surface tension from pendant droplets of the solution. A Teflon needle, 20 Gauge diameter, blunt point was used for measurements. The surface tensions of a growing droplet was recorded

and analyzed. The surface tension measured at the break of the droplet was used for further data analysis.

Figure B-5 shows the surface tension measurements of PAN solutions with increasing polymer concentrations.

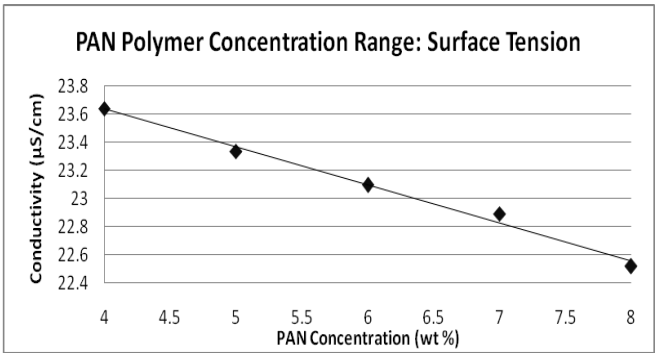

Figure B-5: Surface Tension of PAN solutions with increasing polymer concentrations.

Figure B-6 shows the surface tension measurements of PAN solutions with increasing silicone surfactant concentrations.

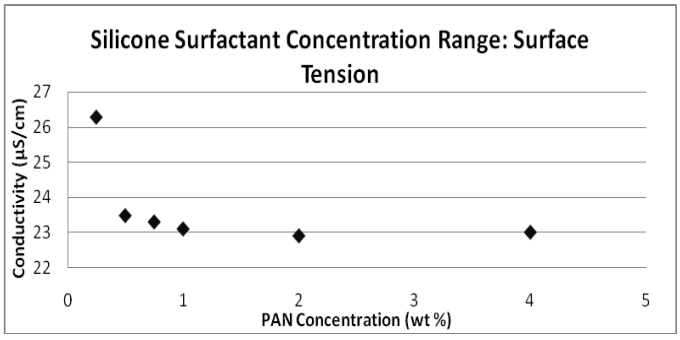

Figure B-6: Surface Tension of Solutions within silicone surfactant concentration range.

The surface tension of PAN solutions decreases with increasing polymer concentration. At higher polymer concentrations the solvent concentration is less, hence a lower surface tension (Surface tension of DMF: 33.7 mN/m at 25 ˚C). The surface tension of the solutions containing increasing amounts of silicone surfactant show a slight decrease in surface tension from 26.3mN/m to 23.5mN/m for solutions with 0.25 wt% to 0.5 wt% silicone surfactant concentration, respectively. Surface tensions of solutions containing 0.5 wt% - 4 wt% silicone surfactant, remain relatively constant at an average of 23.1 mN/m.

B.2 Bubble-Electrospinning

All solutions were bubble-electrospun at room temperature (temperatures and relative humidities are indicated). The field strength was set at 35kV/15cm (Voltage applied to solution bath: 25+kV. Voltage applied to collector: 10-kV). The average number of jets per bubble and average bubble size were recorded. The average number of jets and average bubble size data was calculated from 5 bubble-electrospinning bubbles.

B.1.4 Polymer Concentration Range

The average number of jets, average bubble size and the ambient conditions are listed in Table B-1.

Table B-1: Average number of jets and average bubble size during bubble electrospinning solutions within the PAN concentration range.

Polymer Concentration (wt%)	Surfactant Concentration (wt%)	Average number of Jets (5 bubbles)	Average size per bubble (mm)	Temperature (˚C) / Rel. Humidity (%)
4	**1**	5	14.74	22.5 ˚C / 49%
5	**1**	7	17.67	20.4 ˚C / 48%
5.5	**1**	5	19.00	21.8 ˚C / 46%
6	**1**	15	16.32	25.5 ˚C / 45%
6.5	**1**	2	16.74	21.3 ˚C / 47%
7	**1**	9	17.66	19.6 ˚C / 50%
8	**1**	3	17.01	21.8 ˚C / 45%

The 6 wt% PAN solution had the highest average number of jets per bubble. The bubble size did not vary significantly between the various solutions except for the 4 and 5.5 wt% PAN solutions. From observations, the 4 wt% PAN solution was difficult to spin simply because the larger bubbles were very unstable in the presence of an electric field.

The 6 wt% PAN solution gave the largest number of jets, hence the highest productivity of all solutions.

B.1.5 Surfactant Concentration Range

The average number of jets, average bubble size and the ambient conditions are listed in Table B-2.

Table B-2: Average number of jets and average bubble size during bubble electrospinning solutions within the silicone surfactant concentration range.

Polymer Concentration (wt%)	Silicone Surfactant Concentration (wt%)	Average number of Jets (5 bubbles)	Average size per bubble (mm)	Temperature (˚C) / Rel. Humidity (%)
6	**0.25**	6	13.42	26.1°C / 44%
6	**0.50**	8	17.18	25.4°C / 44%
6	**0.75**	8	16.94	25.6°C / 45%
6	**1.00**	15	16.32	25.5°C / 45%
6	**1.25**	6	17.45	21.8°C / 47%
6	**1.50**	6	18.16	21.8°C / 47%
6	**2.00**	3	15.75	25.8°C / 44%
6	**4.00**	4	15.34	25.4°C / 46%

The 1 wt% silicone surfactant solution showed the highest number average of jets per bubble. The bubbles from the 1 wt% silicone surfactant solution produced a large number of jets with every bubble that was electrospun. The 0.75 wt% silicone surfactant solution also showed easy spinning, producing a good number of jets with every bubble. The 0.5 wt% silicone surfactant solution showed a good number of jets but the ability to get a stable bubble that ejects jets, was more difficult when compared to the bubble-electrospinning of 0.75 wt% and 1.00 wt% silicone surfactant solutions.

The average bubble size was small for the solution containing 0.25 wt% silicone surfactant in comparison to the other solutions within the range. This can be explained by the high surface tension of the 0.25 wt% silicone surfactant solution. Maximum bubble size of a spinning bubble was achieved with the solution containing 0.5 wt% silicone surfactant. The bubble size then decreased slightly with further increases in surfactant concentrations.

The maximum number of jets produced during bubble-electrospinning was with the solution containing 1 wt% silicone surfactant. The maximum bubble size was achieved with solutions containing 0.5 wt% silicone surfactant concentration but the solution had difficulty forming stable bubbles that spun.

B.3 SEM images and Fiber Diameters

Fiber samples were imaged using A Leo® 1430VP Scanning Electron Microscope (SEM) – Central Analytical Facility, Stellenbosch University. Approximately 100 fibers were measured using a SEM Image Studio programme.

B.1.6 Polymer Concentration Range

The fibers bubble-electrospun from solutions is shown in Figure B-7.

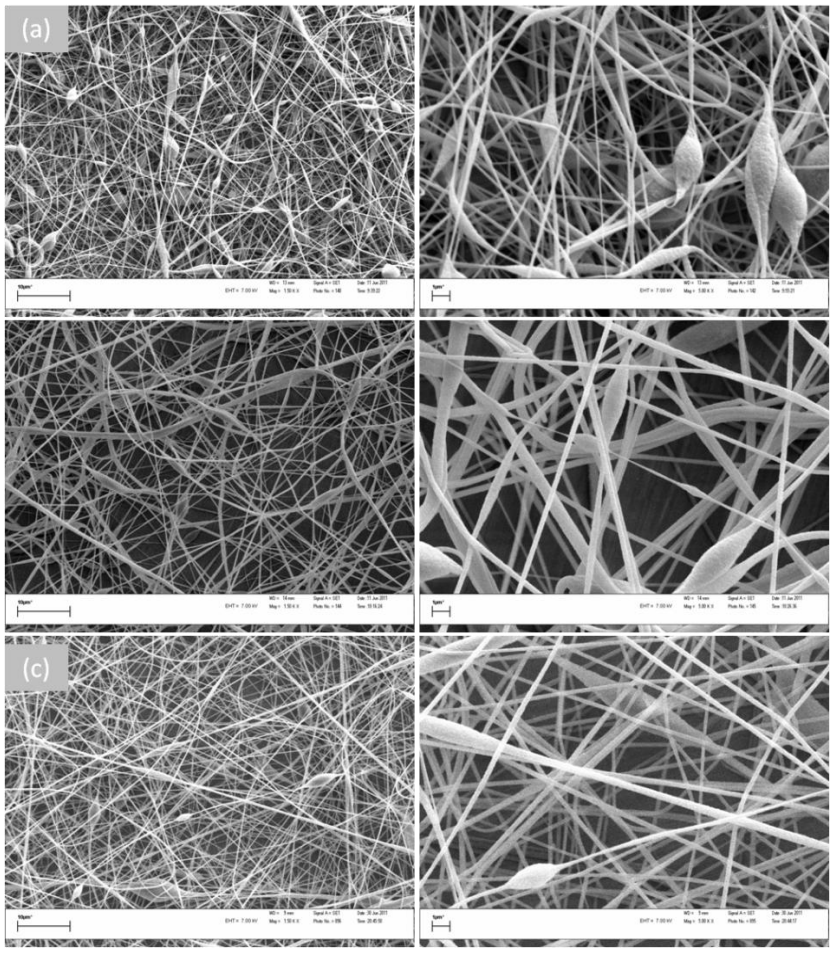

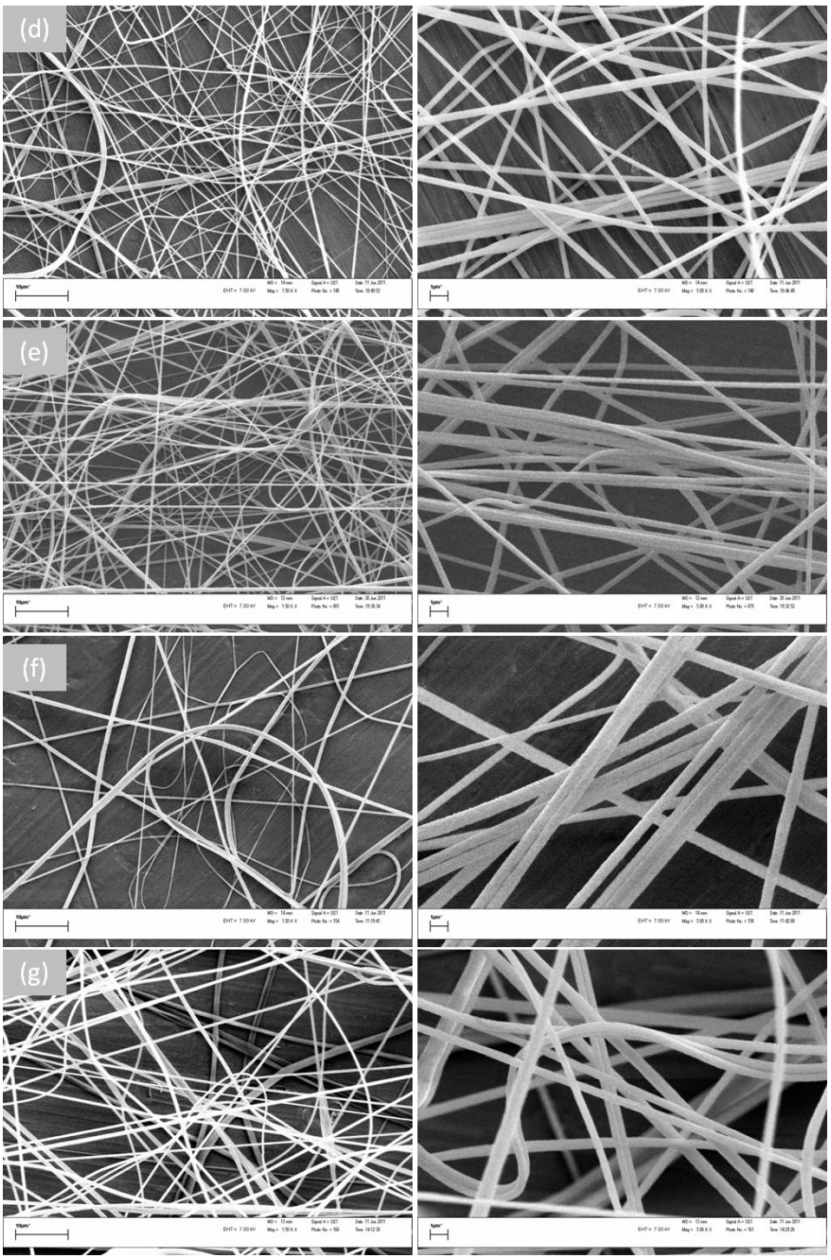

Figure B-7: SEM images of bubble-electrospun solutions in PAN concentration range at 1500x (left) and 5000 x (right) magnifications. Fiber samples from solutions containing (a) 4 wt % PAN; (b) 5 wt % PAN; (c) 5.5 wt % PAN concentration; (d) 6 wt % PAN; (e) 6.5 wt % PAN; (f) 7 wt % PAN; and (g) 8 wt% PAN.

The average fiber diameters of the bubble-electrospun fibers are shown in Figure B-8.

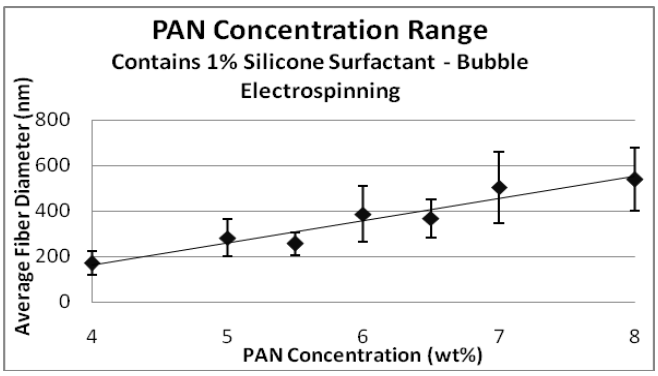

Figure B-8: Average fiber diameters of fibers bubble-electrospun from solutions within the polymer concentration range.

From Figure B-7 it was observed that the number of beads decrease with increasing polymer concentration from 4 to 6 wt % PAN. Solutions with polymer concentrations of 6 wt% and above appear to have no beading but the fibers have a larger range in fiber diameters, as reflected in the standard deviation of the average fiber diameters (refer to Figure B-8). The fibers also increase in average fiber diameter with increasing polymer concentrations which was expected from the significant increases in solution viscosity.

The 4 wt% PAN solution bubble-electrospun with difficulty and formed smaller bubbles in comparison to other solutions and formed a large number of beaded fibers. The 5 wt% PAN solution showed a lesser degree of beading with more uniformity in fiber diameter. The 8 wt% PAN solution had poor bubble stability during bubble-electrospinning and a few number of jets per bubble. 7 and 8 wt% PAN solutions showed a large standard deviation in bubble-electrospun fiber diameters.

The results are based on the solution properties of the solutions. Solutions of low viscosity and high surface tension give beaded fibers, whilst solutions of high viscosity form fibers with large fiber diameters.

B.1.7 Surfactant Concentration Range

Below in Figure B-9 are SEM images of fibers bubble-electrospun from solutions within the silicone surfactant concentration range.

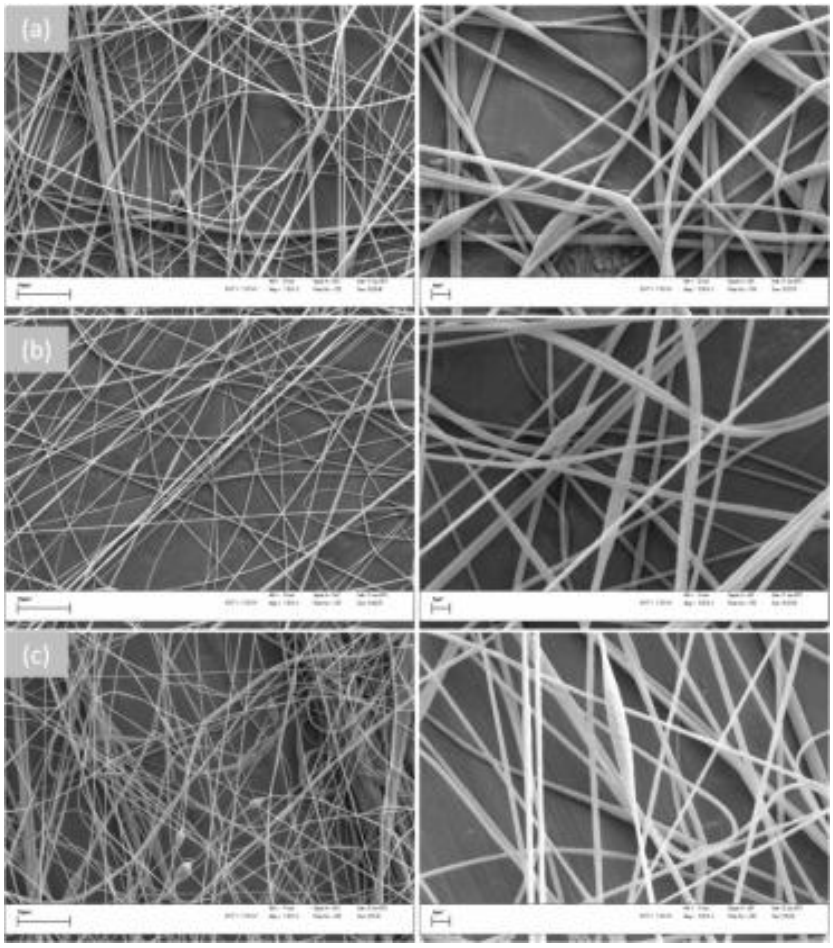

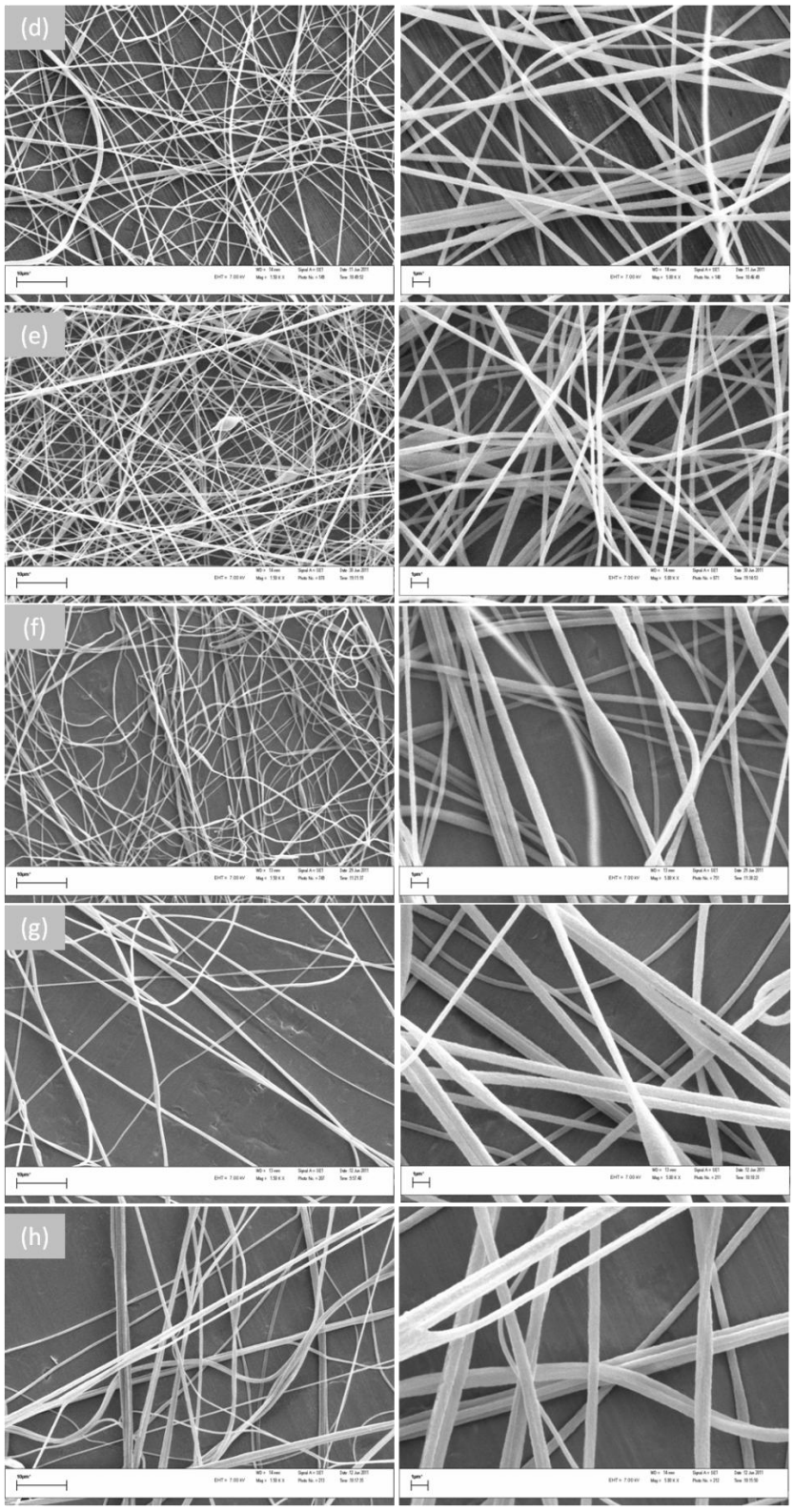

Figure B-9: SEM images of bubble-electrospun solutions in silicone surfactant concentration range at 1500 x (left) and 5000x (right) magnifications. Fiber samples from solutions containing (a) 0.25 wt% silicone surfactant; (b) 0.50 wt% silicone surfactant; (c) 0.75 wt% silicone surfactant; (d) 1.00 wt% silicone surfactant; (e) 1.25 wt% silicone surfactant; (f) 1.50 wt% silicone surfactant; (g) 2.00 wt% silicone surfactant; and (h) 4.00 wt% silicone surfactant.

The average fiber diameters of the bubble-electrospun fibers are shown in Figure B-10.

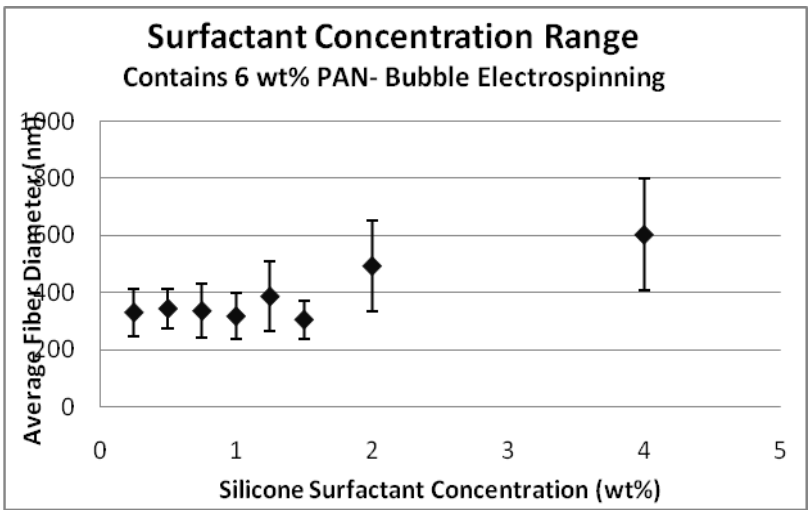

Figure B-10: Average fiber diameters of fibers spun from solutions within the silicone surfactant concentration range.

From Figure B-9 it can be seen that fibers from solutions containing 0.25 wt% to 0.75 wt% silicone surfactant concentrations, showed decreasing amounts of beading, respectively.

The fibers appear uniform along the fiber length (no beading) for solution containing 1 wt% silicone surfactant, whilst showing non-uniformity along the fiber length for solutions containing 2wt% and 4 wt% silicone surfactant. The fibers produced from the 4 wt% silicone surfactant solution have a large standard deviation (refer to Figure B-10) and appear ―messy" in terms of fiber diameter distribution and clustering of fibers along their lengths. The clusters of fibers are due to insufficient solvent evaporation of fibers with large fiber diameters.

Figure B-10 shows the average fiber diameters of fibers bubble electrospun from solutions within the silicone surfactant concentration range. The average fiber diameters remain generally unchanged for solutions containing 0.25 wt% to 1.0 wt% silicone surfactant concentration. The average fiber diameter then increases with further increases in silicone surfactant concentration possibly due to increasing number of interactions between the polymer and surfactant molecules, which in turn increases the solution viscosity.

B.4 Conclusion

Results based on bubble-electrospinning of solutions in the polymer concentration range, indicated that the 6 wt% PAN solution had the highest productivity, gave uniform fibers and had an average fiber diameter of 316.78nm. Solutions containing 5 wt% PAN gave mostly uniform fibers with slight traces of beads whilst the 7 wt% PAN solution gave fewer jets during bubble-electrospinning but still uniform fibers.

Due to the possibility that the solutions containing 6 wt% PAN gives the largest average number of jets and most uniform fibers with a small average fiber diameter, it was decided to use the following polymer concentrations for future experiments with PAN solutions: 5, 6, and 7 wt%. 5 and 7 wt% PAN solutions were selected based on its ability to form large bubbles and sufficient number of jets during bubble-electrospinning, and on the fiber quality produced in these trail experiments.

From results based on the bubble-electrospinning of solutions within the surfactant concentration range, it was observed that the solution containing 1 wt% silicone surfactant gave the highest average number of jets per bubble. The solution containing 0.5 wt% silicone surfactant on average formed the largest bubbles during bubble-electrospinning but formed bubbles with difficulty. Fibers spun from the 1 wt% silicone surfactant solution also contained no beads.

Solutions containing 2 and 4 wt% silicone surfactants gave wider and more non-uniform fibers in appearance. The solution containing 4 wt% silicone surfactant produced clusters of fibers due to insufficient solvent evaporation.

Based on the large average number of jets and fiber quality of PAN solution containing 1 wt% silicone surfactant, the surfactant concentration was selected as the centre-point of the concentration range for future experiments with PAN solutions. 0.5 wt% and 2 wt% concentrations was also selected based on its ability to sufficiently stabilise bubbles during bubble-electrospinning and produce uniform fibers.

Addendum C: PVOH Solution Properties over Time

Polyvinyl Alcohol (PVOH) solutions, containing sodium lauryl ether sulphate (SLES) surfactant, were prepared to investigate possible changes in solution properties over time. PVOH solutions were prepared with the following polymer and surfactant concentrations:

PVOH concentrations (wt%): 8, 10, and 12.

SLES concentrations (x CMC*): 0.5, 1, and 2.

*(The critical micelle concentration (CMC) of SLES surfactant is 0.0008M)

The solution properties (solution viscosity, electrical conductivity and surface tension) of the PVOH solutions were measured at specific time intervals (1 h, 3.5 h, 24 h and 96 h after the solutions was prepared). The bulk solution (100 ml) was firstly separated into four containers for the four specific tests at the four time intervals i.e. no solution was measured twice.

All solution properties were measured at 25˚C (± 1.0˚C). Solutions were heated at 80˚C for 30 minutes, and then cooled to 25˚C, prior to measurements taken at 3.5, 24, and 96 hours. Solutions were made in triplicate.

C.1 Solution Viscosity

The solution viscosity was measured using a Brookfield RVTD Viscometer, fitted with a small sample adapter, and a cylindrical spindle (nr.21). The shear rate of the spindle was 60 rpm for all measurements.

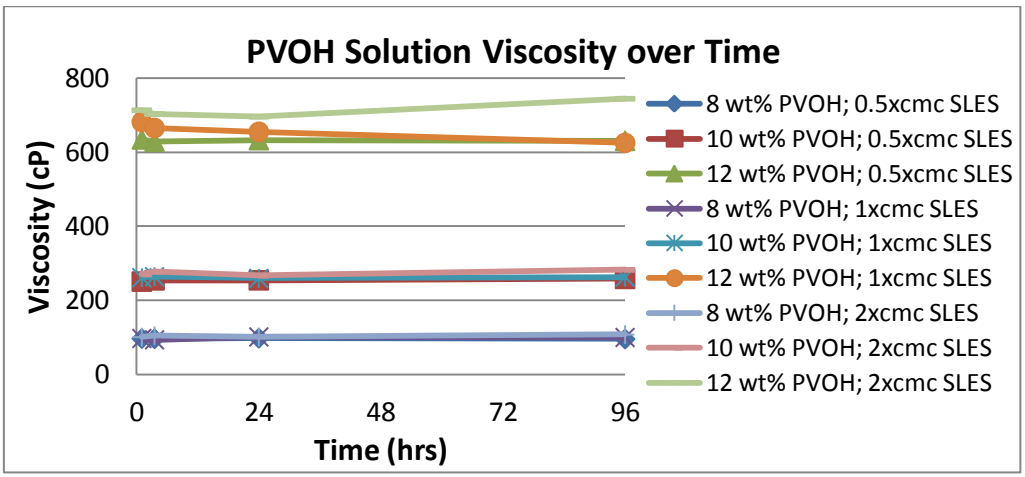

Figure C-1: PVOH solution viscosity over time. Measurements took place after 1h, 3.5h, 24h, and 96h after homogeneous polymer solution was removed from heated oil bath. Measurements took place at 25˚C.

Figure C-1 is a graph showing the influence of solution age on solution viscosity. The general observed trend with regards to time is that the solution viscosity remains consistent over 96 hours. The coefficient of variance (%) was calculated for each solution to see the variance in solution viscosity over time:

Polymer Concentration (wt%)	8			10			12		
Surfactant Concentration (x cmc)	0.5	1	2	0.5	1	2	0.5	1	2
Coefficient of Varriance (%)	1.0	3.5	3.0	1.2	0.7	2.6	0.4	3.6	3.0

A general % variance of 0.4 to 3.6% was observed.

C.2 Solution Conductivity

A Hanna Instruments, EC 215 Conductivity meter was used for solution conductivity measurements. The calibration solutions were supplied by SPRAYTECH, EC84.

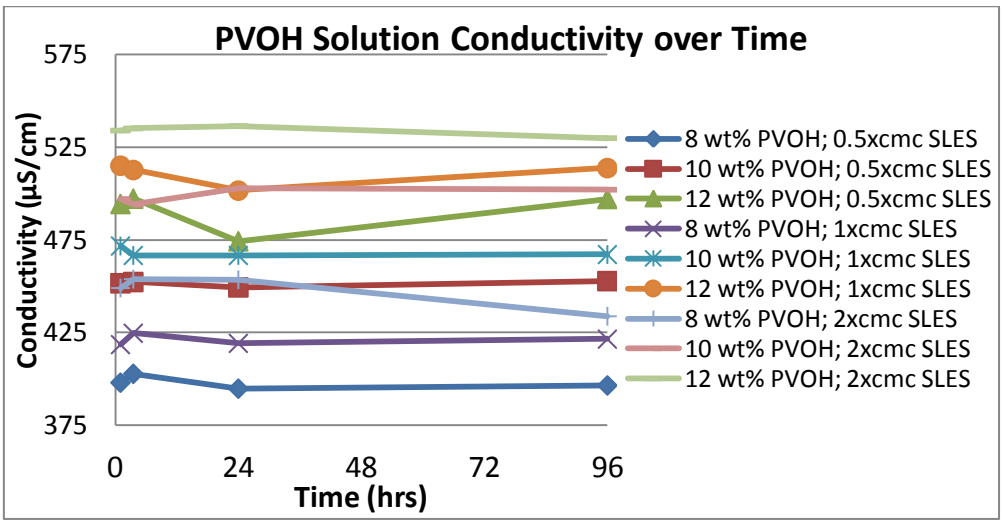

Figure C-2: PVOH solution conductivity over time. Measurements took place after 1h, 3.5h, 24h, and 96h after homogeneous polymer solution was removed from heated oil bath. Measurements were taken at 25˚C.

Figure C-2 is a graph showing the influence of solution age on the solution electrical conductivity. The general observed trend with regards to time is that the solution conductivity remains consistent over 96 hours. The coefficient of variance (%) was calculated for each solution to see the differences in solution conductivity over time:

Polymer Concentration (wt%)	8			10			12		
Surfactant Concentration (x cmc)	0.5	1	2	0.5	1	2	0.5	1	2
Coefficient of Variance (%)	0.9	0.7	2.1	0.3	0.5	0.8	2.3	1.2	0.5

The percentage variance in solution conductivity over time varies between 0.3 and 2.3%.

C.3 Solution Surface Tension

The surface tension of PVOH solutions were measured using a GBX digital droplet contact angle analyzer (pendant drop method). 5 drops were measured for each solution. The surface tension at the break of the droplet was calculated for each droplet.

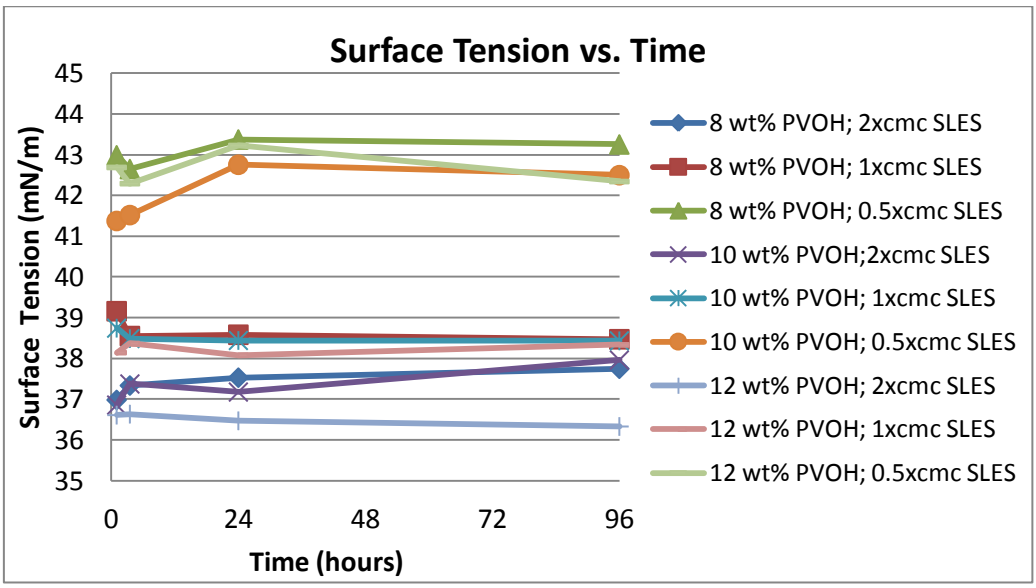

Figure C-3: PVOH solution surface tension over time. Measurements took place after 1h, 3.5h, 24h, and 96h after homogeneous polymer solution was removed from heated oil bath. Measurements were taken at 25˚C.

The surface tension varied slightly over time, specifically with regards to 12 wt% PVOH solutions. All solutions appeared to show slight changes in surface tension between 1 and 3.5 hours. The variance in surface tension could possibly be caused by further heating of 30 minutes for solutions measured at 3.5 hours and later. The coefficient of variance (%) was calculated for each solution to see the variance in solution surface tension over time:

Polymer Concentration (wt%)	8			10			12		
Surfactant Concentration (x cmc)	0.5	1	2	0.5	1	2	0.5	1	2
Coefficient of Variance (%)	0.7	0.8	0.9	1.6	0.4	1.2	1.0	0.4	0.4

Solutions varied between 0.4% and 1.6% for measurements between 1 and 96 hours. It is required that all solutions endure the same time interval of heating prior to all measurements. Surface tension measurements remain significantly consistent after 3.5 hours.

C.4 Conclusion

Solution properties generally remained consistent over time. Solutions would need to be heated for equal periods of time prior to all measurements.

The suggested procedure for the preparation and measurements of solutions was to make polymer solutions and allow the solutions to stir at room temperature for a minimum of 3.5 hours. The solution was separated into two separate containers of 80 ml and 20 ml. Each solution would be heated to 80˚C for 30 minutes prior to any measurements.

Solution surface tension measurements, needle-electrospinning and bubble-electrospinning of solutions would all be done within at 24 hours after the bulk solution was prepared (80 ml solution). Solution conductivity and viscosity would be measured between 3.5 and 96 hours after the bulk solution was prepared (20 ml solution).

Addendum D: PAN Solution Properties over Time

PAN solutions were prepared, containing silicone surfactant, in DMF solvent to investigate the influence of time on the solution properties of the solution. Polymer and surfactant concentrations were as follows:

Polymer concentration (wt%): 5, 6, and 7 wt%

Silicone surfactant (wt%): 0.5, 1, and 2 wt%

The solution properties (solution viscosity, electrical conductivity and surface tension) of the PAN solutions were measured at specific time intervals after removing a homogeneous polymer solution from the 50˚C bath. The homogeneous solution was separated into three containers for the three specific tests at the 1h, 3.5h, and 24h time intervals i.e. no solution was measured twice.

All solution properties were measured at 25˚C (± 1.0˚C). Solutions were heated at 50˚C for 30 minutes, and then cooled to 25˚C, prior to measurements taken at 3.5 and 24 hours.

D.1 Solution Viscosity

The solution viscosity was measured using a Brookfield RVTD Viscometer, fitted with a small sample adapter, and a cylindrical spindle (nr.21). The shear rate of the spindle was 60 rpm for measurements of 5 and 6 wt% PAN solutions, whilst 30 rpm for 7 wt% PAN solutions.

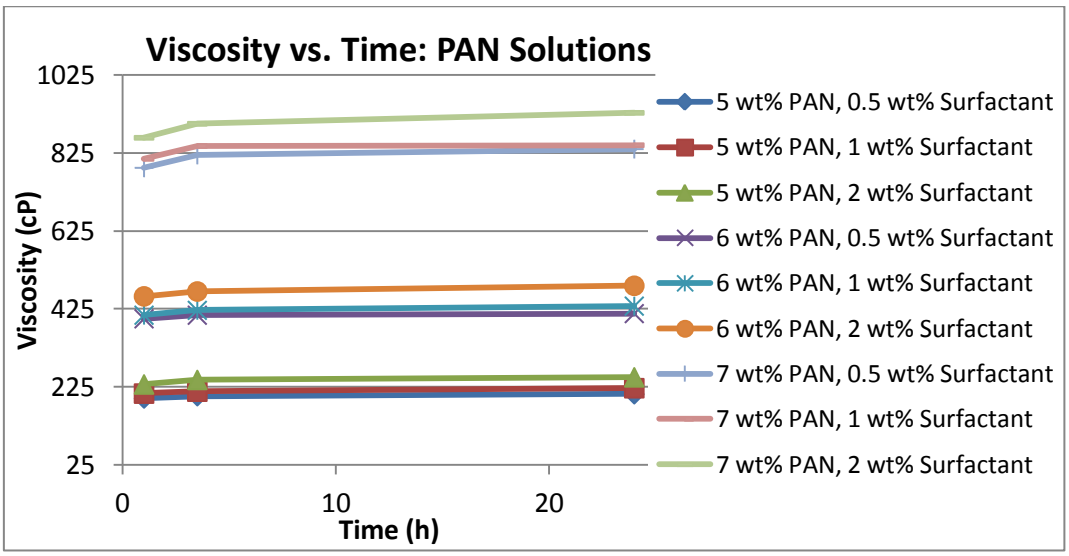

Figure D-1: PAN solution viscosity measurements over time.

Figure D-1 shows the influence of time on the viscosity of the solution. The viscosity of the solution changed over time. All solutions had their lowest viscosity at the 1 h interval.

Table D-1: PAN solution viscosity over time.

		Viscosity (cP)		
Polymer Concentration (wt%)	**Surfactant concentration (wt%)**	**0.5**	**1**	**2**
		Time (h)		
5	**1**	195.8	208.3	231.7
5	**3.5**	201.7	213.3	243.3
5	**24**	206.7	222.1	250
6	**1**	400	409.2	457.5
6	**3.5**	409.2	421.7	470
6	**24**	413.3	432.5	484.6
7	**1**	787	810	864
7	**3.5**	820	843	900
7	**24**	835	845	928

From Table D-1 it is clear that the solution viscosity definitely increased with slight increments over time. Increases in viscosity are possibly due to increasing polymer-polymer and polymer-surfactant interactions over time, and possible loss of solvent content.(84,85)

It was expected that solutions with higher viscosities, would have more difficulty flowing along the bubble wall from the solution bath towards the solution jet, hence the bubbles would rupture earlier. The resultant fibers were also expected to have larger diameters due to more limited mobility of polymer chains.

It was decided to measure the solution whilst the solution viscosity was lowest, i.e. 1 h interval.

D.2 Solution Conductivity

A Hanna Instruments, EC 215 Conductivity meter was used for solution conductivity measurements. The calibration solutions were supplied by SPRAYTECH, EC84.

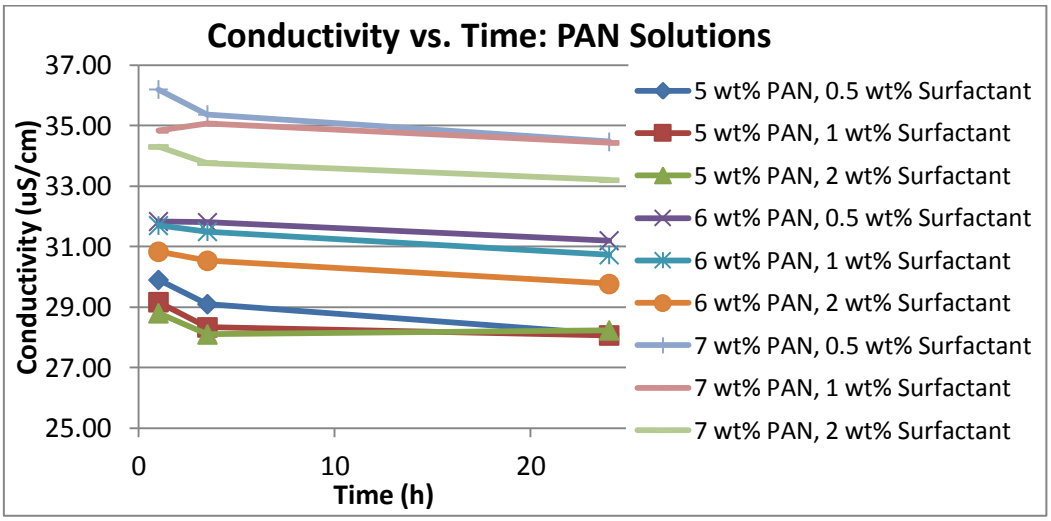

Figure D-2: PAN solution conductivity over time.

From Figure D-2 it was observed that the solution conductivity decreased over time. Solutions with higher conductivity were expected to dominate surface tension forces at the bubble wall easier, form a larger number of jets per bubble and, thus, have a higher productivity during bubble-electrospinning. The resultant fibers were expected to be more uniform due to more rapid whipping than solutions of low conductivity.

It was decided to measure the solution whilst the solution conductivity was at its highest, i.e. 1 h interval.

D.3 Solution Surface Tension

The surface tension of PVOH solutions were measured using a GBX digital droplet contact angle analyzer (pendant drop method) and Teflon needles (1.25mm outer diameter). 5 drops

were measured for each solution. The surface tension at the break of the droplet was calculated for each droplet.

The influence of time on the solution surface tension was measured and data displayed in Figure D-3.

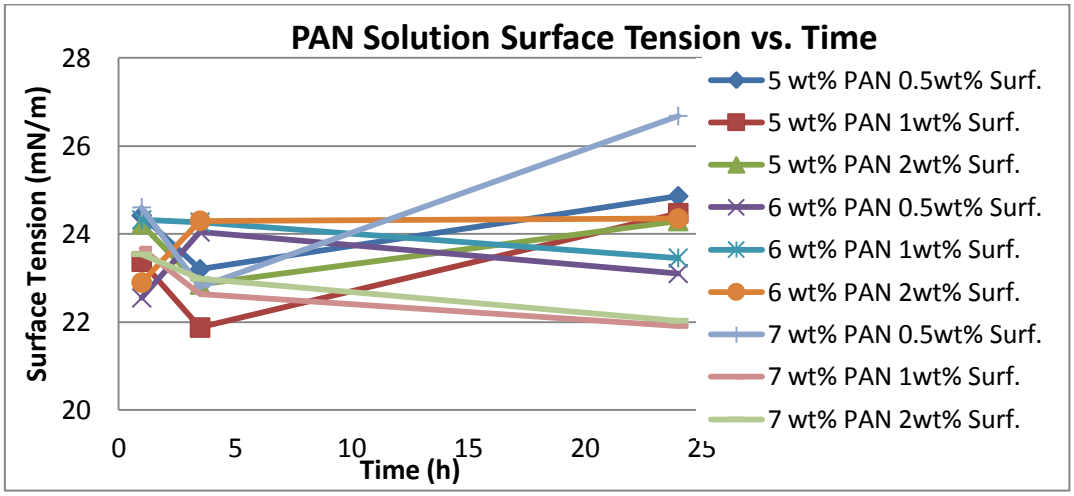

Figure D-3: PAN solution surface tension vs. Time

The data did not correspond with any trend identified in solution conductivity or solution viscosity. The tests were repeated but the interpretation of data remained obscure. It was discovered that the malleable Teflon needles changed in cross section shape over time which effected the calibration of the solution droplets (the needle outer diameter is used for calibration).

Due to time constraints it was decided to measure 4 sets of solutions, of 3 polymer and surfactant concentrations, at a 1 h interval and define a range of surface tension measurements as a guideline for further experiments. The average results over 4 sets of solutions are displayed in Figure D-4.

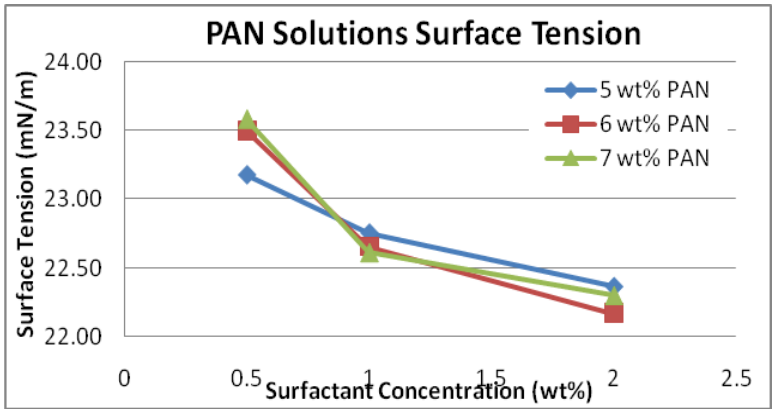

Figure D-4: PAN solution surface tension at 1 hour interval.

It was clear that the surface tension was reduced by increasing surfactant concentration which was expected due to the low surface energy of surfactants.

D.4 Conclusion

Based on results it was found that the solution viscosity increased and conductivity decreased over 24 h.

In addition, surface tension measurements with Teflon needles and Digidrop equipment gave inconsistent results due to the malleability of the needles. Results from surface tension measurements at a 1 h interval showed that the surface tension decreased with increasing surfactant concentration. It was decided to use results as a guideline for future surface tension measurements.

Based on the results, the experimental procedure for future experiments will be as follows:

The solutions were used for solution property measurements, needle- and bubble-electrospinning 1h after the solution was made. No PAN solutions were reheated for measurements. All measurements and electrospinning took place within 3.5 hours after the solution was removed from the heated stirrer.

Addendum E: Surface Tension Data Analysis Procedure

The surface tension of solutions was measured using GBX Digital Drop Contact Angle Analyzer. The data obtained from the droplet analyses could not easily be converted to information due the solution properties of the solutions. For this reason a suitable procedure for data analysis was constructed to obtain the surface tension at the break of any solution droplet. This section describes the analysis procedure of solution droplets to obtain a single surface tension value for each solution.

Five droplets per solution were recorded and analyzed using GBX Digital Drop Contact Angle Analyzer Windrop++ software. The surface tension vs. time data was then exported to and analyzed in Excel. Details on analysis procedures are described in Addendum C.

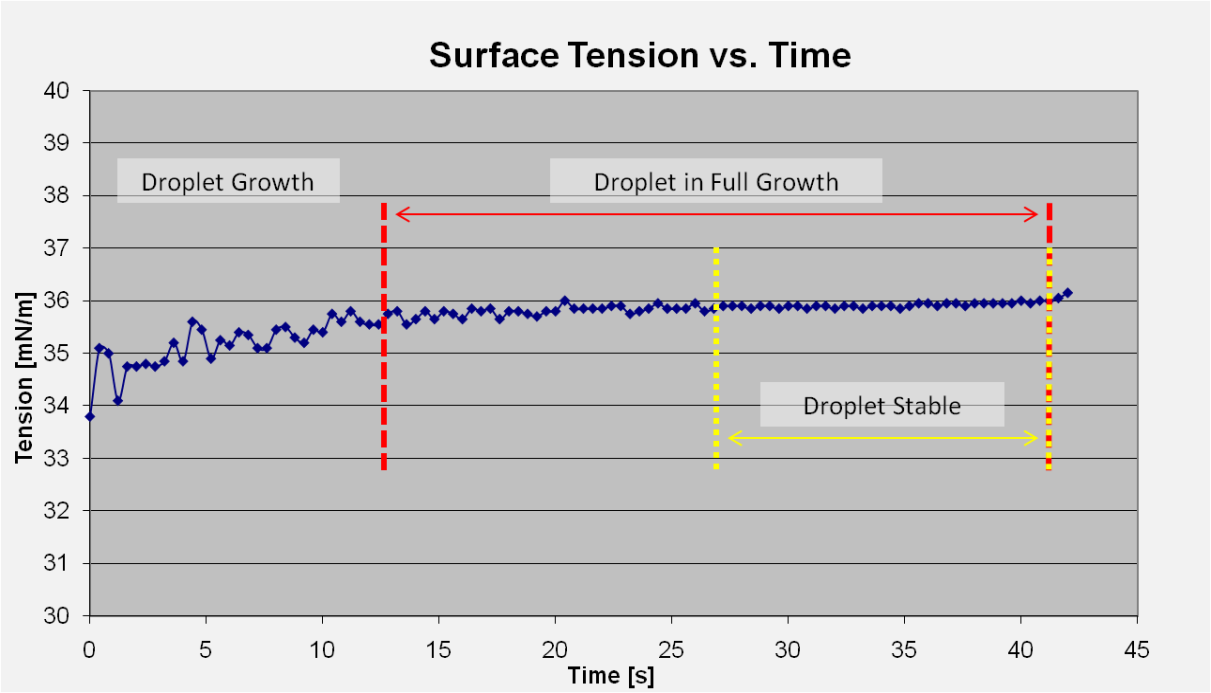

Figure E-1: Illustration of a droplet lifetime.

Figure E-1 is a graph of surface tension data from one droplet under continuous increases in droplet volume. The droplet undergoes an increase in surface tension as it grows. The droplet forms a pear-shape at the point of full growth. The volume of the droplet continues to increase whilst the droplet maintains its pear-shape. The surface tension of the droplet

becomes stable after a time interval specific to the solution. The droplet finally reaches maximum volume and breaks away from the needle.

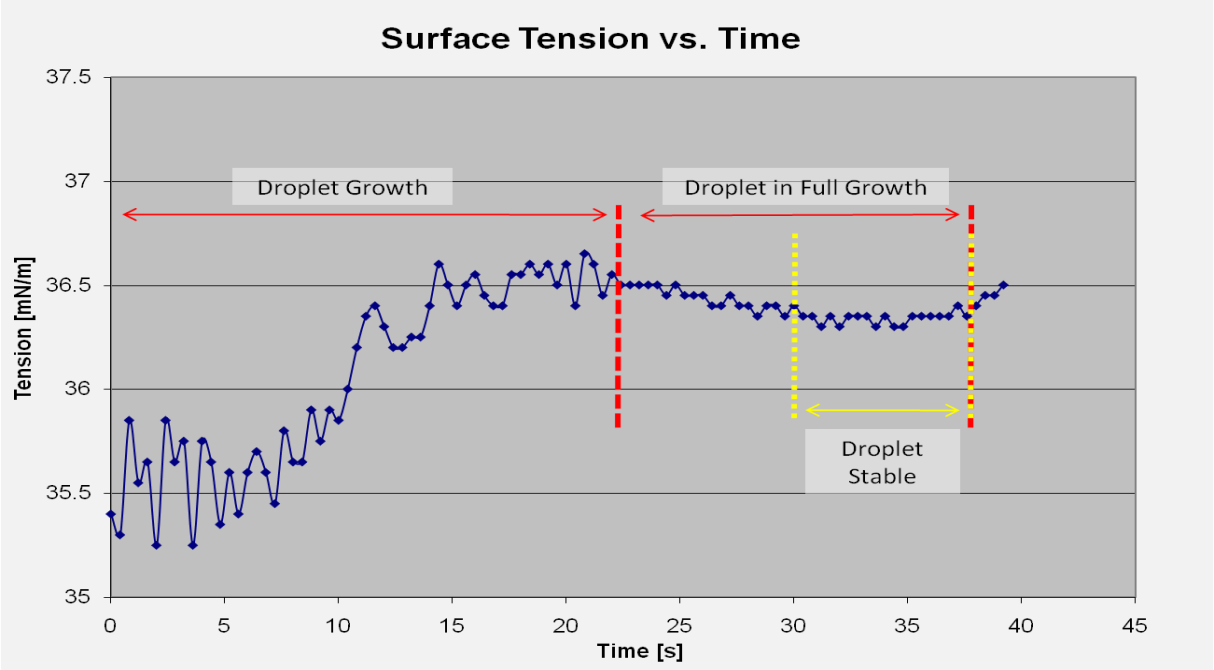

Figure E-2: Illustration of a highly polymer-concentrated solution droplet lifetime

Figure E-2 illustrates a droplet surface tension vs. time profile from a solution of higher polymer concentration than before. The surface tension vs. time profile appears slightly different to that of Figure E-1 but certain areas of droplet growth and stability can be identified.

In both Figure E-1 and Figure E-2, slight ~~-n~~oise" levels are observed, generally caused by vibrations in the surroundings. The vibrations experienced by the machine were minimized using insulation. The different surface tension vs. time profiles obtained from different solutions, and the slight noise levels displayed in data, lead to the decision to use the following procedure to obtain the surface tension at the break of the droplet:

Data from the stable region in the graph was isolated from the rest of the data and re-plotted on a new surface tension vs. time graph. A linear trendline equation was used to calculate the surface tension of the droplet directly prior to the break of the droplet.

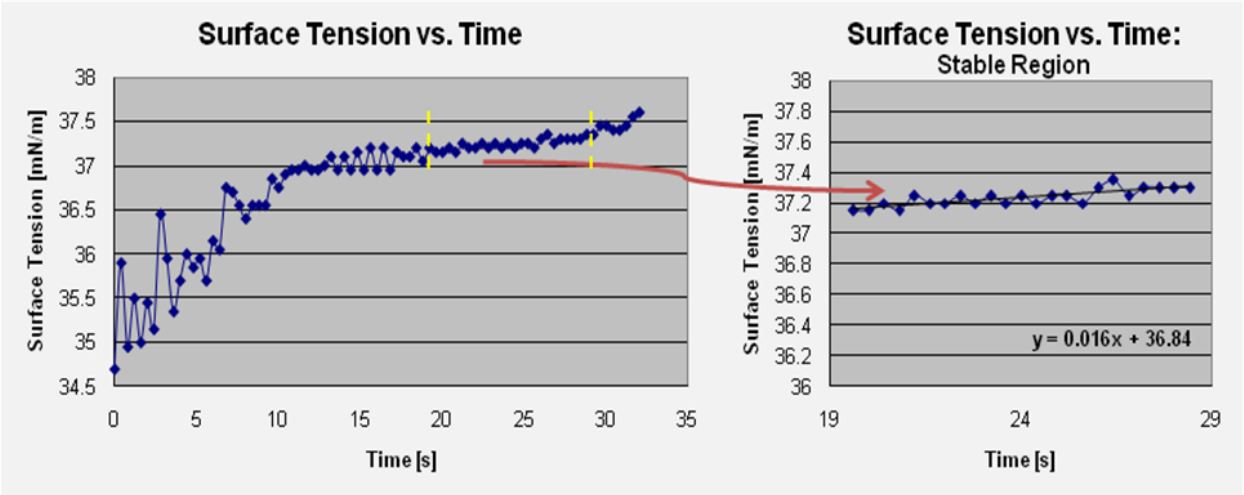

Figure E-3: Surface tension data analysis. Selection of the stable region from the original data and the application of a trendline.

The trendline equation was used to calculate the surface tension at the break of the droplet i.e. last data point on the stable region graph.

Five drops were analyzed per solution. Data from a minimum of three drops were used to calculate the average surface tension of a solution. The solution temperature was controlled at 25.0˚C (± 1.0˚C) throughout the measurement process.

Addendum F: Tables

This addendum includes all tables with regards to average solution properties, average bubble-electrospinning results, and average fiber diameters for both polymer solutions.

F.1 PVOH and PAN Solution Properties

The solution viscosity, conductivity and surface tension was measured for all solutions. The solution surface tension was not measured in triplicate. Table F-1 and Table F-3 list the average solution properties of PVOH and PAN solutions, respectively. Table F-2 and Table F-4 are the standard deviations of average PVOH and PAN solution properties, respectively. The solution properties of both solutions were measured at 25 °C (±1.0 °C).

Table F-1: Average solution properties of PVOH solutions.

Polymer (wt%)	Surfactant (xcmc)	Viscosity (cP)	Conductivity (µS/cm)	Surface Tension (mN/m)
8	**0.5**	93.88	383.78	48.08
8	**1**	95.97	408.44	44.77
8	**2**	96.23	442.89	43.06
10	**0.5**	229.73	434.67	48.07
10	**1**	263.50	462.44	45.38
10	**2**	259.02	495.78	41.96
12	**0.5**	617.96	487.33	47.47
12	**1**	578.57	504.22	43.86
12	**2**	673.03	531.44	41.30

Table F-2: Standard deviations of average PVOH solution properties.

Polymer (wt%)	Surfactant (xcmc)	Viscosity (cP)	Conductivity (µS/cm)	Surface Tension (mN/m)
8	**0.5**	4.46	5.27	-
8	**1**	5.65	6.85	-
8	**2**	3.17	2.14	-

10	**0.5**	47.72	8.67	-
10	**1**	12.88	6.95	-
10	**2**	10.49	0.51	-
12	**0.5**	32.92	3.00	-
12	**1**	11.42	3.84	-
12	**2**	65.29	5.85	-

Table F-3: Average solution properties of PAN solutions.

Polymer (wt%)	Surfactant (wt%)	Viscosity (cP)	Conductivity (µS/cm)	Surface Tension (mN/m)
5	**0.5**	201.06	29.03	24.55
5	**1**	209.02	28.38	23.54
5	**2**	218.77	26.93	23.24
6	**0.5**	414.43	32.71	24.41
6	**1**	412.10	31.33	23.48
6	**2**	448.18	31.54	22.89
7	**0.5**	781.45	34.57	23.60
7	**1**	810.83	33.82	22.64
7	**2**	860.50	32.23	22.80

Table F-4: Standard deviation of average PAN solution properties.

Polymer (wt%)	Surfactant (wt%)	Viscosity (cP)	Conductivity (µS/cm)	Surface Tension (mN/m)
5	**0.5**	8.32	0.99	-
5	**1**	8.15	0.91	-
5	**2**	10.11	0.23	-
6	**0.5**	11.03	2.53	-
6	**1**	7.71	2.12	-
6	**2**	7.92	1.79	-
7	**0.5**	18.67	0.74	-
7	**1**	23.63	1.68	-
7	**2**	10.33	0.86	-

F.2 Needle-Electrospun Fiber Diameters

All solutions were needle-electrospun with a field strength of +10 kV/15 cm. The solutions were spun at room temperature. The tables below list average fiber and bead diameters and the related standard deviations. Table F-5 and Table F-7 list the average fiber and bead diameters of PVOH and PAN fibers, respectively. Table F-6 and Table F-8 list the standard deviations of fiber and bead diameters for both PVOH and PAN fibers, respectively.

Table F-5: Average needle-electrospun PVOH fiber and bead diameters.

Polymer Concentration (wt%)	Surfactant Concentration (x cmc)	Average Fiber Diameter (nm)	Average Bead Diameter (nm)
8	**0.5**	83.67	349.34
8	**1**	88.38	285.49
8	**2**	84.56	301.75
10	**0.5**	136.34	290.52
10	**1**	126.35	308.37
10	**2**	116.39	301.45
12	**0.5**	185.34	-
12	**1**	162.45	-
12	**2**	147.48	-

Table F-6: Standard deviation of needle-electrospun PVOH fiber and bead diameters.

Polymer Concentration (wt%)	Surfactant Concentration (x cmc)	Fiber Diameter (nm)	Bead Diameter (nm)
8	**0.5**	21.51	72.10
8	**1**	24.33	61.28
8	**2**	26.59	77.49
10	**0.5**	22.87	63.35
10	**1**	24.43	50.22
10	**2**	25.50	60.83

12	**0.5**	33.16	-
12	**1**	29.95	-
12	**2**	25.96	-

Table F-7: Average needle-electrospun PAN fiber and bead diameters.

Polymer Concentration (wt%)	Surfactant Concentration (wt%)	Average Fiber Diameter (nm)	Average Bead Diameter (nm)
5	**0.5**	173.48	798.44
5	**1**	207.28	890.79
5	**2**	228.10	1066.95
6	**0.5**	300.80	1120.05
6	**1**	378.36	1070.50
6	**2**	454.59	1513.84
7	**0.5**	538.97	1406.67
7	**1**	595.44	-
7	**2**	729.58	2217.66

Table F-8: Standard deviation of needle-electrospun PAN fiber and bead diameters.

Polymer Concentration (wt%)	Surfactant Concentration (wt%)	Fiber Diameter (nm)	Bead Diameter (nm)
5	**0.5**	47.72	305.92
5	**1**	52.19	346.77
5	**2**	74.50	439.33
6	**0.5**	67.48	571.13
6	**1**	81.74	424.36
6	**2**	107.98	391.74
7	**0.5**	98.53	375.78
7	**1**	117.15	-
7	**2**	187.27	792.68

F.3 PVOH and PAN Bubble-Electrospinning Data

The bubble lifetime, bubble size, average number of jets per bubble and the bubble stability (average number of failed attempts in bubble formation prior to a new stable bubble formed). Table F-9 and

Table F-10 list the average bubble-electrospinning data for PVOH and PAN solutions, respectively. Table F-11 and Table F-12 list the standard deviations of bubble-electrospinning data for PVOH and PAN solutions, respectively. All solutions were bubble-electrospun at room temperature.

Table F-9: Average bubble-electrospinning data for PVOH solutions.

Polymer (wt%)	Surfactant (x cmc)	Bubble Size (mm)	Bubble lifetime (s)	Number of jets
8	**0.5**	23.96	182.62	1.00
8	**1**	28.29	115.55	1.00
8	**2**	22.95	140.54	1.11
10	**0.5**	25.88	142.57	1.03
10	**1**	27.76	58.16	1.10
10	**2**	22.26	114.21	1.22
12	**0.5**	25.29	227.88	2.21
12	**1**	29.74	25.63	1.18
12	**2**	24.01	65.82	1.60

Table F-10: Average bubble-electrospinning data for PAN solutions.

Polymer (wt%)	Surfactant (wt%)	Bubble Size (mm)	Ave no jets	Bubble Lifetime (s)
5	**0.5**	17.17	3.88	16.05
5	**1**	17.83	4.63	20.47
5	**2**	17.48	4.30	10.07
6	**0.5**	18.08	5.23	9.83
6	**1**	18.79	3.80	9.03
6	**2**	18.07	3.13	2.72
7	**0.5**	17.62	4.47	3.90
7	**1**	16.78	3.97	3.60
7	**2**	18.85	2.62	2.16

Table F-11: Standard deviation of average bubble-electrospinning data for PVOH solutions.

Polymer (wt%)	Surfactant (x cmc)	Bubble Size (mm)	Number of jets	Bubble lifetime (s)
8	**0.5**	0.65	0.00	149.76
8	**1**	3.05	0.00	62.92
8	**2**	1.41	0.18	60.49
10	**0.5**	3.63	0.06	18.26
10	**1**	1.12	0.14	38.71
10	**2**	0.97	0.17	84.92
12	**0.5**	1.97	0.91	140.86
12	**1**	1.84	0.04	31.08
12	**2**	1.64	0.51	19.63

Table F-12: Standard deviation of average bubble-electrospinning data for PAN solutions.

Polymer (wt%)	Surfactant (wt%)	Bubble Size (mm)	Ave no jets	Bubble Lifetime (s)
5	**0.5**	1.82	1.25	0.47
5	**1**	1.40	0.96	3.22
5	**2**	1.03	1.20	4.54
6	**0.5**	0.93	2.61	4.85
6	**1**	2.12	1.26	1.62
6	**2**	1.29	0.06	0.82
7	**0.5**	2.86	0.51	0.37
7	**1**	1.07	1.37	0.30
7	**2**	1.15	0.53	0.61

Table F-13: Temperatures and relative humidities during needle- and bubble-electrospinning of PAN and PVOH solutions

PVOH Solutions			
Polymer Concentration (wt%)	**Surfactant Concentration (x cmc)**	**Solution Set**	**Temp/ Humidity**
8	**0.5**	A	22.8˚C/40%
8	**0.5**	B	22.1˚C/43%
8	**0.5**	C	23.0˚C/42%
8	**1**	A	21.9˚C/42%
8	**1**	B	22.8˚C/42%
8	**1**	C	22.8˚C/42%
8	**2**	A	22.5˚C/41%
8	**2**	B	22.8˚C/41%
8	**2**	C	23.0˚C/44%
10	**0.5**	A	22.9˚C/43%
10	**0.5**	B	23.1˚C/41%
10	**0.5**	C	21.9˚C/41%
10	**1**	A	22.7˚C/44%
10	**1**	B	21.1˚C/45%
10	**1**	C	23.0˚C/45%
10	**2**	A	21.8˚C/46%
10	**2**	B	21.8˚C/45%
10	**2**	C	22.6˚C/47%
12	**0.5**	A	22.8˚C/45%
12	**0.5**	B	22.4˚C/44%
12	**0.5**	C	22.9˚C/47%
12	**1**	A	22.7˚C/47%
12	**1**	B	22.6˚C/43%
12	**1**	C	21.4˚C/48%
12	**2**	A	22.8˚C/44%
12	2	B	22.8˚C/45%
12	2	C	22.1˚C/43%

PAN Solutions			
Polymer Concentration (wt%)	**Surfactant Concentration (wt%)**	**Solution Set**	**Temp/ Humidity**
5	**0.5**	A	22.8˚C/40%
5	**0.5**	B	22.1˚C/43%
5	**0.5**	C	23.0˚C/42%
5	**1**	A	21.9˚C/42%
5	**1**	B	22.8˚C/42%
5	**1**	C	22.8˚C/42%
5	**2**	A	22.5˚C/41%
5	**2**	B	22.8˚C/41%
5	**2**	C	23.0˚C/44%
6	**0.5**	A	22.9˚C/43%
6	**0.5**	B	23.1˚C/41%
6	**0.5**	C	21.9˚C/41%
6	**1**	A	22.7˚C/44%
6	**1**	B	21.1˚C/45%
6	**1**	C	23.0˚C/45%
6	**2**	A	21.8˚C/46%
6	**2**	B	21.8˚C/45%
6	**2**	C	22.6˚C/47%
7	**0.5**	A	22.8˚C/45%
7	**0.5**	B	22.4˚C/44%
7	**0.5**	C	22.9˚C/47%
7	**1**	A	22.7˚C/47%
7	**1**	B	22.6˚C/43%
7	**1**	C	21.4˚C/48%
7	**2**	A	22.8˚C/44%
7	**2**	B	22.8˚C/45%
7	**2**	C	22.1˚C/43%

F.4 Bubble-Electrospun Fiber Diameters

All solutions were bubble-electrospun with field strengths of 40 kV/15 cm (PVOH solutions) and 35 kV/15 cm (PAN solutions). The tables below list average fiber and bead diameters, as well as their related standard deviations. Table F-14 and Table F-16 list the average fiber and bead diameters of bubble-electrospun PVOH and PAN fibers, respectively. Table F-15 and Table F-17 list the standard deviations of bubble-electrospun PVOH and PAN fibers, respectively.

Table F-14: Average bubble-electrospun PVOH fiber and bead diameters.

Polymer Concentration (wt%)	Surfactant Concentration (x cmc)	Average Fiber Diameter (nm)	Average Bead Diameter (nm)
8	**0.5**	108.78	410.70
8	**1**	102.00	527.53
8	**2**	97.51	459.75
10	**0.5**	144.88	949.42
10	**1**	157.70	706.01
10	**2**	131.66	792.26
12	**0.5**	248.73	857.64
12	**1**	241.13	1898.05
12	**2**	190.18	1609.43

Table F-15: Standard deviation of bubble-electrospun PVOH fiber and bead diameters.

Polymer Concentration (wt%)	Surfactant Concentration (x cmc)	Average Fiber Diameter (nm)	Bead Diameter (nm)
8	**0.5**	33.40	130.89
8	**1**	32.97	251.79
8	**2**	29.80	198.07
10	**0.5**	48.41	367.19
10	**1**	50.01	-

10	**2**	49.22	373.66
12	**0.5**	80.04	-
12	**1**	108.72	865.29
12	**2**	78.70	924.74

Table F-16: Average bubble-electrospun PAN fiber and bead diameters.

Polymer Concentration (wt%)	Surfactant Concentration (wt%)	Average Fiber Diameter (nm)	Average Bead Diameter (nm)
5	**0.5**	208.53	1105.89
5	**1**	221.90	1178.34
5	**2**	253.81	786.90
6	**0.5**	278.73	1096.01
6	**1**	313.56	924.23
6	**2**	356.53	1013.03
7	**0.5**	413.79	-
7	**1**	438.20	-
7	**2**	437.41	-

Table F-17: Standard deviation of bubble-electrospun PAN fiber and bead diameters.

Polymer Concentration (wt%)	Surfactant Concentration (wt%)	Fiber Diameter (nm)	Bead Diameter (nm)
5	**0.5**	55.63	594.84
5	**1**	53.493	493.02
5	**2**	55.243	194.65
6	**0.5**	65.863	316.45
6	**1**	73.823	331.65
6	**2**	96.153	204.06
7	**0.5**	112.42	-
7	**1**	137.30	-
7	**2**	116.62	-

Table F-18: Calculation of PVOH fiber production rates.

Referencing		(a)	(b)	(c)	(d)	(e)	(f)	(g)	(h)	(i)
Polymer Conc (wt%)	**Surfactant Conc (wt%)**	**Bubble Size (mm)**	**Bubble Lifetime (s)**	**Fiber Weight per bubble (mg)**	**Bubbles in 1 m bath**	**bubbles in m^2 bath**	**bubbles per hour**	**m^2/h number of bubbles**	**Production per m^2/h (g)**	**Standard Deviation of Production Rate**
Equations					**1000/(a)**	**$(d)^2$**	**3600/(b)**	**(e)x(f)**	**(g)x(c/1000)**	
8	0.5	23.96	182.62	4.79	41.76	1744.54	28.53	49779.22	184.66	68.46
10	0.5	28.29	115.55	3.70	35.61	1277.06	40.21	51345.56	431.07	94.87
12	0.5	22.95	140.54	6.14	43.69	1913.52	29.29	56045.88	644.27	83.47
8	1	25.88	142.57	11.12	39.12	1547.76	25.52	39497.49	147.04	52.81
10	1	27.76	58.16	9.03	36.06	1301.33	79.52	103487.79	454.59	153.60
12	1	22.26	114.21	7.49	44.98	2025.52	66.62	134947.49	1100.85	857.47
8	2	25.29	227.88	23.67	39.71	1583.46	19.45	30796.67	300.94	64.50
10	2	29.74	25.63	6.13	33.69	1137.13	530.97	603774.71	533.49	115.76
12	2	24.01	65.82	7.32	41.79	1751.44	58.15	101846.26	739.30	217.88

F-46

Table F-19: Calculation of PAN fiber production rates.

Referencing		(a)	(b)	(c)	(d)	(e)	(f)	(g)	(h)	(i)
Polymer Conc (wt%)	**Surfactant Conc (wt%)**	**Bubble Size (mm)**	**Bubble Lifetime (s)**	**Fiber Weight per bubble (mg)**	**Bubbles in 1 m bath**	**bubbles in m^2 bath**	**bubbles per hour**	**m^2/h number of bubbles**	**Production per m^2/h (g)**	**Standard Deviation of Production Rate**
Equations					**1000/(a)**	**$(d)^2$**	**3600/(b)**	**(e)x(f)**	**(g)x(c/1000)**	
5	0.5	17.17	16.05	1.84	58.24	3392.03	224.47	761414.83	1404.39	117.70
5	1	17.83	20.47	2.40	56.10	3146.73	179.08	563523.79	1352.46	160.78
5	2	17.48	10.07	1.16	57.21	3272.78	400.86	1311928.22	1516.01	546.08
6	0.5	18.08	9.83	1.64	55.30	3058.04	472.79	1445808.30	2369.52	271.28
6	1	18.79	9.03	1.17	53.21	2831.34	700.30	1982801.06	2324.28	193.81
6	2	18.07	2.72	0.69	55.35	3063.68	1395.57	4275581.94	2969.15	278.99
7	0.5	17.62	3.90	1.16	56.75	3220.98	928.20	2989713.90	3471.39	1294.00
7	1	16.78	3.60	1.03	59.59	3551.53	1004.37	3567043.43	3685.94	1022.82
7	2	18.85	2.16	0.72	53.06	2815.34	1744.25	4910649.58	3546.58	826.77

F-47